JAB-99-123

Nevada Test Site Terminal Waste Storage Program
Subtask 1.3: Facility Hardening Studies
DESIGN COST SCOPING STUDIES

by

Peter I. Yanev

and

G. Norman Owen

URS/John A. Blume & Associates, Engineers
130 Jessie Street (at New Montgomery)
San Francisco, California

April 1978

Prepared under Contract EY-76-C-08-0099
for the Nevada Operations Office
United States Department of Energy

Blank Page

ABSTRACT

As part of a program being conducted by the U.S. Department of Energy, Nevada Operations Office, to determine the feasibility of establishing a terminal waste storage repository at the Nevada Test Site, URS/John A. Blume & Associates, Engineers, made approximate determinations of the additional costs required to provide protection of structures against seismic forces. This report presents a preliminary estimate of the added costs required to harden the surface structures, underground tunnels and storage rooms, and vertical shafts of the repository against ground motion caused by earthquakes and underground nuclear explosions (UNEs). The conceptual design of all of the structures was adapted from proposed bedded-salt waste-isolation repositories.

Added costs for hardening were calculated for repositories in three candidate geological materials (Eleana argillite, Climax Stock granite, and Jackass Flats tuff) for several assumed peak ground accelerations caused by earthquakes (0.3g, 0.5g, and 0.7g) and by UNEs (0.5g, 0.7g, and 1.0g).

Hardening procedures to protect the tunnels, storage rooms, and shafts against incremental seismic loadings were developed from (1) qualitative considerations of analytically determined seismic stresses and (2) engineering evaluations of the dynamic response of the rock mass and the tunnel support systems.

The added costs for seismic hardening of the surface structures were found to be less than 1% of the estimated construction cost of the surface structures. For the underground structures, essentially no hardening was required for peak ground accelerations up to 0.3g; however, added costs became significant at 0.5g, with a possible increase in structural costs for the underground facilities of as much as 35% at 1.0g.

CONTENTS

CONTENTS (continued)

TABLES

FIGURES

SUMMARY

Purpose

The U.S. Department of Energy, Nevada Operations Office, is currently conducting a program to determine whether a terminal waste storage repository can be established at the Nevada Test Site (NTS). This report presents a preliminary estimate of the costs required for hardening terminal waste storage repositories at candidate NTS locations against ground motion caused by earthquakes and underground nuclear explosions (UNEs). These hardening costs are the additional costs that are required beyond static design and construction costs.

Description of Repository Structures

No appropriate conceptual design for the waste repository was available at the initiation of the study. Thus, it was necessary to assume a configuration that would represent a prototype facility and would be applicable to a variety of sites with different geologic conditions. Five proposed repository concepts were reviewed: three bedded-salt waste-isolation facilities and two retrievable surface storage facilities. The concept selected for study was based primarily on the bedded-salt waste-isolation facilities and was developed for storage of high-level waste (HLW) only.

The structures of the repository were classified according to the three seismic categories generally used in the nuclear industry. Category I, which includes all structures whose continual functioning or integrity is essential for the safe containment of waste materials, is generally the only category whose structures require hardening beyond the requirements of local building codes. The following repository structures were assumed to be Category I structures; they include eight of the surface structures and all of the underground structures.

- HLW building
- Control room building
- Emergency power building
- HLW hoist building
- Suspect waste and laundry building

- Mine storage filter building
- Water pumphouses (two)
- Vertical shafts and all underground structures (tunnels, storage rooms, etc.)

All of the surface structures in this category were based, architecturally and functionally, on available bedded-salt repository configurations and were assumed to be reinforced concrete, shear-wall structures. It was further assumed that the tornado design criteria that apply to safety-related nuclear power plant structures would be required for surface repository structures. For the tornado risk area in which the NTS is located, exterior walls and roofs of nuclear power plant structures are generally designed to be around 18 in. thick to resist the impact of tornado-generated debris. Consequently, 18-in.-thick reinforced concrete walls and roofs were assumed for the Category I surface structures of the repository.

In the conceptual design selected for analysis, the underground facility is connected to the surface structures by four vertical shafts that are from 11 ft to 26 ft in diameter and differ in design, use, and functional constraints:

- Man and material shaft
- HLW shaft
- HLW ventilation shaft
- Construction ventilation shaft

The underground structures, which include all tunnels and HLW storage rooms, were assumed to be located 2,000 ft below the surface. Although this depth was selected because of the geology of the NTS, it is representative of other proposed repository concepts as well. The underground facility may encompass an area of several hundred acres. It is conceptualized as a grid of intersecting tunnels and storage rooms. Because actual configurations and design details were not available, a common 18-ft diameter cross section was assumed for all the structures at the underground level. This assumption was adopted directly from one of the bedded-salt facilities reviewed and was selected to simplify the cost-estimating effort. The actual cross sections will probably have the horseshoe shape conventionally used for tunnels. The size of the cavity was selected on the basis of approximate functional requirements,

described in the literature on bedded-salt concepts, to be compatible with the geology of the candidate sites at the NTS.

The Candidate Geological Materials

Four geological materials, characteristic of the following candidate construction sites, were reviewed:

1. Eleana Formation argillite (hereafter called shale)
2. Climax stock granite
3. Jackass Flats tuff
4. Jackass Flats alluvium

Engineering geology information obtained from data available at the NTS was used to provide a basis for the preliminary design of support systems for the underground repository structures. Data on the candidate materials taken from bore holes and existing tunnels were assumed, for the analysis, to be uniform for all sites at the NTS where the material occurs. Properties were then assigned to the materials on the basis of the acquired data. Evaluation of the Jackass Flats alluvium was discontinued at this point in the investigation because the available data for the material were insufficient for even a conceptual design.

The Eleana shale was found generally to have low hardness and strength properties. Some portions of the shale exhibited high slaking potential and closely-spaced fracturing. Portions may be difficult to mine and support because squeezing ground may be encountered. The tuff and the granite were observed to have high strength properties.

Ground Motion Criteria

The peak ground motion accelerations assumed for this study were specified by Sandia Laboratories as follows:

1. From earthquakes -- 0.3g, 0.5g, and 0.7g.
2. From UNEs -- 0.5g, 0.7g, and 1.0g.

For dynamic structural analysis, the frequency content of ground motion, as well as the peak ground acceleration, is usually required. This information

can be provided by response spectra, which are idealized peak response plots. For the purposes of this study, the response spectra recommended by NRC *Regulatory Guide 1.60* were adopted for the surface structures, for both earthquakes and UNEs. A value of 7% of critical damping -- a typical value for concrete structures at high stresses -- was used.

A literature survey was conducted to determine seismic motion criteria for the underground structures. While most of the empirical data indicated that motion amplitudes decrease with depth, there were some instances of amplification. Because the time constraints and budget of this preliminary study did not permit a comprehensive analysis of depth effects, this characteristic was disregarded, and a simple seismic wave approach was adopted for the investigation of stresses and strains at depth. Peak ground motions associated with the NRC spectra were assumed for analysis of the underground structures. The general effect of these assumptions was intended to be conservative.

Hardening Costs

On the basis of the available sources of information for bedded-salt repositories, the cost of the surface structures assumed to be in Category I was estimated to exceed $40 million and the cost of the entire repository to exceed $500 million. Thus, most of the cost of the repository is associated with the underground structures. For that reason, the cost scoping of the surface structures was not given extensive treatment.

The following added costs for hardening were computed on the basis of many assumptions generally used in cost estimating. The stated dollar cost figures are presented primarily for internal comparison and should be used with caution. Expression of added costs as a percentage of the static design cost of the structures (also presented) provides a better basis for comparison.

Added Costs for Hardening of the Surface Structures. Response spectrum analyses with single-degree-of-freedom models were conducted for the surface structures. Approximate fundamental frequencies and seismic forces and stresses were computed for the specified ground motions. Wherever the seismic stresses exceeded the allowable stresses, the structures were hardened and then were reanalyzed; this process was iterated until the stress criteria were met. The added costs for hardening were then computed.

The thick exterior walls required for tornado hardening also provide major resistance to seismic motion; therefore, the added costs for hardening the surface structures were small. No hardening was required for a peak ground acceleration of 0.5g or below, from either earthquakes or UNEs. Hardening was required at 0.7g and 1.0g for the HLW building and at 1.0g for the emergency power building. No hardening was required for the other Category I structures. The added costs were small, amounting to $30,000 for 0.7g and $105,000 for 1.0g peak ground acceleration. If, however, tornado hardening is not required, the added costs for ground motion hardening will be increased. A separate study of added earthquake hardening costs for various types of conventional surface structures was performed to obtain a preliminary indication of that cost. The added cost was estimated to exceed $400,000.

Added Cost for Hardening of the Underground Structures. The analysis and design of deep underground structures for seismic motion require methodologies different from those available for the analysis of surface structures. In both cases a reasonably detailed and reliable prediction of the seismic motion to which the structure is expected to be exposed is essential. However, such a prediction for deep tunnels requires detailed and time-consuming analyses not appropriate to this study. Furthermore, because the current state of the art for static tunnel design relies heavily on observational and empirical modification during construction, specific preconstruction stabilization evaluations that depend on detailed calculations of stresses and strains usually are not justifiable. Seismic analyses currently are most useful for making a general evaluation of the magnitudes of seismic stresses or strains relative to in-situ and ultimate stresses and strains. (Thus, a close working relationship between the seismic consultants and those responsible for static load considerations should be maintained.)

For the foregoing reasons, a simplified but conservative approach was taken for the investigation of stresses and strains at depth. Dilatational and shear waves were assumed to be propagating through the medium in the directions that impose maximum strains on underground structures. Various combinations of these waves were then considered in order to obtain the largest possible strain. The additional hardening requirements for underground structures are based not only on incremental seismic stresses (which must be compared to the in-situ static stresses in the rock formation) but also on a

practical and experience-oriented evaluation of the effects of seismicity on underground openings. It was concluded that the primary effort in hardening tunnels and shafts must be to improve construction details to achieve a more coherent system between the rock and the tunnel. With this methodology, a program for the incremental improvement of the underground support structures was developed.

Before seismic hardening can be designed, it is necessary to have a conceptual design of the static support systems for the tunnels and the shafts. Review of the properties of available cores of the Eleana shale indicated that pockets of squeezing ground may exist. For that reason, it was assumed that the static stabilization of the tunnels and shafts would require steel sets with the necessary blocking. For the candidate tuff and granite materials, it was assumed that rock bolts and wire mesh would be used to provide static support. A 15- to 18-in.-thick concrete liner was assumed for the shafts (not to provide static stability but rather to ensure water-tightness).

The hardening features assumed for conceptual designs in the different candidate materials consist of the following:

- Eleana shale: additional packing between the overbreak and the lagging and additional and larger tie rods between the steel sets.
- Tuff and granite: additional rock bolts around the perimeter of the excavation, additional thickness of shotcrete on the surface, and increased rock bolt bonding to the rock material.

At the initiation of the study, it had been planned to compute only the added costs for hardening. However, as the work progressed, it became clear that hardening costs could not be entirely separated from static construction costs. Therefore, the static costs were estimated for all structures. These URS/Blume cost estimates were based on data for conventional structures (such as rapid transit tunnels) that do not involve such costs as licensing, nuclear quality assurance, security, etc. Thus, all cited dollar costs should be used only for relative comparisons among the candidate sites. (It should be noted that construction costs for the Eleana shale without seismic hardening that were estimated concurrently by Fenix & Scisson, Inc., used different assumptions.)

Estimated base costs in 1978 dollars per linear foot of length for the tunnels and shafts are as follows:

Tunnels (18 ft ø)			Man and Materials Shaft (26 ft ø)			HLW and Construction Ventilation Shafts (16-1/2 ft ø)			HLW Shaft (11 ft ø)		
Granite	Tuff	Shale	Granite	Tuff	Shale	Granite	Tuff	Shale	Granite	Tuff	Shale
730	770	1,400	3,400	3,500	4,900	2,700	2,700	3,500	1,800	1,900	2,100

On the basis of the assumption that squeezing ground will dominate the shale design, that material is the least desirable from the cost viewpoint. Construction of the tunnels in shale is roughly twice as expensive as construction in tuff or granite for the static condition. The shaft construction costs in the shale are roughly 15% to 40% greater than those in tuff and granite.

Figure S.1 illustrates the changes in the total cost per linear ft of the tunnel as a function of peak ground acceleration. Above 0.5g, there is little difference among geologic materials in the added costs for hardening.

Table S.1 summarizes the added costs for hardening at the various peak ground accelerations by illustrating these costs as a percent of static cost. The static cost can change significantly without substantially affecting the stated percentages.

The added costs of hardening tunnels against ground motion can be quite significant at 0.5g or above. There is generally little difference in cost between tuff and granite; the granite seems to be the slightly more desirable material economically. As a percentage over base cost, the cost of hardening for the shale is less than for the tuff or granite because of the greater amount of static support required for the shale.

The added costs of hardening shafts against ground motion are insignificant (all approximately 1%) with the single exception of the shafts in shale for 1.0g peak ground acceleration.

TABLE S.1

SUMMARY OF ESTIMATED HARDENING COSTS AS PERCENTAGE INCREASE

PGA Range (g)	Cost Increase per Linear Foot (%)					
	Tunnels			Four Shafts Combined		
	Granite	Tuff	Shale	Granite	Tuff	Shale
0.0 to 0.3	0	0	0	0	0	0
0.0 to 0.5	3	18	2	1	1	1
0.0 to 0.7	27	26	13	1	1	1
0.0 to 1.0	34	35	13	1	1	10

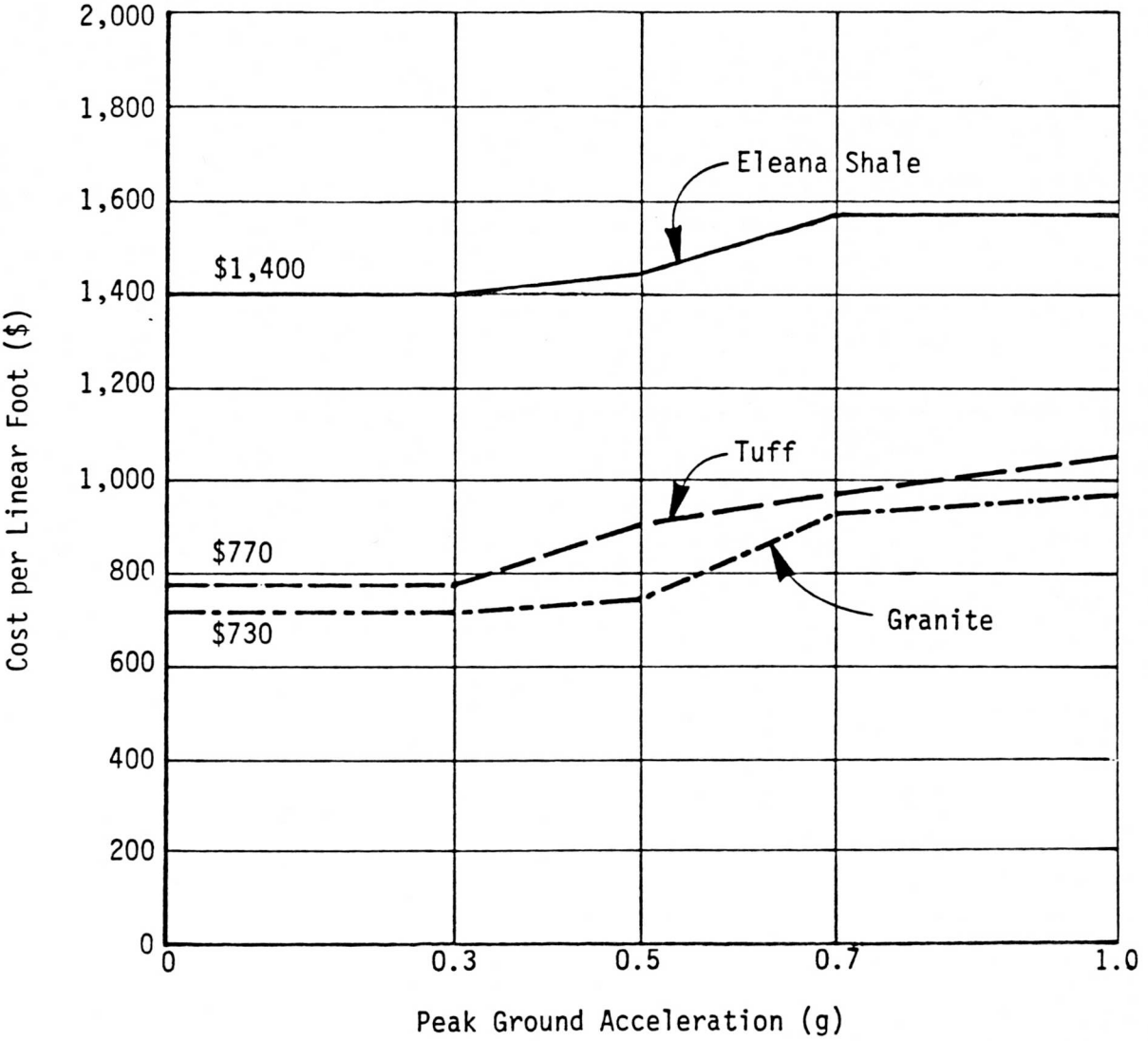

Note:

These dollar amounts should be used only in the context of this report. They are relative figures and may vary significantly.

FIGURE S.1 SUMMARY OF ESTIMATED TUNNEL COST PER LINEAR FOOT

Conclusions

On the basis of the assumptions that were made, no significant added costs for hardening against ground motion are expected for surface structures or for underground structures at or below 0.3g peak ground acceleration. However, the added costs for hardening become significant at 0.5g or above and could increase the total cost as much as 35%. These cost estimates are quite sensitive to the criteria, assumptions, and procedures used in the design for seismic hardening. In particular, the final performance and design criteria selected for the terminal waste repositories will strongly influence total costs.

1. INTRODUCTION

1.1 Purpose

The U.S. Department of Energy, Nevada Operations Office (DOE-NV), is currently directing a program to determine whether a terminal waste storage repository can be established at the Nevada Test Site (NTS).[1] A part of this effort requires an early indication of whether the facility can be hardened (strengthened) at a reasonable cost against ground motion caused by weapons testing and by natural seismicity at the NTS and in its surrounding areas.

This report presents a preliminary estimate of the costs at candidate NTS locations for hardening terminal waste storage repositories against ground motion caused by weapons testing at the NTS as well as the costs for hardening against assumed earthquake ground motions. The estimates are calculated as additional costs -- that is, those beyond the design and construction costs that would be incurred in the absence of such seismic considerations. In the report, these costs are referred to as added costs for hardening; the terminal waste storage repository is referred to simply as the repository.

1.2 Scope of the Studies

The detailed scope of work originally conceived for the design cost scoping studies[2] was somewhat altered as the work progressed; analysis and design variables were redefined within the context of the evolving work. The final scope of work includes the following:

1. Identifying alternative structural configurations for the repository and selecting one to be adapted to the candidate sites at the NTS.
2. Collecting the available preliminary seismological data, for both underground nuclear explosions (UNEs) and natural seismicity, for use in formulating preliminary design ground motion criteria at various depths below the ground surface, using the following peak ground accelerations in each of the three component directions (two horizontal and one vertical):

   UNEs -- 0.5g, 0.7g, and 1.0g
   Earthquakes -- 0.3g, 0.5g, and 0.7g
3. Collecting geological data for the candidate sites sufficient for formulating the preliminary design

ground motion criteria at selected depths below the ground surface; reviewing the data for the purpose of formulating preliminary structural configurations of the underground structures of the repository. The four candidate sites, in order of priority, are:

- Eleana argillite (shale)*
- Climax stock granite
- Jackass Flats tuff
- Jackass Flats alluvium

4. Adapting the selected repository configuration, including the surface and underground structures, to the NTS candidate sites.
5. Classifying the structures and the structural components according to their use and function, using the NRC nuclear power plant methodology as a guideline.
6. Formulating preliminary criteria for the design and analysis of the structures; conducting the necessary analysis and design of the structures for static conditions and for the imposed ground motion criteria.
7. On the basis of the preliminary analyses and designs, estimating the added costs for hardening the facility against UNE and earthquake ground motions.
8. Conducting parallel studies (also called secondary studies) to assess and/or substantiate the results of item 7, above. (Two brief studies were conducted to determine the added costs for hardening existing or planned structures in seismic areas, one for underground facilities and one for surface facilities.)
9. Making recommendations for the initiation of a follow-up study if the preliminary cost studies suggest that more detailed estimates are feasible and warranted.
10. Preparing a written report that summarizes the work and the resulting recommendations.

1.3 Acknowledgments

The work was carried out in support of various facility hardening studies for the NTS Terminal Waste Storage Program. This report is in support of Subtask 1.3 of the program.[1] Technical direction for URS/John A. Blume & Associates, Engineers (URS/Blume), was provided by Sandia Laboratories (Sandia), Albuquerque, New Mexico. The project was sponsored by DOE-NV

*Eleana argillite is referred to as Eleana shale in the remainder of this report.

under U.S. Department of Energy Contract No. EY-76-C-08-0099. Extensive contributions were made by the engineering staff and management of URS/Blume. Professor Tor L. Brekke of the University of California, Berkeley, and George E. Wickham of Jacobs Associates, San Francisco, provided valuable consulting services. Mary H. Stauduhar of URS/Blume edited the report and coordinated its publication.

2. DESCRIPTION OF THE STRUCTURAL SYSTEM OF THE REPOSITORY

2.1 General Description of the Repository

The repository is designed to receive and store commercial radioactive high-level waste (HLW) products. For the purposes of this cost estimate, it may be assumed that these products will be received over a 20-year period and may be stored for an indefinite period of time.[3]

Figure 2.1[4] presents a conceptual design of a repository. The facility consists of a large number of excavated storage rooms and interconnecting tunnels located a few thousand feet below the ground surface. Receiving and handling facilities for canisters that contain waste or spent fuel are located on the surface. It is planned that the waste will be delivered by truck or rail. Vertical shafts connect the surface receiving facilities to the underground facility, where the waste canisters are delivered to a transporter vehicle that moves the waste to its final storage location. There, the canisters containing HLW are lowered into holes in the floor of the underground storage rooms. The holes are then backfilled or plugged for radiation shielding. In the case of low-level waste, the canisters may be stacked in the storage rooms for disposal. If spent fuel is delivered to the plant, it is assumed for this study that the canisters that contain it will be dealt with in the same way as reprocessed HLW.[4]

The extent of the land area associated with particular repositories may vary, depending on the local geologic conditions. Surface facilities may occupy from 100 to 200 acres and will be the only visible evidence of the repository.

2.2 Selection of the Structural System

At the initiation of the study, the configuration and details of the structures were not available, nor had they been defined. Thus, it was necessary to assume a configuration that would be representative of a typical repository and would be applicable to a variety of sites with different geologic conditions.

Several different proposed repository concepts were reviewed, including the following:

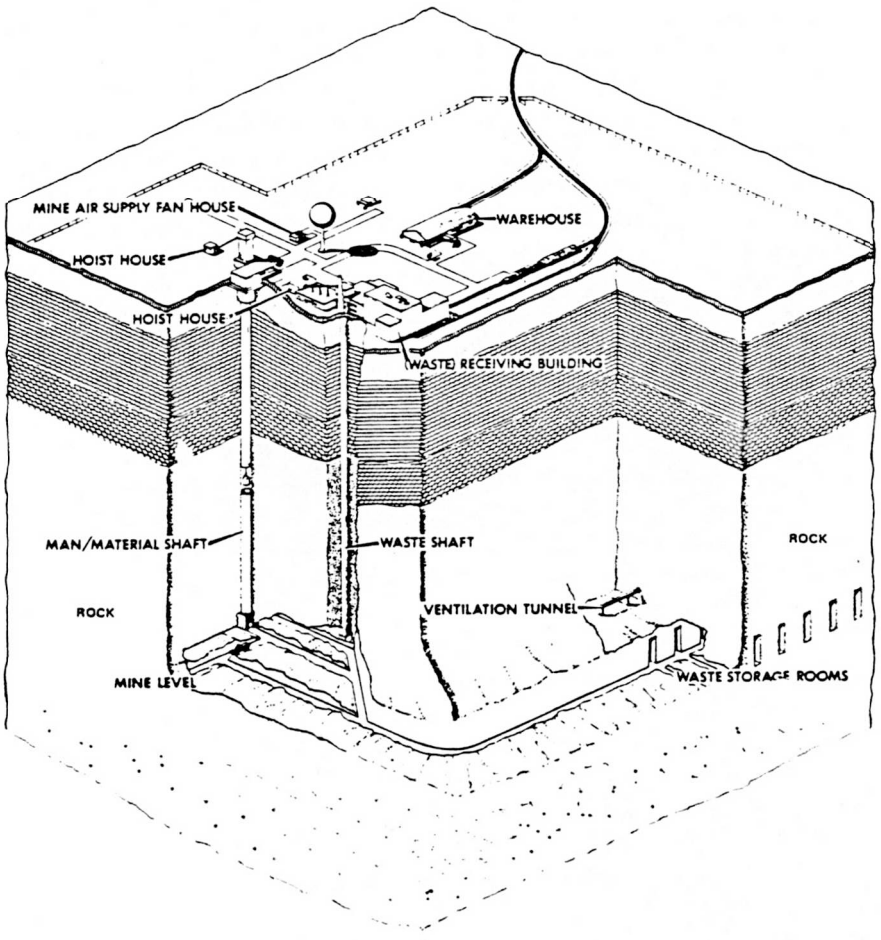

Source: Reference 4.

FIGURE 2.1 SIMPLIFIED CUTAWAY OF A REPOSITORY

1. The bedded salt waste isolation facility[3,5,6]
2. Gorleven Center, West Germany, bedded salt facility[7]
3. Retrievable surface storage facilities[8]
4. Spent unreprocessed fuel facility[9]

For deep repositories, References 3 and 5 present the most detailed structural configurations for both the surface and the underground structures. On this basis, it was decided to use the structural configurations described in Reference 5, insofar as they are applicable, for the surface structures. The vertical shaft configurations presented in Reference 5 were also used. References 3 and 5 were used for defining the general structural configurations and the size of the underground structures.

In order to simplify the cost estimating of the various proposed hardening procedures, it was also decided to develop the repository concept for storage of HLW only. Thus, it was possible to assume that all of the underground tunnels were of the same cross section; the cost estimating then could be conducted on the basis of cost per linear foot of tunnel.

2.3 Classification and General Description of the Structures

2.3.1 Classification. Some of the structures of the repository will house HLW; other structures will not. Therefore, it was necessary to classify all of the structures according to their function and use before the conceptual design for costing could be initiated. It is assumed that all of the structures of the repository will be designed to withstand natural phenomena such as winds, earthquakes, and tornados so that no loss of function will occur if that function is required for public safety.[3] It is generally assumed that the following specified levels of operational reliability and containment capacity will be met in the event of such natural phenomena. These classification categories are not to be confused with other categories, such as those for nuclear power plants, which cover a variety of design accidents that cannot occur in a repository.

> Category I: Structures, systems, and equipment whose failure might permit the uncontrolled release of radioactive material or those that are essential for the safety of plant personnel in the event of a radiological accident caused by the design earthquake.

Category II: Structures, systems, and equipment designed to permit waste-handling operations to continue without endangering the public health and safety during or following the design earthquake.

Category III: Structures, systems, and equipment whose failure will not result in release of excessive amounts of radioactivity or those that are not essential to continued waste-receiving and -storing operations.

2.3.2 General Assumptions for Structures. This section describes in general the facilities that meet the design requirements and provide the basis for a cost estimate. The structures and their assigned classifications are summarized in Table 2.1. The following general comments apply to these structures:

1. All buildings contain areas that may be classified as Category I, II, or III. The buildings may house equipment and equipment systems that are in Categories I through III. For the purposes of this study, it was conservatively assumed that if any portion of a building, or any equipment it contains, is Category I, then the entire structure is Category I. In the case of the administration building, it was assumed that the control room area could be structurally separated from the remaining structure by a gap. Under that assumption, the control room building is Category I, while the administration building becomes Category III. The required gaps between adjacent Category I and non-Category I structures are assumed to be large enough that interaction between the structures can not occur in case of the failure of a non-Category I structure.
2. Category I structures are assumed to be constructed of reinforced concrete for tornado-generated missile protection. Fenestrations of Category I structures that open to the atmosphere are also protected against missiles. Category II areas are assumed generally to be steel framed and to have insulated corrugated-metal panel siding; however, for structural considerations and economy, some Category II areas are constructed of reinforced concrete. Category III buildings are assumed generally to be constructed of reinforced concrete block with built-up roofing over metal decking.

2.3.3 Hardening Assumptions for Tornado Design. Tornado loads often govern the design of the exterior structural (shear) walls and roofs of the Category I structures of nuclear power plants. Because it is expected that tornado

TABLE 2.1

PRELIMINARY DESIGN CLASSIFICATION

OF ALL REPOSITORY STRUCTURES

Structure	Design Categorization	
	From Reference 5	Assumed by URS/Blume
Surface Structures, Major Facilities		
1. HLW building	I	
2. Control room building	I	
3. Administration building		III
Surface Structures, Support Facilities		
1. Emergency power building	I	
2. HLW hoist building	I	
3. Suspect waste and laundry building	I	
4. Mine storage filter building	I	
5. Water pumphouses (two)	I	
6. Man and materials building	III	
7. Warehouse and shops	III	
8. Vehicle maintenance building	III	
9. Man and materials hoist building	III	
10. Sewage treatment plant		III
11. Sewage effluent lagoon		III
12. Site entrance gatehouse	III	
13. Surface tailings storage and conveyance		III
14. Transformer and switch yard	II	
Underground Facilities		
1. HLW shaft		I
2. HLW shaft transfer cell		I
3. HLW ventilation shaft		I
4. Construction ventilation shaft		I
5. Man and materials shaft		I
6. Shops in tunnels		I
7. Storage rooms		I
8. All other tunnels		I

design will be required for the surface structures studied here, it was conservatively assumed that tornado design criteria similar to those for nuclear power plants will be employed. NRC *Regulatory Guide 1.76 -- Design Basis Tornado for Nuclear Power Plants*[10] details the design basis tornado criteria that are required in the design of Category I structures. Reference 10 also indicates that the state of Nevada in general is located in tornado region III, the lowest-risk tornado region. On that basis, it was further assumed that the NTS is located in tornado region III. In the cost scoping studies, to account for the effects of various tornado-generated missile impact forces and other pressure forces on the Category I surface structures, all exterior structural shear walls and roofs of Category I structures were assumed to be a minimum of 18 in. thick.[11] It is important to note that this assumed thickness is based on estimates of response such as the energy-balance and the impulse-momentum methods.[12,13] Recent tests[14,15] have indicated that these methods are often too conservative, and modifications to the current design methodology for tornado loads on nuclear power plant structures are therefore expected. In some cases, other design factors, such as radiation shielding, governed wall thickness. If a thickness greater than 18 in. was required, that thickness was assumed for this study.

As the Category I surface structures are generally of the shear-wall type, the tornado design assumptions have the effect of significantly stiffening the structures. Thus, for low-profile structures, tornado design also provides much of the required seismic design. However, some basic differences between tornado and seismic design remain, such as the detailing of connections between slabs and shear walls, detailing of the interior shear walls, and detailing of roof and floor slabs.

2.4 Surface Structures

Table 2.1 lists surface structures of the repository. Seven structures were assumed to be Category I; ten structures were assumed to be non-Category I. Because only Category I structures are likely to be hardened beyond the requirements of the applicable building codes, they were the only structures to receive further analysis. The seven Category I structures are described briefly in the following paragraphs. All of the accompanying figures are taken from Reference 5. The non-Category I structures are described in Reference 5.

2.4.1 HLW Building. The HLW building, as shown in Figures 2.2 and 2.3, provides facilities for personnel and equipment involved in the transfer of HLW from the incoming waste shipping canisters to the vertical shaft that is located beneath the building. A hot-cell and clean-cell arrangement allows for expansion of the facility by the addition of as many as three hot cells that lead into a common clean cell. The major portion of this facility is a tornado-hardened structure, with all fenestrations protected to prevent the penetration of tornado-borne missiles.

The inside dimensions of the rectangular building are approximately 126 ft by 155 ft. The structural framing is typically a reinforced concrete system. The floors and the roof are beam-and-slab systems supported on concrete columns and concrete bearing walls. The roof and the exterior walls are 18 in. thick. The area that contains the hot cell and the clean cell is enclosed by 4-ft-thick walls and roof. A hoist system upper sheave room, located directly above the vertical shaft, is considered to be part of the building. The high-bay area for shipping and receiving is also assumed to be a reinforced concrete system with 12-in.-thick walls and roof. The foundations are typically constructed as a system of individual columns and continuous-wall spread footings. Combined mat footings that bear directly on grade are required in some areas.

2.4.2 Control Room Building. Reference 5 assumes that the control room is an integral portion of the administration building. As described in Section 2.3.2 of this report, the control room is assumed to be a separate building (structurally disconnected and distant from the administration building). Whereas the administration building provides general support services for all facilities and activities at the repository site, the control room is assumed to perform all safety-related control operations. It will house the facility computers and the various monitoring and control systems.

Figure 2.4 shows the administration and control room buildings. The single-story control room building is approximately 144 ft by 36 ft. The structural framing is typically a reinforced concrete system. The roof is a concrete slab supported on concrete walls and columns. Both the exterior walls and the roof are assumed to be 18 in. thick. The floor is typically a concrete

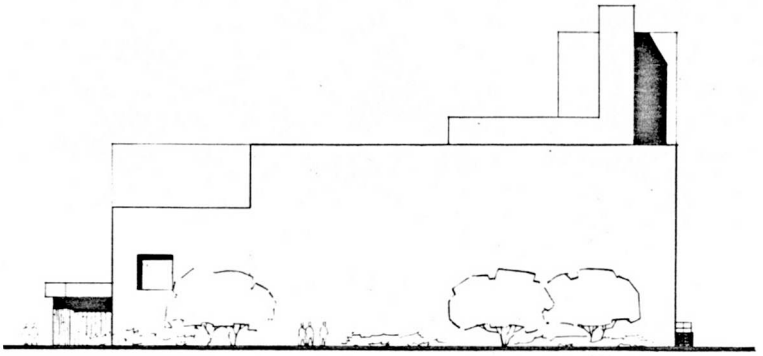

Front Elevation

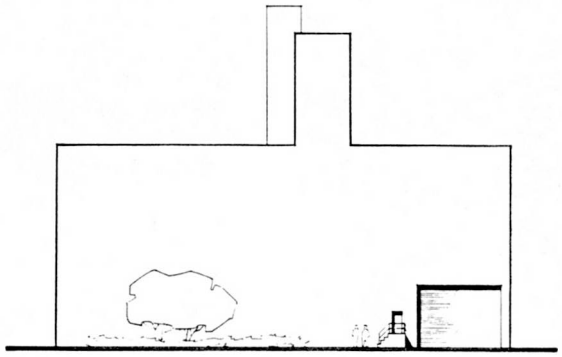

Side Elevation

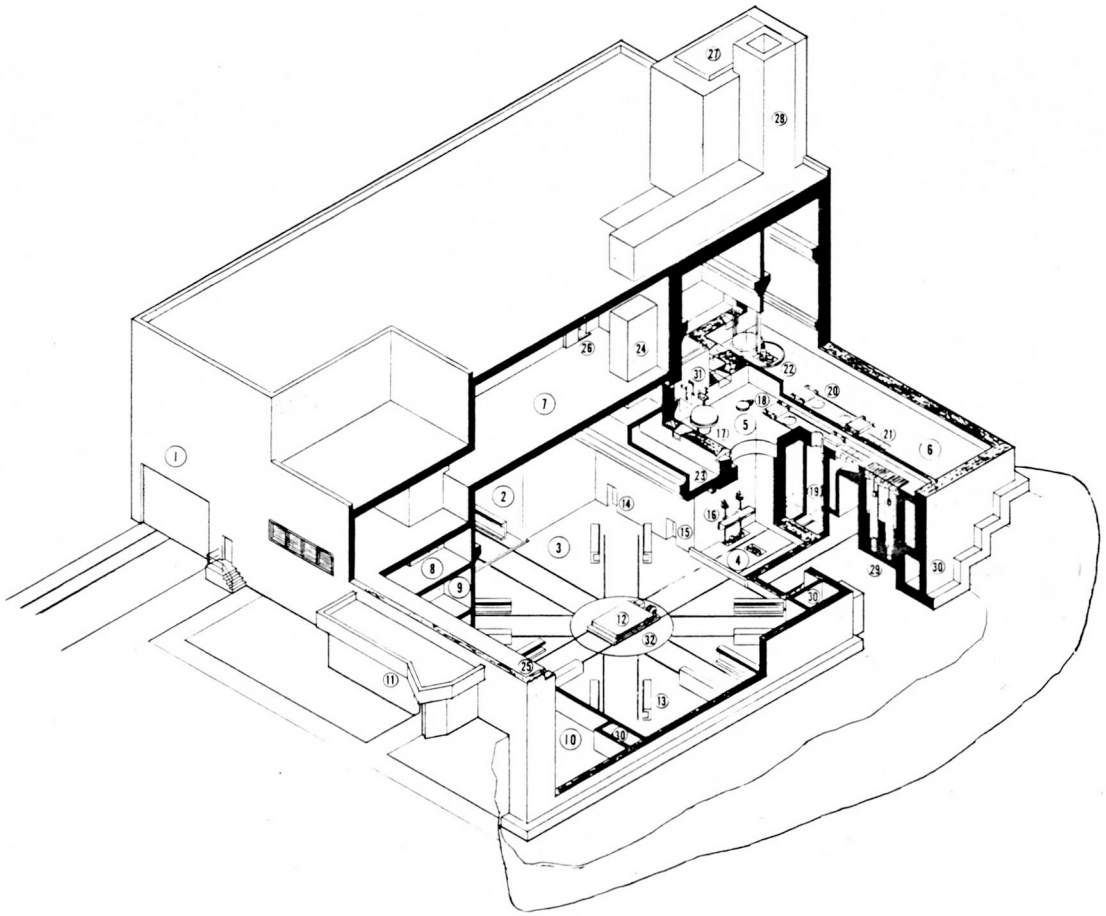

1. SHIPPING / RECEIVING HIGH BAY
2. TRANSFER GALLERY
3. PREPARATION & DECONTAMINATION
4. CASK ELEVATOR RM
5. HOT CELL
6. CLEAN CELL
7. HVAC ROOM
8. Offices
9. Health Physics / Lockers & Showers
10. Mechanical Equipment
11. Entrance
12. Cask Transfer Vehicle
13. Cask Cooldown Station
14. Lower Sheave Rm
15. Decon Repair
16. Elevator
17. Overpack Welder
18. Overpack Leak Test
19. Canister Decontamination
20. Canister Transfer Ports
21. Filters
22. Mine Cage Loading Station
23. Control Rm
24. Crane Repair Shield Doors
25. HVAC Access
26. Emergency Exit
27. Upper Sheave Rm
28. Exhaust Stack
29. Canister Storage Pits
30. Duct
31. Master Slave Manipulator
32. Turn Table

General View

Source: Reference 5

FIGURE 2.2 HLW BUILDING

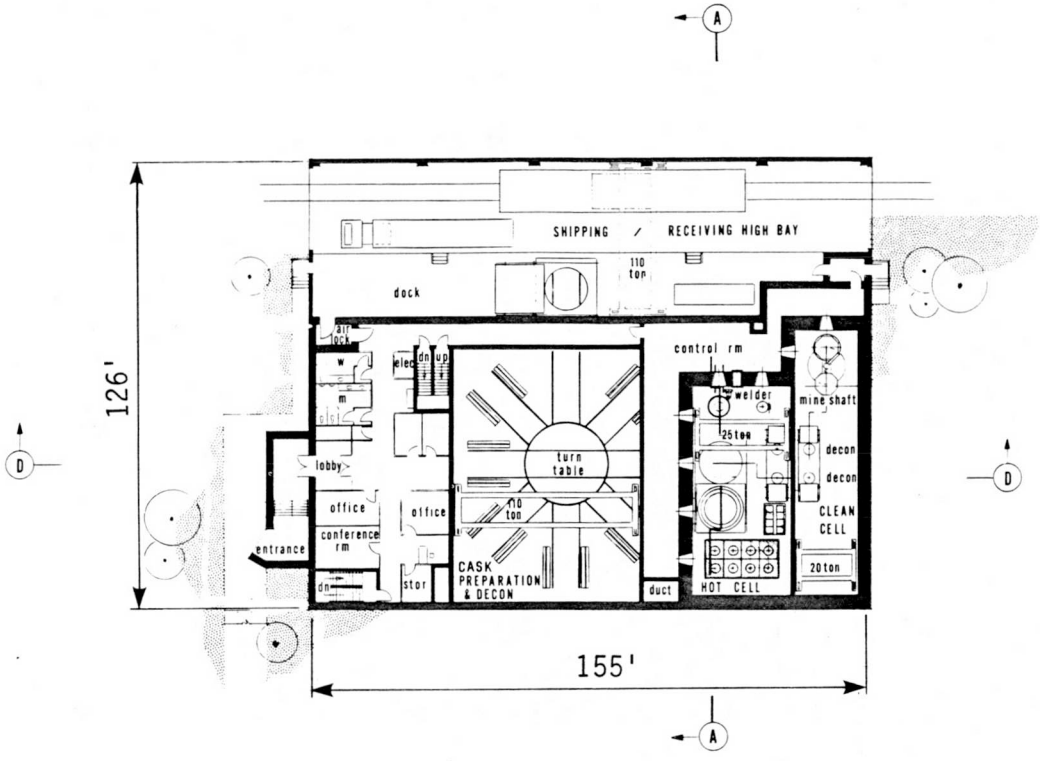

Floor Plan at Elevation +4'-0"

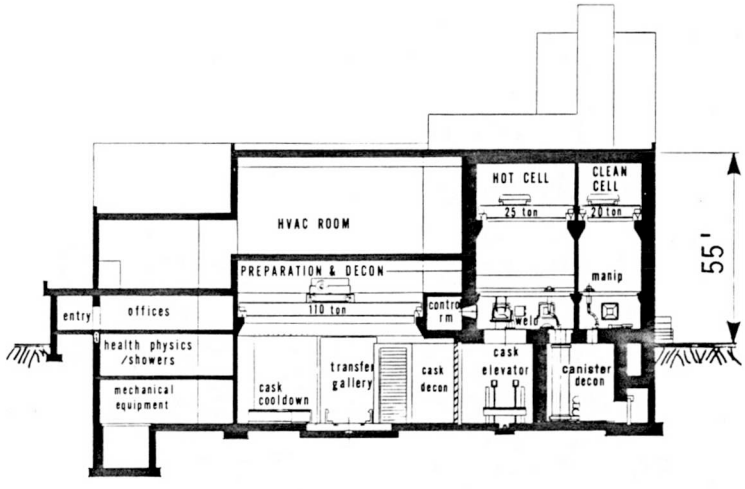

Section D-D

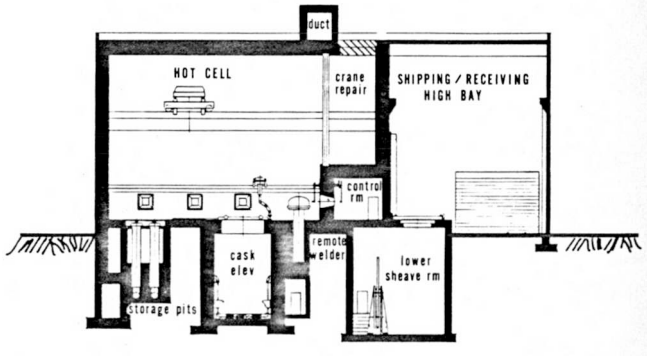

Section A-A

Plan and Sections

Source: Reference 5

FIGURE 2.3 HLW BUILDING

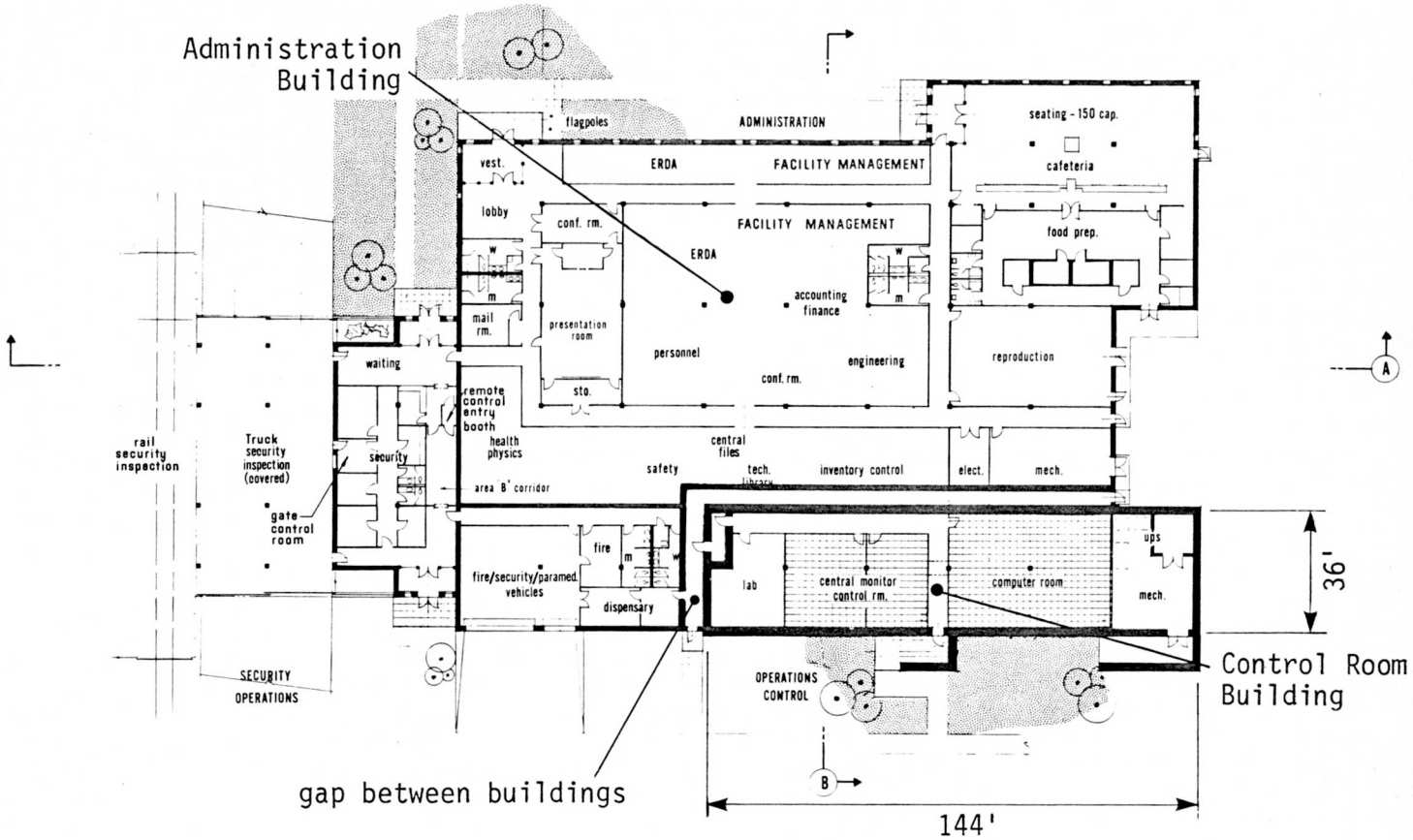

Floor Plan

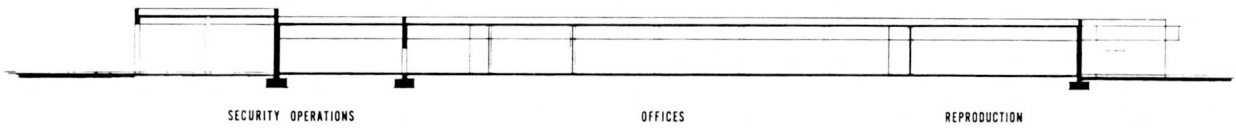

Section A-A

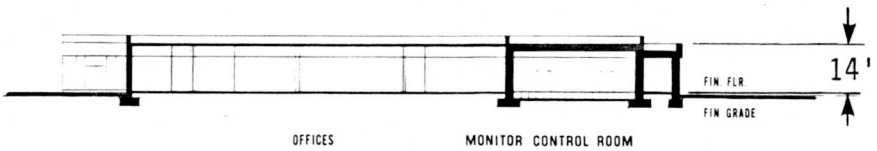

Section B-B

Source: Reference 5

FIGURE 2.4 ADMINISTRATION AND CONTROL ROOM BUILDING

slab on grade. Foundations are individual columns and continuous-wall spread footings.

2.4.3 Emergency Power Building. The emergency power building, as shown in Figure 2.5, houses the repository's emergency power generators and the normal and vital power switchgear. This split-level, single-story building is approximately 105 ft by 86 ft. The structural framing is a reinforced concrete system, with the beam-and-slab roof supported on a system of concrete columns and concrete bearing walls. The exterior shear walls and the roof slab are assumed to be 18 in. thick. The floor is a slab on grade. The foundations are individual columns and continuous-wall spread footings.

2.4.4 HLW Hoist Building. The HLW hoist building is a small, rectangular underground structure that houses the hoist equipment for the HLW shaft. Access to the hoist area is controlled at grade level. The underground area provides a hoist room and an office area. The hoist room has a removable roof panel above the hoist drum for installation and maintenance of the drum and other hoist equipment. A tunnel connects the hoist room to the lower sheave room of the HLW building and provides adequate space for cable guides, visual inspection, and preventive maintenance of the cables. The building is approximately 64 ft by 40 ft and 24 ft high. The roof level is approximately at finished grade. The exterior walls and the roof slab are assumed to be 18 in. thick. The structural framing is a reinforced concrete beam-and-slab system supported on exterior concrete walls. The floor is a concrete slab on grade. Building foundations are continuous-wall spread footings.

2.4.5 Suspect Waste and Laundry Building. The suspect waste and laundry building, shown in Figure 2.6, provides space for a laundry (to process protective clothing) and space for equipment tanks and controls (to collect and process radioactive wastewater for recycling or discharge to the suspect waste pond). The building is a small, rectangular structure, 80 ft by 60 ft. The structural framing is a reinforced concrete system, with a beam-and-slab roof system supported on concrete columns and concrete walls. The roof slab and exterior shear walls are 18-in.-thick concrete. The floor is a reinforced concrete slab on grade. Foundations are individual columns and continuous-wall spread footings. Combined mat footings, bearing directly on the ground, are required in some areas.

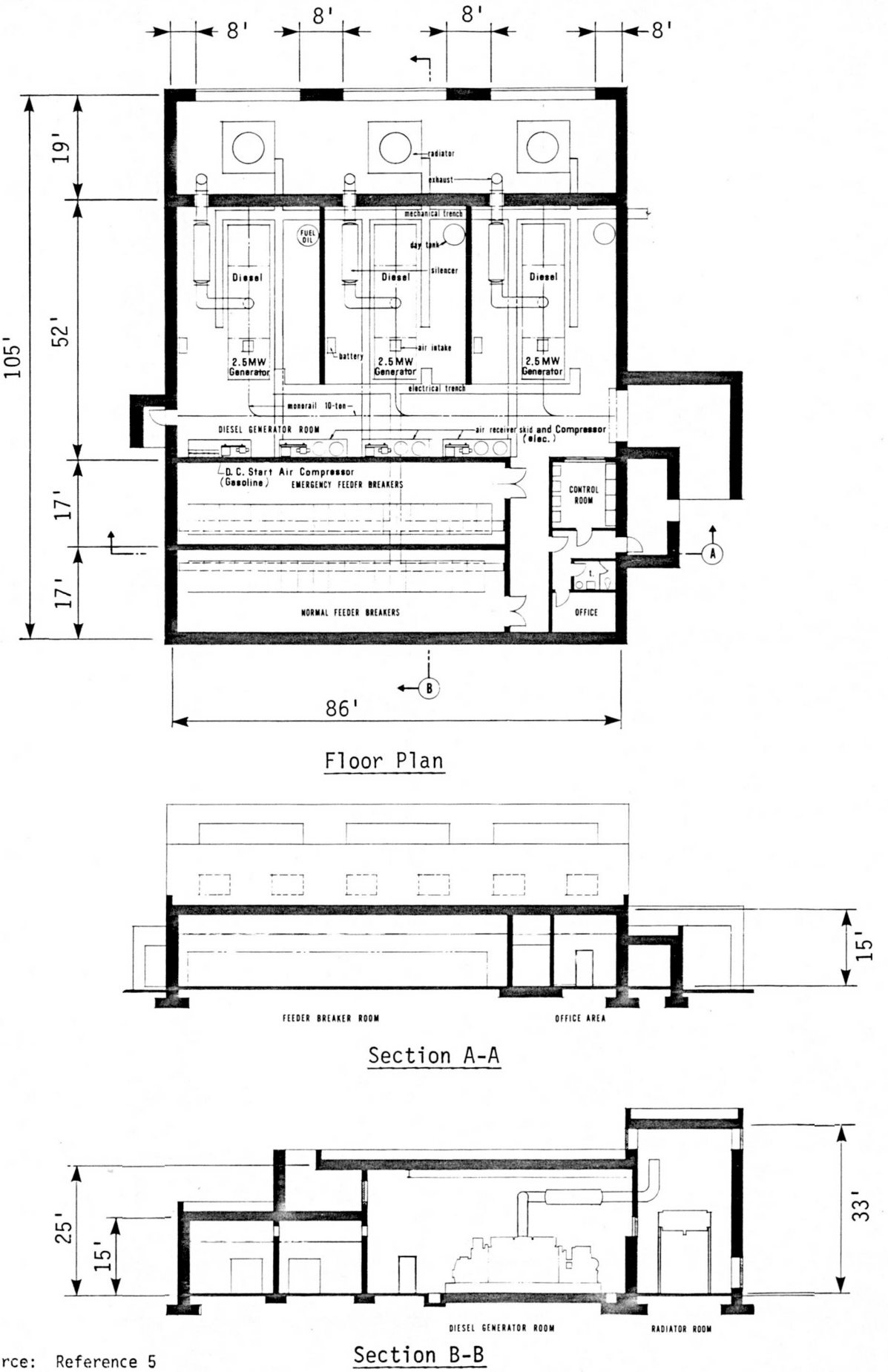

Source: Reference 5

FIGURE 2.5 EMERGENCY POWER BUILDING

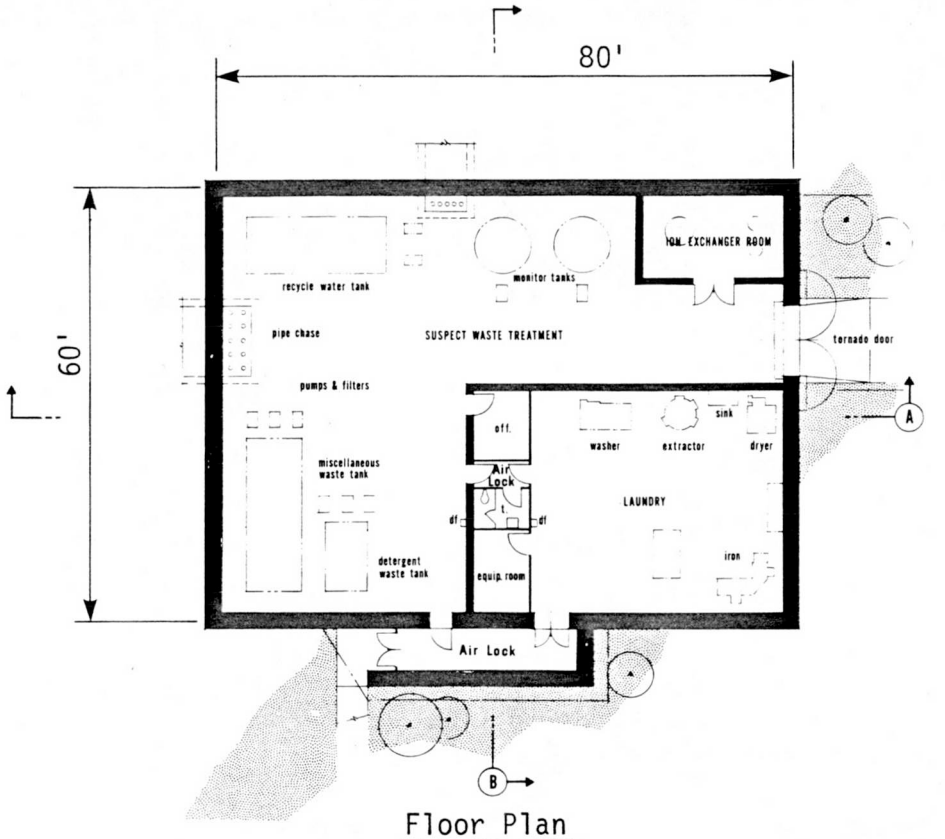

Floor Plan

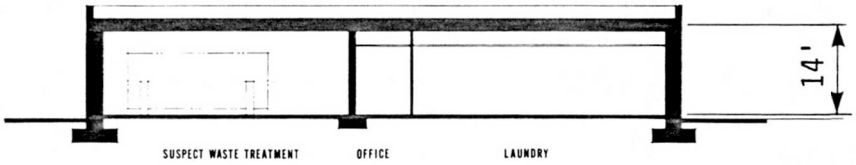

Section A-A

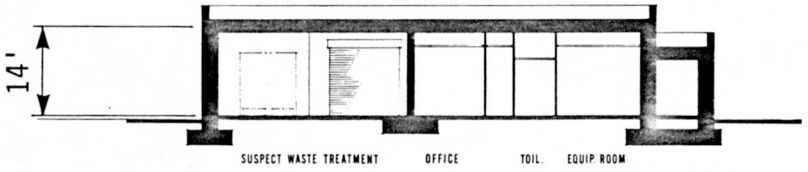

Section B-B

Source: Reference 5

FIGURE 2.6 SUSPECT WASTE AND LAUNDRY BUILDING

2.4.6 Mine Storage Filter Building. The mine storage filter building, shown in Figure 2.7, is a two-level structure that houses the ventilation equipment required to move and filter air from the waste storage horizons of the repository. Mine exhaust air is discharged from the building through a 98-ft-high stack. The rectangular building is approximately 120 ft by 80 ft. The structural framing is a reinforced concrete beam-and-slab floor, and the roof system is supported on interior concrete columns and exterior concrete walls. The exterior shear walls and the roof slab are assumed to be 18 in. thick. The lower floor is a concrete slab on grade. Foundations are individual columns and continuous-wall spread footings.

2.4.7 Water Pumphouses. The two water pumphouses contain the domestic-water and fire-protection pumps and are located at opposite ends of the site. Water chlorination equipment and a storage area for chemicals are also provided. The buildings are buried structures; a vertical, fixed stairwell provides access into the entrance pit of each building. Both of the pumphouses are single-story buildings that are 37 ft by 20 ft and 10 ft high. The roof level is approximately at finished grade. The structural framing is a reinforced concrete beam-and-slab system supported on 18-in.-thick reinforced concrete exterior walls. The floor is a concrete slab on grade. Foundations are continuous-wall spread footings.

2.5 Shafts

It is assumed that there will be four vertical mine shafts associated with the operation of the repository. In general, the shafts connect surface structures with the underground facility, which is assumed to be 2,000 ft below the surface. The location of the shafts is illustrated in Figures 2.8 and 2.9. The four shafts are the man and materials shaft, the HLW shaft, and the HLW and construction ventilation shafts. These shafts all differ in size, design, usage, and functional constraints. For the purposes of this study, all of the shafts are assumed to be Category I, as summarized in Table 2.1.

The general features and structural design of the shafts are discussed below. In Chapter 6, the structural design of the shafts and the assumed hardening procedures are discussed in detail.

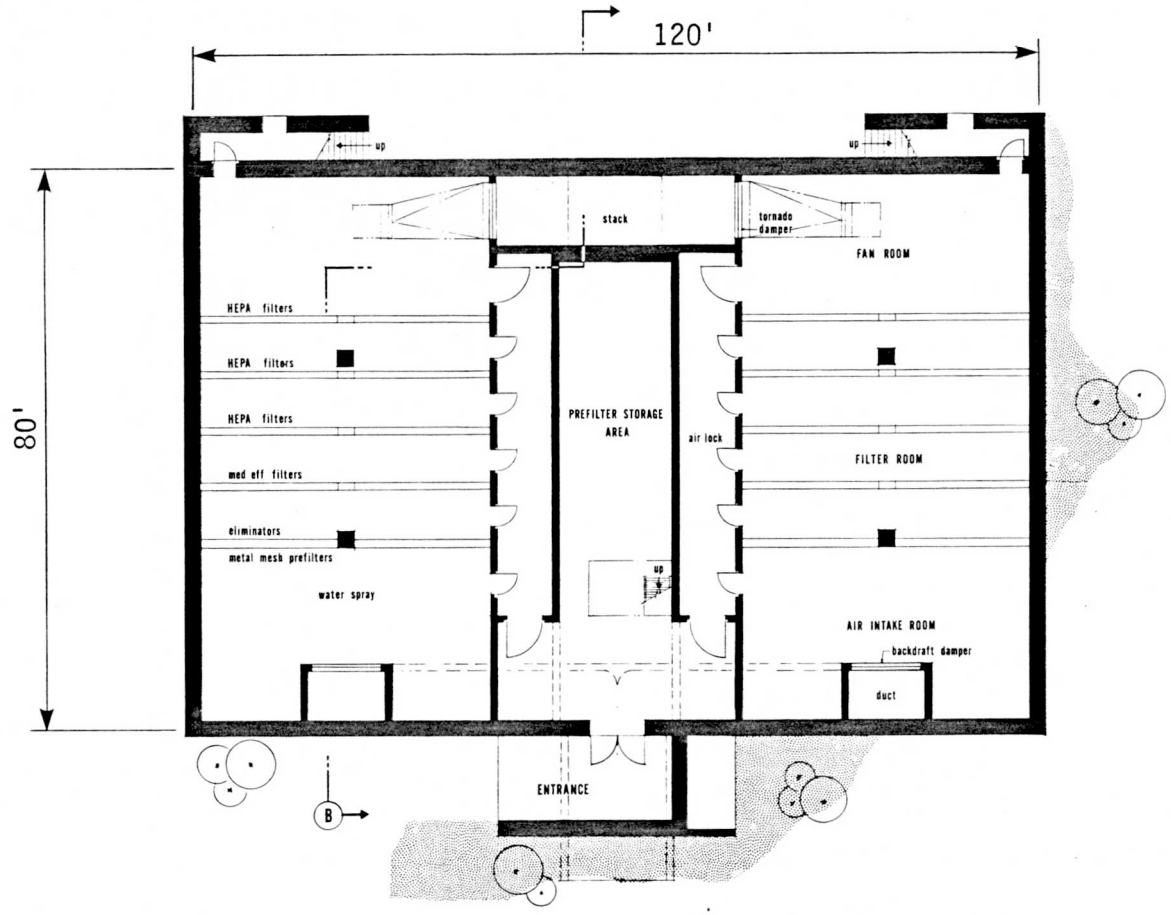

First Floor Plan

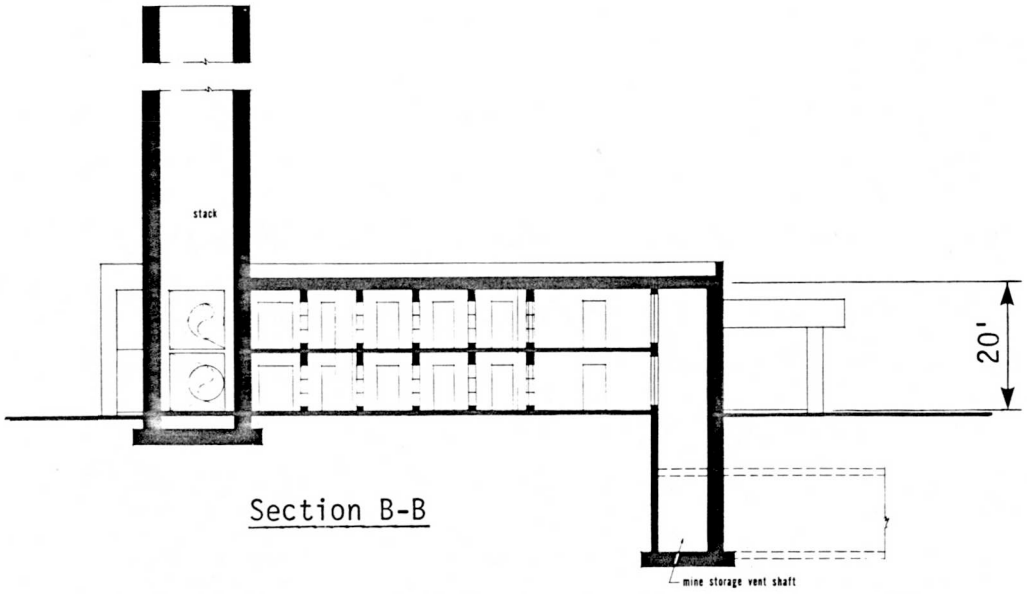

Section B-B

Source: Reference 5

FIGURE 2.7 MINE STORAGE FILTER BUILDING

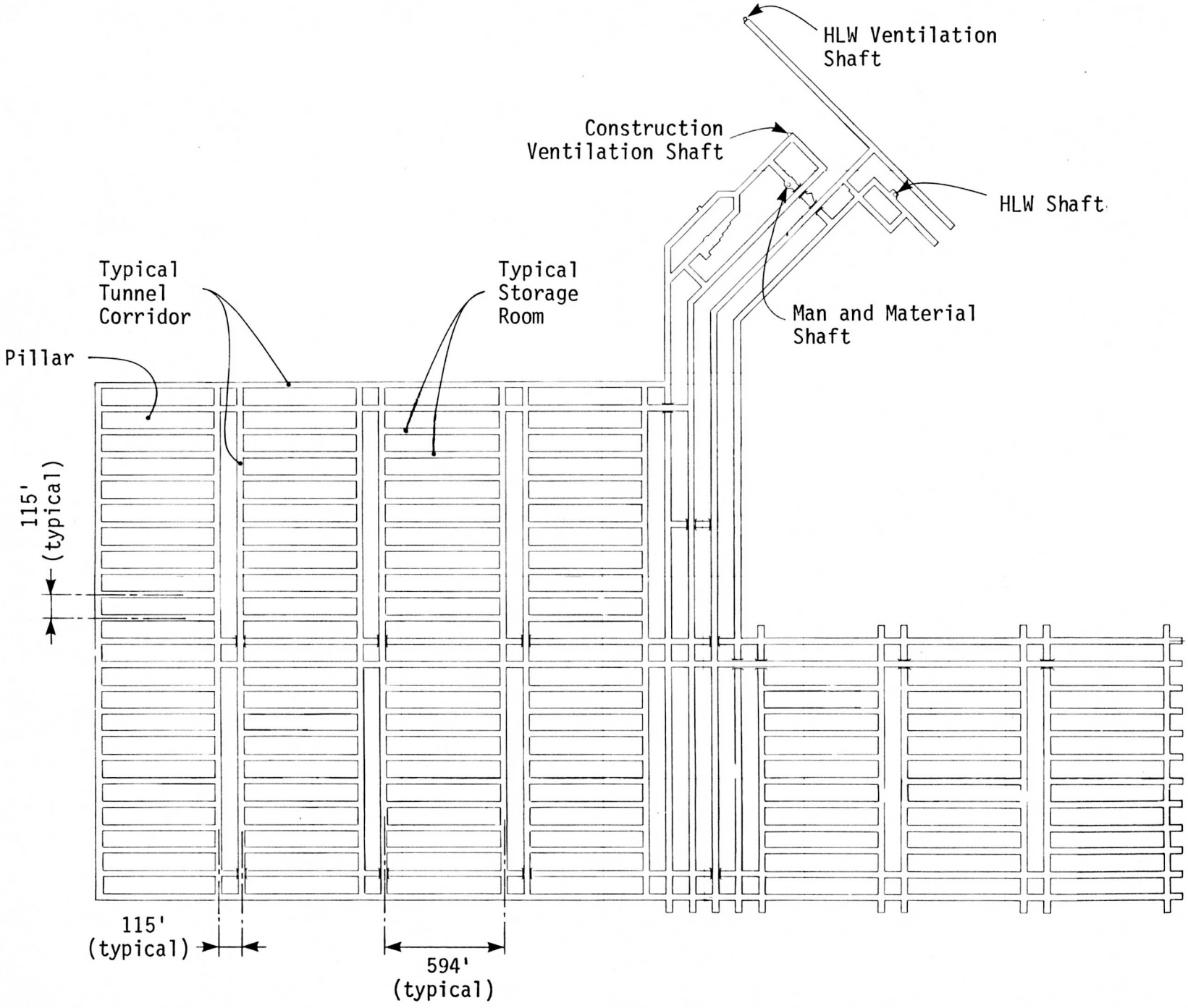

Source: Reference 5

FIGURE 2.8 PLAN OF THE ASSUMED UNDERGROUND FACILITY

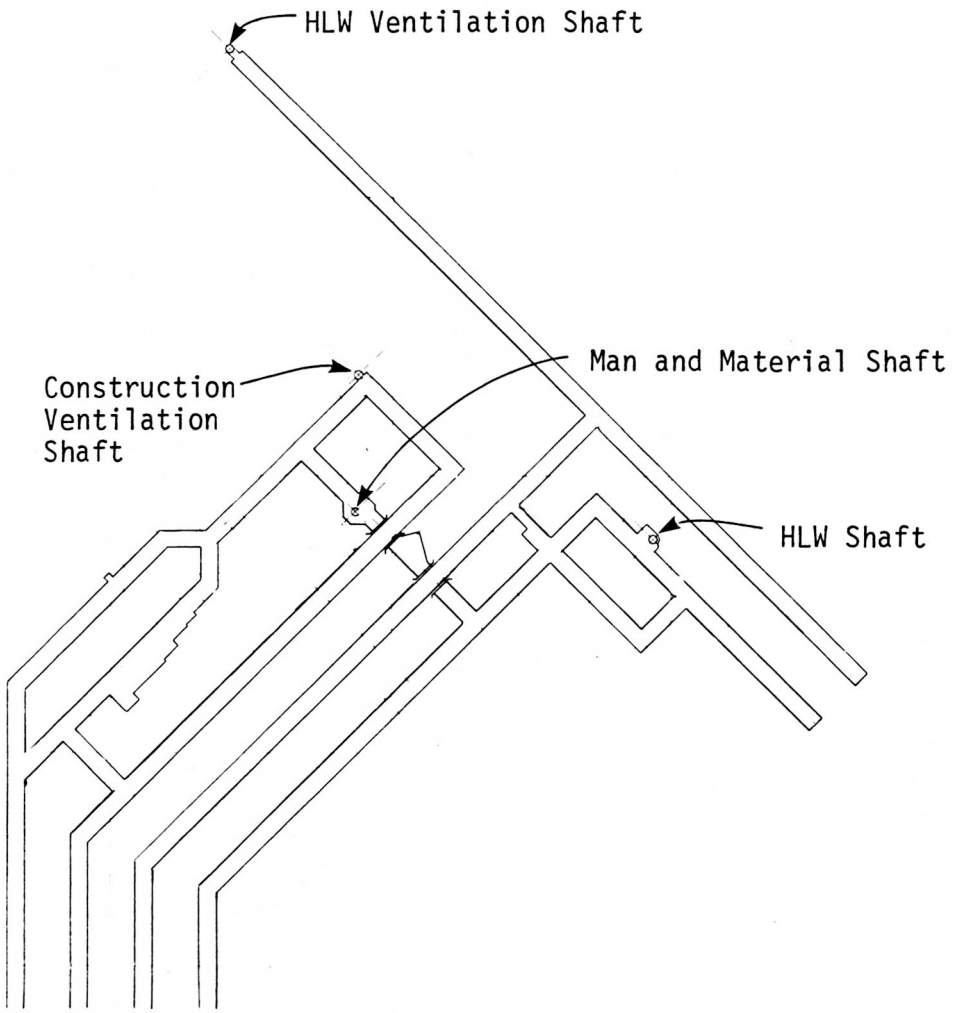

Source: Reference 5

FIGURE 2.9 PLAN OF THE HLW WASTE RECEIVING AND SHAFT AREA

2.5.1 HLW Shaft. The HLW shaft connects the clean cell of the HLW building with the transfer cell of the underground facility and is used to move HLW canisters. The general arrangement of the shaft is illustrated in Figure 2.10. Its design was governed by the sizes, configurations, and quantities of HLW receivals.[5] The shaft is assumed to have an inside diameter of 8 ft and to extend from the floor of the clean cell of the HLW building to 44 ft below the level of the underground facility. The underground transfer cell, shown in Figure 2.10, is an integral part of the HLW shaft. The cell is similar to the clean cell on the surface and has all equipment necessary for transferring the canisters from the shaft conveyance to the HLW transporter. The roof of the cell can withstand the loads imposed on it by the transporter during this operation.

2.5.2 HLW and Construction Ventilation Shafts. Two exhaust ventilation paths are required to separate the storage and construction exhaust airstreams. The HLW shaft is not used for ventilation because the large airflows would require extensive modification of the surface facilities and because the uncontaminated construction exhaust air would be passed through a potentially contaminated area. Therefore, two shafts for exhaust air are provided.[5]

The HLW ventilation shaft is assumed to have a 14-ft inside diameter; it connects the underground facility with the mine storage filter building, Figure 2.7. The construction ventilation shaft is also assumed to have an inside diameter of 14 ft; it connects the surface with the construction area of the underground facility. The uncontaminated air exhausted through this shaft by fans installed at the shaft collar at the surface is released without having been filtered.

2.5.3 Man and Materials Shaft. The man and materials shaft connects the surface with the underground facility and is used to move men and materials, remove mined materials, and supply fresh air. Its size is dictated by the amount of excavated material to be removed, the size of equipment to be lowered underground, and fresh air requirements for the underground level. It is the largest of the four shafts in the repository, with an inside diameter of 23 ft. A 130-ft extension of the shaft below the underground level is assumed for the skip-loading station.

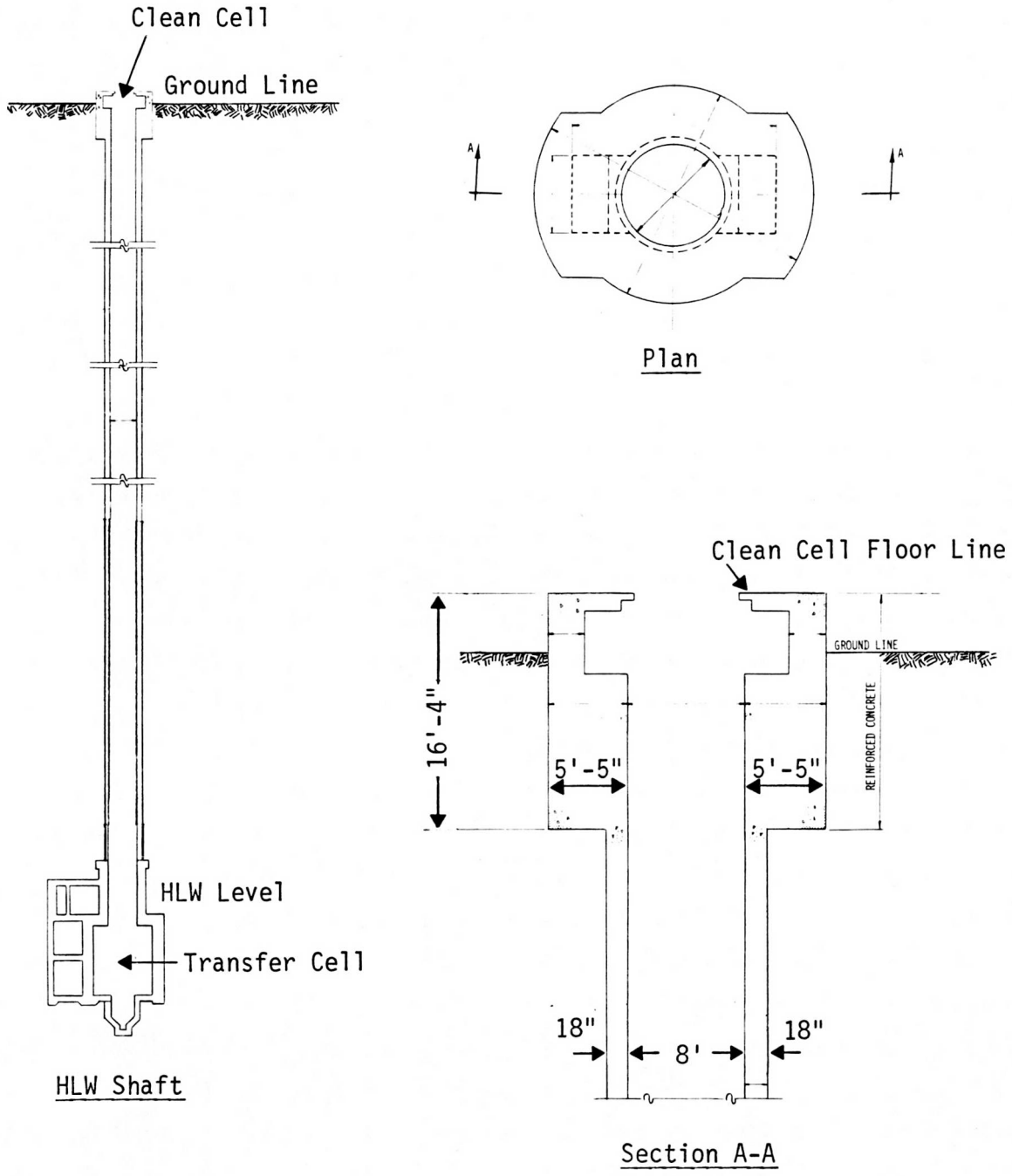

Source: Reference 5

FIGURE 2.10 GENERAL ARRANGEMENT OF THE HLW SHAFT

2.6 Underground Structures

In the context of this report, the underground structures are defined to be the tunnels and storage rooms located at the HLW storage level, which is assumed to be 2,000 ft below the surface. Review of the geological conditions at the four NTS candidate sites indicated that the desired geological formations extend to 2,000 ft or deeper below the surface at all but the alluvium site in Jackass Flats. The 2,000-ft depth was selected somewhat arbitrarily; however, it is representative of depths proposed in various bedded salt plant configurations.[3,5,6] The depth is also sufficient to affect the added costs for hardening the underground structures against ground motion because the relatively long vertical transport path somewhat increases the costs for transporting the hardening materials, such as shotcrete, steel sets, rock bolts, etc.

The underground facility (the HLW storage level) is reached by four shafts, as described in the previous paragraphs. It may encompass an area of several hundred acres. Although it is shown in Figure 2.8 to be arranged in a rectangular grid pattern, that pattern is not a requirement and does not affect the costs per linear foot of the tunnels. In general, the shorter tunnels of Figure 2.8 are the HLW storage rooms, whereas the larger tunnels are used for ventilation, access, and transport.

For the purposes of cost estimating, it is assumed that all of the tunnels, with the exception of some of those in the waste receiving area (see Figure 2.9), have an excavated (outside) diameter of 18 ft. Thus, the use of steel sets to support the tunnel walls would cause the clear diameter of the tunnels to be smaller whereas the use of rock bolts would leave the diameter essentially unchanged except for the small decrease in size that would result from surfacing with shotcrete. In order to simplify the cost estimating effort for the candidate sites, particularly in regard to the added cost for hardening, all tunnels were assumed to be circular rather than to have the horseshoe shape that is usually used in such construction. It was felt that this assumption would have a roughly equal effect on the costs for all candidate sites and therefore that the relative added costs for hardening would be valid. Further descriptions, details, and constraints of the structural configurations of proposed underground facilities can be found in References 3 and 5.

3. PRELIMINARY ENGINEERING GEOLOGY

Although the collection and reduction of engineering geology data were not part of the original scope of work, it was necessary to conduct such work for the design cost scoping studies. The amount of information required varies with the design level. For the purposes of the studies reported here, it was necessary to collect engineering geology information sufficient to provide a basis for preliminary tunnel designs that could then be hardened against the assumed ground motion. These data were collected from the extensive geologic data on the NTS that were available for three of the four candidate repository sites (essentially no data were available for Jackass Flats alluvium).

The four candidate repository sites, as shown in Figure 3.1, are:

1. Eleana shale, Syncline Ridge
2. Jackass Flats tuff, Skull Mountain
3. Climax stock granite, Quartzite Mountain
4. Jackass Flats alluvium, Jackass Flats

Appropriate data and information were collected from selected representative bore holes in the Eleana shale (well UE17e) and the Climax granite (well UE15f). Engineering geology information is not available on the Jackass Flats tuff; therefore, for the purpose of this report, the Tunnel Beds Formation (tunnel U12e.14 UG10) was evaluated as an example of typical ash-fall tuff. It was assumed that the data are applicable to the Jackass Flats tuff. As noted above, it was determined that appropriate engineering geology data on the Jackass Flats alluvium either did not exist or could not be found within the duration of this study. Because such data are necessary for the cost scoping studies of the tunnels, it was decided to discontinue further evaluation of this candidate material for the present cost scoping studies.

All of the well bore data that were collected were assumed to be generalized to the entire site. Furthermore, it was presumed that geologic conditions of varying favorability exist within a particular study material. The site-

Repository Sites:

Study Materials:

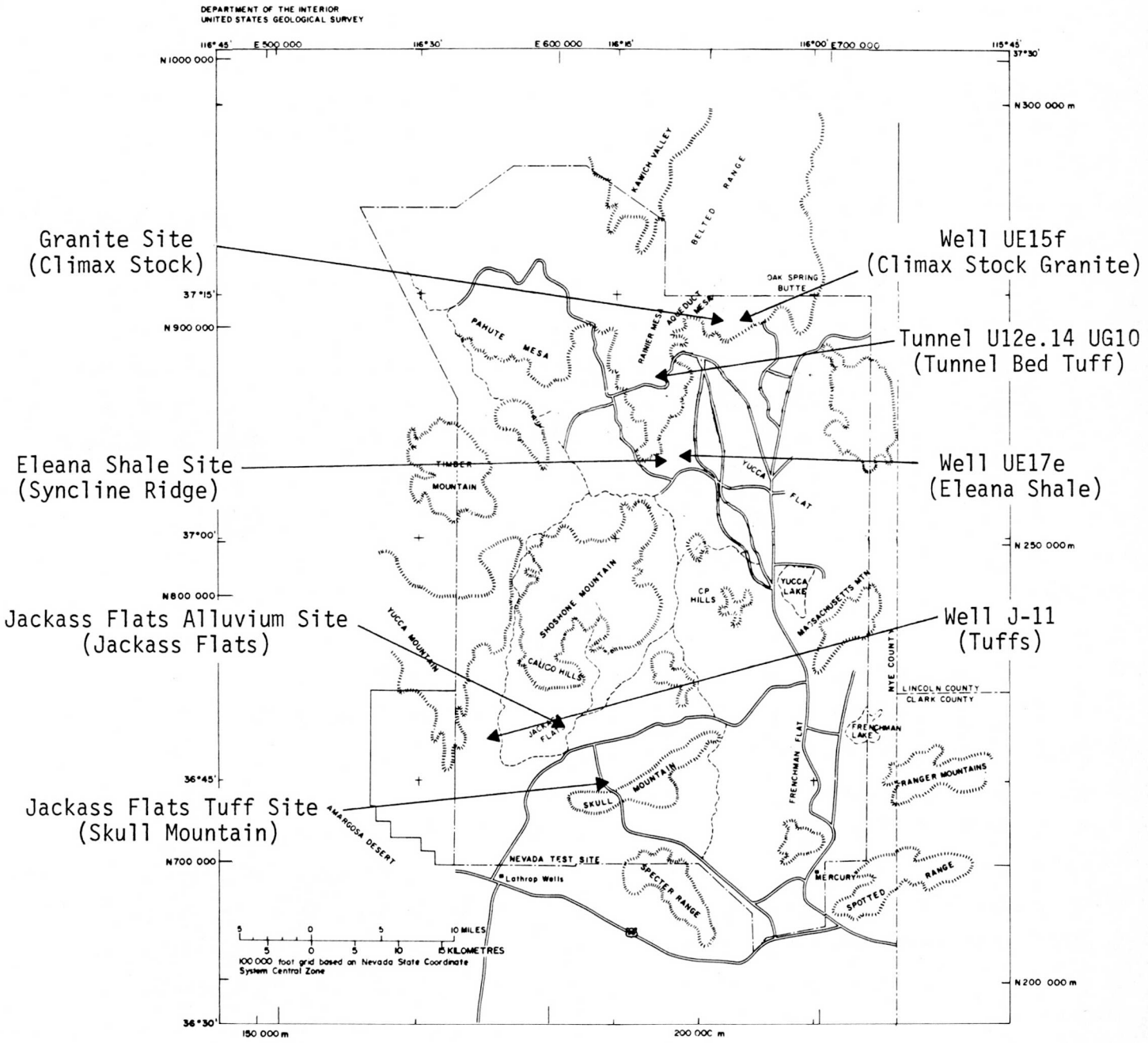

Source: U.S. Geological Survey

FIGURE 3.1 LOCATIONS OF CANDIDATE REPOSITORY SITES AND STUDY MATERIALS

specific data remain pertinent because it was assumed that the most favorable conditions are to be selected for the eventual repository site.

3.1 Geologic Profiles at the Candidate Sites

3.1.1 Eleana Shale Site. The proposed Eleana shale repository site is situated in the Syncline Ridge area (Figure 3.1). The site geological profile is composed of alluvium, Tippipah limestone, and Eleana Formation unit J. The proposed repository is in the argillite of the upper portion of the Eleana Formation unit J. A typical Eleana shale section is in well UE17e, as shown in Figure 3.2, at location coordinates N 853,205, E 646,448.

Well UE17e indicated that the Eleana Formation upper unit J is divisible into a quartzite and an argillite interval (Figure 3.2). The quartzite interval is composed of cyclical deposits of argillite (55% of the deposit), sillite (25%), and quartzite (20%) and is approximately 240 ft thick. The argillite is clay-rich and is dark gray to black, while the quartzite is yellowish and orange-brown to gray with coarse to silt-size quartz grains. The argillite interval at well UE17e is roughly 2,800 ft thick and is probably uniform throughout the Syncline Ridge area.[16] The argillite is very dark gray to black, massive, and clay-rich. It consists of alternating beds containing a high (greater than 20%) and low (less than 20%) quartz content that is uniformly distributed through the interval. Intervals of high- and low-quartz argillite range in thickness from a few inches to 12 ft. Throughout the argillite interval are 1/16-in. to 1/8-in. white quartz veins and 1/4-in. to 1/2-in. pyrite nodules and nodule clusters.

3.1.2 Tunnel Beds Tuff Site. This site, which was used as an analog for the Jackass Flats tuff, is on the east flank of Rainier Mesa. Rainier Mesa is a complex sequence of ash-flow and ash-fall tuffs deposited in hollows of a deeply eroded pre-Tertiary rock surface.[17] The Tertiary-age formation sequence is composed of the Tunnel Beds (formerly Indian Trail) and the Piapi Canyon. The Piapi Canyon Formation is subdivided into the Tonopah Spring and the Rainier Mesa members. The cited study material is from the Tunnel Beds tuff (tunnel bore hole U12e.14 UG10, located at coordinates N 886,327.42, E 632,297.04, at construction station 11+18, as-built bearing N 14°40'42" W; see Figure 3.2).

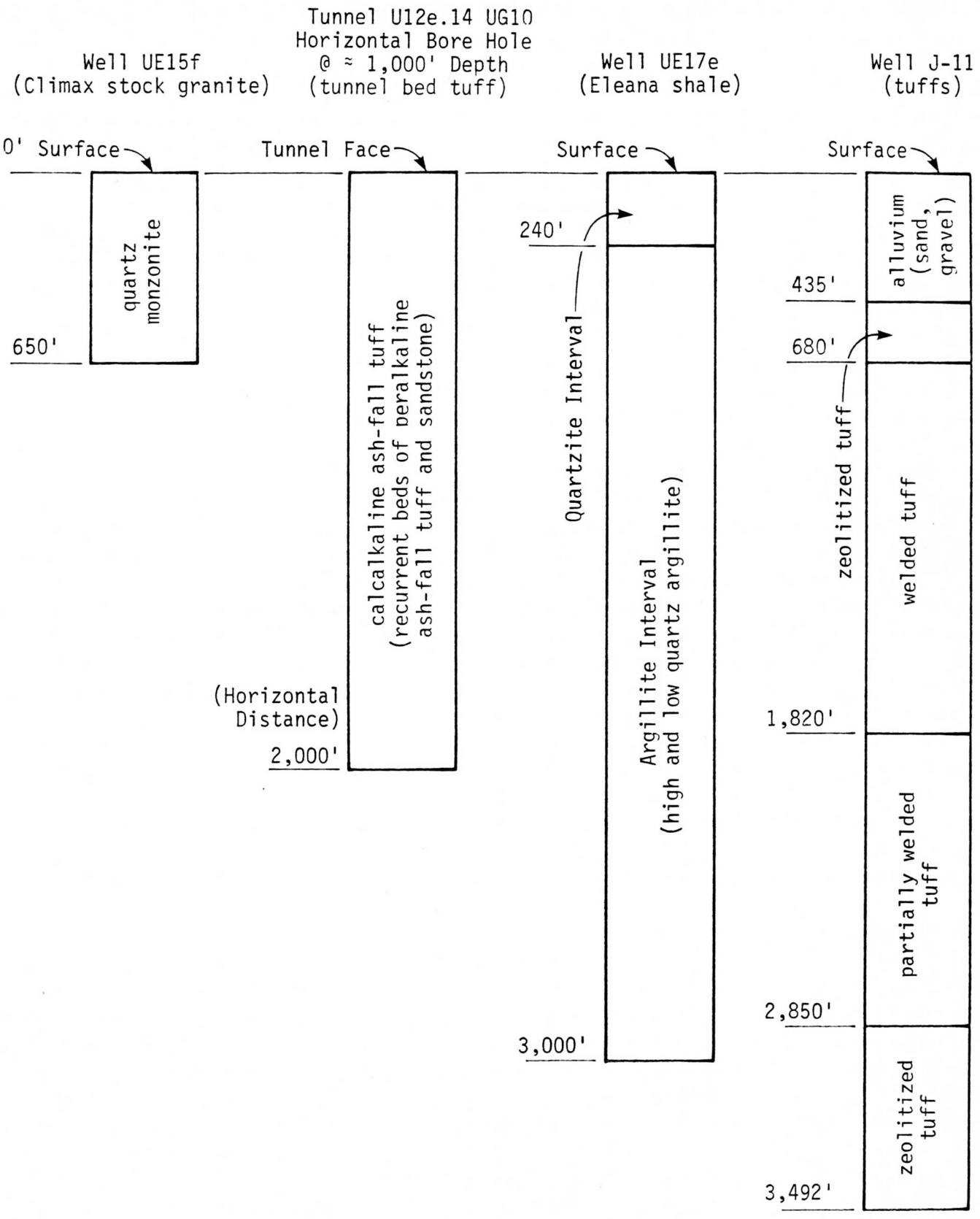

FIGURE 3.2 GEOLOGIC PROFILES OF THE STUDY MATERIALS

The Tunnel Beds tuff is approximately 1,000 ft thick at U12e.14 UG10, with a possible formation thickness of nearly 3,000 ft.[18] It is composed of a sequence of four ash-flow and ash-fall tuff units.[18] Tunnel bore hole U12e.14 UG10 was drilled 2,003 ft horizontally into an ash-fall tuff unit and penetrated a calcalkaline ash-fall tuff with recurrent beds of peralkaline ash-fall tuff and sandstone. This unit is described as: calcalkaline and peralkaline tuffs, periodically reworked; pale orange, pale yellow, and pink; zeolitized; occasionally argillized; and containing 1-in. to 2-in. white pumice lenses.[19]

3.1.3 Climax Stock Granite Site. The candidate Climax stock granite site is located at Quartzite Mountain. The Climax stock is described as a composite intrusive of older granodiorite and younger quartz monzonite, both cut by dikes and sills, and hydrothermally altered.[17] The candidate repository site is situated in the quartz monzonite represented by well UE15f (at coordinates N900,912, E 677,907).

Well UE15f penetrated 653 ft of quartz monzonite porphyry, which has a projected thickness of over 3,000 ft (Figure 3.2). The average composition of the quartz monzonite porphyry is quartz (28%), potassium and/or sodium feldspar (25%), plagioclace (40%), and biotite (6%). It is described as: light bluish gray; medium- to occasional fine-grained; composed of crystal of quartz, feldspar, and biotite (less than 3%) with sparse 1-in. feldspar phenocrysts; and slightly kaolinized feldspars.[20] Mineralization of iron oxide, manganese, pyrite, clay, and calcite is prevalent within discontinuities.

3.2 Engineering Rock Properties

The engineering rock properties of the designated repository site materials were evaluated with respect to those properties that are essential for the seismic analysis and the design and stabilization of the tunnels. The pertinent material properties are classified as to (1) rock type and (2) in-situ discontinuity properties. Rock type properties are concerned with the strength of the materials' composition, e.g., mineralogy, cementation, and slaking potential. The discontinuity properties of the rock mass are related to its in-situ strength. Examples of rock type and discontinuity relative interpretive scales are shown in Tables 3.1 and 3.2. For the purpose of this report,

TABLE 3.1
ROCK TYPE INTERPRETIVE SCALES[a]

Type of Field Test	Unconfined Compressive Strength (psi)	Hardness	Strength
Difficult to break into 4-in. pieces	20,000	Very hard, VH	Very strong, VS
Broken into 4-in. pieces with one hammer blow	8,000 to 20,000	Very hard, VH	Strong, S
Scraped or dented slightly with pick	2,500 to 8,000	Hard, H	Moderately strong, MS
Crumbled with pick, scraped with knife	1,000 to 2,500	Moderately hard, MH	Weak, W
Crumbled with fingers	< 1,000	Friable, F	Friable, F

[a]Adapted from Reference 21.

TABLE 3.2
DISCONTINUITY RELATIVE INTERPRETIVE SCALES[a]

Bedding	Joints	Bedding or Joints (per ft)	Spacing (in.)		Splitting
Massive	Massive	1	120	48	Massive
Wide	Wide	1 to 3	24 to 120		
Moderate	Moderate	3 to 9	12 to 24	24	Blocky
Close	Close	9 to 60	2 to 12	--	Slabby
Very close	Very close	60	2	2	Flaggy
				0.4	Shaly, platy
				0.08	Papery

[a]Adapted from References 21 and 22.

preliminary engineering rock properties were evaluated from cores, geophysical logs, and the available laboratory test analyses.

3.2.1 Preliminary Rock Type Properties. A summary of the significant preliminary rock type properties of the study materials is presented in Table 3.3.

Engineering properties for the Eleana shale were determined from field observations and laboratory tests of the core from drill hole UE17e. The limited data presented in Reference 23 on modulus of elasticity (E) and Poisson's ratio (ν) are associated with calculated dilatational wave velocities on the order of 5,000 fps (using the relationships given in Reference 24). Such wave speed values are low compared to velocity logs for drill holes UE1, UE16d, UE16f, and UE17e.[25] The dilatational wave velocities in the Eleana Formation range between 10,000 and 12,000 fps; a good representative value is 11,000 fps.[25] Average values for density and Poisson's ratio, 2.6 and 0.33, respectively, were obtained from laboratory tests on 15 samples from hole UE17e.[25] The modulus of elasticity calculated from these values was observed to be at the high end of the range of values reported from the same laboratory tests.

Engineering properties for the tuff were approximated from Reference 26 using only the zeolitized tuff samples as representative of an ash-fall tuff. The unconfined compressive strength was estimated from geologic field observations of the core samples. The range of values for strength is probably too great because the observed samples had dried out from their original in-situ state.

Hardness and relative strength for the granite site were obtained through field observations of core samples. Values for unconfined compressive strength, bulk density, modulus of elasticity, and Poisson's ratio were derived from Reference 27. Wave velocities were calculated from these values.

The Eleana shale rock type properties are different for the high- and low-quartz argillite.[23] The high-quartz argillite is harder than the low-quartz argillite, as noted in URS/Blume field observations. The low-quartz argillite slakes severely; the high-quartz argillite has a less significant slaking potential from environmental changes such as drying and wetting.

TABLE 3.3

ROCK TYPE ENGINEERING GEOLOGY PROPERTIES

Rock Materials		Hardness	Strength		Unit Weight (pcf)	Modulus of Elasticity (psi)	Poisson's Ratio	Dilatational Wave Velocity (fps)
			Relative	Unconfined Compression (psi)				
Eleana Formation: shale[a,b]	Low quartz	Friable	Friable	3,000 to 8,000	162	2.85×10^6	.33	11,000
	High quartz	Moderately hard	Weak					
Tunnel Beds Formation: ash-fall tuff[c,d]		Hard	Strong	8,000 to 20,000	122	1.70×10^6	.20	8,500
Climax Stock Granite: quartz monzonite[e]		Very hard	Very strong	14,000 to 40,000	165	7.32×10^6	.22	15,300

[a]From laboratory tests, Reference 25.

[b]From velocity logs, Reference 25.

[c]From URS/Blume field observations.

[d]From Reference 26.

[e]From Reference 27.

TABLE 3.4

ENGINEERING GEOLOGY DISCONTINUITY PROPERTIES

Rock Materials		Splitting	Bedding	Structure	Mineralization
Eleana Formation: shale	Low quartz	Flaggy	Massive	Cracked and flaked	Calcite
	High quartz	Slabby	Massive	Laminar	Quartz and calcite
Tunnel Beds Formation: ash-fall tuff		Blocky	Not apparent	Porous[a]	None
Climax stock granite: quartz monzonite		Blocky	Not apparent	Massive	None

[a]This property is specific to well U12e.14 UG10.

The Tunnel Beds Formation and the Climax stock granite appear to have high strength properties throughout the observed sections. However, the pumice lenses in the Tunnel Beds Formation are friable and indicate a possible deterioration after repeated drying and wetting.

3.2.2 Preliminary Discontinuity Properties. Representative preliminary discontinuity properties of the study materials are presented in Table 3.4.

The Eleana Formation argillite is considered to be highly fractured; the high-quartz argillite is fractured to a lesser degree than the low-quartz argillite. The rock is fragmented by fractures dipping 90° to the core axis and approximately 45° to the core axis. The 90° fractures are relatively rough and generally are filled with calcite or quartz. The 45° fractures are smooth to polished. Bedding is sealed and indistinct. Fissility is confined to the low-quartz argillite.

For the purposes of the work discussed in this report, the Tunnel Beds Formation and the Climax stock granite are regarded as competent and intact rock. Fracture spacing is from 24 in. to 48 in. The fractures are grouped 90° to the core axis and 30° to 60° to the core axis. All fractures are rough, with no apparent mineralization.

4. GROUND MOTION CRITERIA

4.1 Purpose

The purpose of this chapter is to describe the procedures and results of studies conducted to establish preliminary ground motion criteria to be used in the design cost scoping studies. While such preliminary ground motion criteria constitute essential input for the cost scoping studies, neither the assigned scope of work nor the time available for this study allowed any effort to be made to formulate definitive ground motion criteria for potential waste storage repositories.

The postulated peak ground motion accelerations were specified by Sandia. They were selected specifically for this study in order to give a range of strong ground motions on which to base comparative hardening cost estimates. The assumed peak ground accelerations (PGAs) used for this study for each of the three component directions are as follows:

1. From earthquakes -- 0.3g, 0.5g, and 0.7g
2. From UNEs -- 0.5g, 0.7g, and 1.0g

4.2 Criteria for the Surface Structures

Two ground motion criteria -- one for earthquakes and another for UNEs -- were formulated for the surface structures of the repository.

4.2.1 Design Response Spectra for Earthquakes. The response spectra selected for earthquakes are the standard response spectra for both horizontal and vertical earthquake components specified by NRC *Regulatory Guide 1.60*.[28] They are based on detailed studies of typical earthquake response spectra and are set at the mean-plus-one-standard-deviation level.[29] The spectra are illustrated in Figure 4.1 for 7% of critical damping. That damping corresponds to the damping that is generally used in reinforced concrete structures. The spectra are normalized to a surface PGA of 1.0g for scaling to the given PGAs (0.3g, 0.5g, and 0.7g for earthquakes). In conforming with *Regulatory Guide 1.60*, PGAs in the vertical and horizontal directions are assumed to be equal. The horizontal and vertical response spectra are

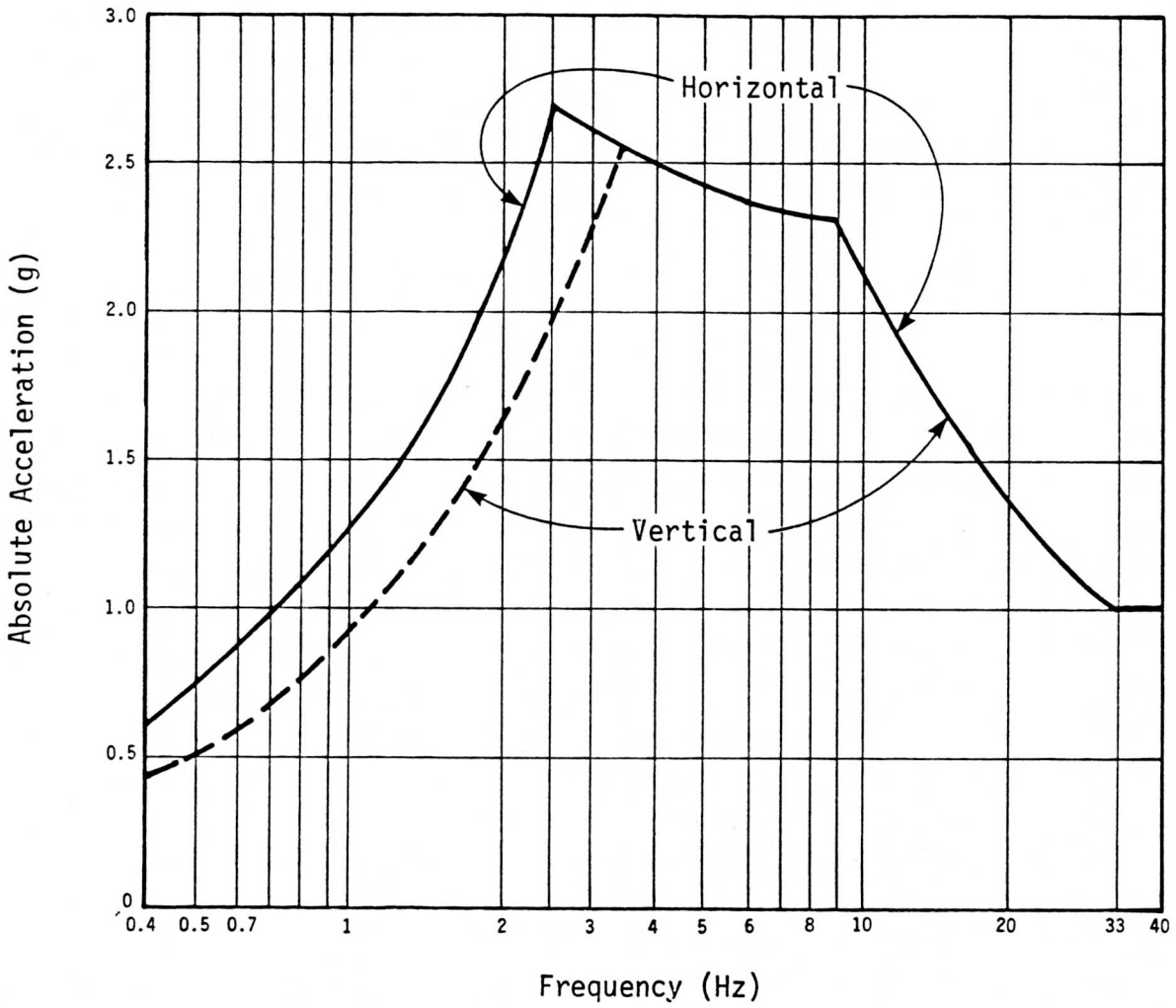

FIGURE 4.1 NRC *REGULATORY GUIDE 1.60* RESPONSE SPECTRA AT 7% DAMPING

different for frequencies below 3.5 Hz in that the vertical spectrum is approximately 2/3 of the horizontal spectrum.

It should be noted that the *Regulatory Guide 1.60* spectra are in general use for nuclear facilities. The current trend in the nuclear industry, however, is toward spectra developed specifically for the project site. It is expected that the final response spectra for a repository at the NTS will be site-specific, reflecting the geology, seismicity, and response characteristics of the soil and rock formation at the repository site.

Site-specific response spectra might be different from those assumed in this study. Differences would affect the design of surface structures and critical surface and underground mechanical systems and could result in either a decrease or an increase in costs. Additional studies would be necessary to determine the effect of site characteristics on the cost of the structures of the repository.

4.2.2 Design Response Spectra for UNEs. At stations removed some distance from the source, the recorded ground motions from UNEs produce spectra that, except in the longer periods, are similar in shape to those of earthquakes. Spectral displacements of UNEs for long periods are smaller than earthquake spectral displacements at the same PGA.[30] Consequently, with appropriate reduction at long periods, the spectral shapes shown in Figure 4.1 can be used for UNEs.

Because the surface structures in this study have natural frequencies in excess of 3.5 Hz (periods less than 0.29 sec; see Chapter 5), the spectral values of concern are not affected by a reduction in the long-period range. The earthquake spectra of Figure 4.1 are therefore used for UNEs in this study. The spectra are normalized to a surface PGA of 1.0g for scaling to the given PGAs (0.5g, 0.7g, and 1.0g for UNEs).

UNE response spectra are particularly sensitive to site-specific factors. The final UNE response spectra for a repository at the NTS are expected to be site-specific; therefore, they could be different from those assumed in this study. Just as with earthquake response spectra, different UNE response spectra could result in changes in costs.

4.3 Criteria for the Underground Structures

Separate ground motion criteria were formulated for use in the analysis of the tunnels and the shafts. The criteria are consistent with the current state of the art for tunnel design. The ground motion criteria utilized in this report for underground structures should be considered to be preliminary.

4.3.1 Attenuation of Seismic Motion with Depth. The literature on the relationship between earthquake motion and its intensity at depth below the free surface was reviewed.[31-37] The studies reviewed indicate that, in general, motion attenuates with depth. There are situations, however, in which instrumental and observational motions underground have been found to be as strong as (and sometimes stronger than) those on the surface.[31,34] Such findings are an indication of the general complexity of this phenomenon. No simple statement can be made to describe the effect of depth upon seismic motion.

The seismic motion at a particular depth consists of the superposition of the several body and surface waves. The motion at that point will reflect whatever seismic energy is present: body waves traveling directly from a seismic source, body waves reflecting off the Moho or other high-impedence contrast surface, body waves reflecting from the free surface or from some other interface below the surface, or surface waves.

The most complete, or ideal, seismic motion characterization for use in underground structure analysis would be a three-component time history of motion that includes the superposition of these waves. Such a rigorous approach for characterizing seismic ground motion at depth is technically possible but requires detailed and elaborate analyses. The time constraints and budget of this preliminary study did not permit such an effort. For these reasons, the possible attenuation of motion with depth was ignored, and a simple approach was adopted for the investigation of stresses and strains at depth (see Chapter 6).

The decision to ignore depth effects does not affect the cost scoping results significantly. The seismic stresses and strains determined without considering possible depth reduction were not used in a strict quantitative fashion to project incremental hardening requirements for the different ground motion

acceleration levels (see Chapter 6). Instead, these dynamic stresses and strains were treated as indicators of possible tunnel damage.

4.3.2 Peak Ground Motion. During ground motion, the tunnels and shafts of the repository will deform with the surrounding medium. Conservatively, they may be analyzed for the peak ground values of acceleration and velocity. (The relative displacement between points is of concern rather than the actual displacement of each point. Because particle velocity is a measure of relative displacement for simple wave motion, peak ground displacements are not required.) Peak ground motion values from earthquakes have been reported in several of the studies[29,38-40] used to develop the standard NRC response spectra.[28] The data from these papers were used to provide a convenient point of reference; there is no assumption that peak ground motion need be associated with existing NRC regulatory guides.

The maximum ground velocity for horizontal motion assumed for this work, scaled to a maximum PGA of 1.0g, is approximately 48 in./sec. This value constitutes an approximate average for a number of surface records on alluvium; it should be significantly reduced for competent crystalline rock.[40] A more recent study[41] investigates further the effect of different soil conditions on response spectra. From that study and from geological information presented in Chapter 3, it was assumed that the alluvium value should be used for the Eleana shale, with a reduction of 30% for the tuff and granite sites.

The peak vertical ground acceleration is often taken as 2/3 of the peak horizontal acceleration, a ratio that also generally agrees with Reference 41. Therefore, it is assumed that the peak vertical ground velocities are 2/3 of the horizontal values. The appropriate values for ground velocities are listed in Table 4.1 for 1.0g. Values for 0.3g, 0.5g, and 0.7g are linearly scaled from this table.

The appropriate values for peak ground velocity and displacement need further research. The studies cited above investigated earthquakes with a broad range of PGA levels -- generally less than 0.5g. The average values were then linearly scaled to 1.0g. Further study would be needed to confirm that peak particle velocity does scale linearly with g-level.

TABLE 4.1

ASSUMED PEAK GROUND VELOCITIES FOR 1.0g PEAK HORIZONTAL GROUND ACCELERATION

Rock Formation	Velocity in the Horizontal Direction (in./sec)	Velocity in the Vertical Direction (in./sec)
Eleana shale	48	32
Tuff and granite	34	22

The effect that possible nonlinear behavior of the materials would have on peak particle velocity raises another question that needs to be addressed at some future time. For example, strain calculations for the Eleana shale (see Section 6.5) imply that the particle velocity of 48 in./sec will cause extensive fracturing. Clearly, if this is the case, the energy will dissipate over some finite distance, and the wave will become elastic with a much smaller particle velocity. This consideration could be used to advantage in a site-specific analysis, permitting smaller peak ground velocities near the repository.

5. ANALYSIS OF THE SURFACE STRUCTURES

5.1 Analytical Assumptions

Only Category I structures were addressed in these analyses. The structures are of reinforced concrete and are of the shear-wall type. Massive 18-in.-thick exterior shear walls are assumed in order to provide protection against tornado-generated missiles. Consequently, these structures are relatively stiff and strong.

Simplified analyses were conducted to determine the approximate frequencies of the structures. After the frequencies were estimated, the spectral acceleration values and corresponding seismic forces and stresses were determined. Analyses were also conducted to determine the approximate stresses caused by torsion of the structures.

5.2 Seismic Analysis

Seismic analysis of the surface structures consisted of engineering calculations that were performed by hand and were based on conservative assumptions; no computer programs were used. The following procedure was applied:

1. The basic configurations shown in Figures 2.2 through 2.7 and in Reference 5 were used. Simplifications in the layout and the geometry of some shear walls were made in order to allow hand calculation.
2. Transverse and longitudinal horizontal shear wall areas, A_s, were computed for each direction for each of the structures. The shear area was assumed to be 5/6 of the gross wall area.
3. The structural weights were estimated from the assumed configurations. Weights for the major equipment items were assumed and were added to the structural weights to give the total weight of each structure, W. The center of mass of each structure was also computed.
4. The frequencies, f, and periods, T (sec), for each direction of the structures were computed with the simplified formula given in Reference 43 for shear-wall buildings:

$$T = \frac{0.05H}{\sqrt{D}} \text{ and } f = \frac{1}{T}$$

where:

H = the height of the structure (ft)

D = the width of the structure in the direction of the assumed earthquake motion (ft)

5. The base shear coefficient was assumed equal to the spectral acceleration, S_a, for the appropriate structural frequency at 7% of critical damping from response spectra[28] normalized to the appropriate PGA level.

6. The total base shear, V, was computed as:

$$V = S_a W$$

7. For individual walls, the amounts of shear, bending, and total displacements were assumed to be:

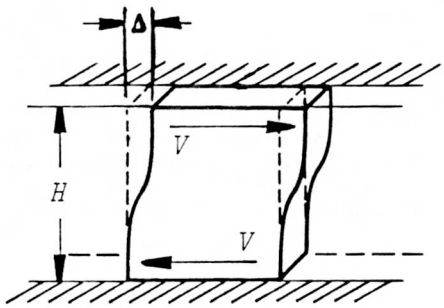

$$\text{Shear displacement} = \Delta_s = \frac{6VH}{5AG}$$

$$\text{Bending displacement} = \Delta_b = \frac{VH^3}{12EI}$$

$$\text{Total applied displacement} = \Delta = \Delta_s + \Delta_b$$

where:

V = resultant shear force

H = vertical wall height

A = horizontal wall area

I = moment of inertia of the wall

E = modulus of elasticity

G = shear modulus

These displacements were based on the assumption that the walls are fixed, both at the top and at the bottom. From these displacements, the absolute lateral stiffness of the ith wall due to bending and shear was calculated:

$$K_i = \frac{12EI}{H^3} + \frac{5AG}{6H}$$

where the following concrete material properties were assumed:

f'_c = 4,000 psi

E = 3,600,000 psi

G = 1,440,000 psi

and where f'_c is the specified compressive strength of concrete in psi.

8. The center of rigidity of each structure was then computed from the calculated wall stiffnesses, K_i.

9. The horizontal shear that is resisted by each individual shear wall was computed from:

$$V_x = \left(\frac{K_x}{\Sigma K_x}\right) V_x + \left(\frac{K_x y}{J_r}\right) V_x e$$

$$V_y = \left(\frac{K_y}{\Sigma K_y}\right) V_y + \left(\frac{K_y x}{J_r}\right) V_y e$$

where:

K_x = lateral stiffness of wall along the x-direction

K_y = lateral stiffness of wall along the y-direction

x or y = perpendicular distance from the center of rigidity to the axis of a particular wall

J_r = rotational stiffness of all walls

= $\Sigma(K_x y^2 + K_y x^2)$

V_x = total base shear in the x-direction

V_y = total base shear in the y-direction

e = distance between the centers of mass and rigidity (stiffness)

10. Finally, the average shear stresses, v, of the walls were computed from:

$$v = \frac{V}{\phi t l}$$

where:

ϕ = 0.85[42]

t = thickness of the wall

l = length of the wall

11. The total allowable design shear stress, v_u, at any section was limited to[42]:

$$v_u \leq 10\sqrt{f'_c} = 630 \text{ psi}$$

12. If the results of step 10 indicated that v exceeded v_u, the exterior shear wall thickness, t, was increased, and steps 7 through 10 were repeated until satisfactory stresses were computed.

Thus, the increased thickness of the exterior shear walls was assumed to be the only parameter that would be necessary for estimating the hardening costs of the surface structures. It was assumed that other details, such as the connections between the horizontal diaphragms and the vertical shear walls, would not be significantly affected.

5.3 Results

Table 5.1 summarizes the results of analysis of the surface structures. The table also lists the various controlling and assumed structural dimensions (wall, roof, and slab thicknesses). The incremental costs are given in terms of the additional cubic yards of reinforced concrete that are required to harden the given structure to the given PGA level.

The HLW building is the only structure that requires additional hardening in order to be strengthened up to 0.7g. The HLW building and the emergency power building are the only buildings that require strengthening to bring their design to the 1.0g PGA level.

Thus, in general, the seismic design of the surface structures is largely governed by the tornado-hardening requirements for licensable Category I structures. Additional seismic hardening for earthquake motion is necessary for only one building, whereas two buildings require additional hardening against the upper-limit ground motion of UNEs.

The added costs for hardening are presented in Chapter 8.

TABLE 5.1

SUMMARY OF ASSUMED STRUCTURAL DIMENSIONS AND INCREMENTAL QUANTITIES OF CONCRETE REQUIRED TO HARDEN THE SURFACE STRUCTURES

Structure	Thickness of Elements[a]	Incremental Cost in Cubic Yards of Concrete				Remarks
		PGA[b]				
		0.3g	0.5g	0.7g	1.0g	
HLW building	Shipping and receiving: walls 12 in., roof 12 in. Cells: walls 48 in., roof 48 in. Other: walls and roof 18 in., floors 12 in.	none[c]	none	100	300	--
Control room building	Roof 18 in., walls 18 in.	none	none	none	none	Control room is separate from administration building
Emergency power building	Roof 18 in., exterior walls 18 in., interior wall (radiator) 18 in., other interior walls 12 in.	none	none	none	50	--
HLW hoist building	(All underground)	none	none	none	none	Assumed adequate by inspection
Suspect waste and laundry building	Exterior walls 18 in., roof 18 in.	none	none	none	none	--
Mine storage filter building	Exterior walls 18 in., interior walls 12 in., roof 18 in., floor 12 in.	none	none	none	none	Stack is separate from building[d]
Water pumphouses	(All underground)	none	none	none	none	Assumed adequate by inspection

[a]For other dimensions, see Chapter 2.

[b]PGA refers to the peak ground acceleration on a typical response spectrum curve; 1.0g is the acceleration of gravity (32.2 ft/sec^2).

[c]Tornado hardening design governs wherever "none" appears.

[d]No analysis of the 98-ft-high stack was conducted because the available preliminary structural design data were insufficient.

6. ANALYSIS OF THE UNDERGROUND STRUCTURES

6.1 Introduction

The underground structures require a methodology for seismic analysis that is entirely different from that available for the surface structures. The detailed and time-consuming calculations required for rigorous seismic analysis of deep tunnels are not appropriate to this preliminary study. Furthermore, the current state of the art for static tunnel design is largely empirical; detailed calculations of stresses and strains are not used in specific stabilization evaluations. Therefore, simple seismic analyses were used to formulate a general engineering evaluation of the magnitudes of the seismic stresses and strains relative to the in-situ ultimate stresses and strains of the medium.

From the outset of the study, it was expected that additional hardening features would require an engineering evaluation of the effects of seismic motion on the stability of the tunnels rather than being based solely on the addition of the seismic stresses and strains to the basic design. Therefore, in addition to the analytical approach, a practical and experience-oriented state-of-the-art approach was initiated. Dr. Tor Brekke, Professor of Geological Engineering, University of California, Berkeley, and Mr. George E. Wickham of Jacobs Associates, San Francisco, California, were engaged as consultants at an early stage of the project to assist URS/Blume in developing this effects evaluation program.

6.2 Literature Pertaining to Underground Seismic Analysis

The literature was surveyed to obtain pertinent information for estimating seismically induced stresses and for formulating empirical criteria for seismic effects in the rock around underground openings. The analysis and design of an underground structure requires a prediction of the seismic motion to which the structure will be exposed. A refined seismic analysis requires a degree of detail precluded by the preliminary nature of this study. Furthermore, there are limitations in underground engineering that prevent the effective use of such analysis. For these reasons, the literature review was not exhaustive. The following discussion summarizes material that was reviewed.

A fairly large body of literature describes criteria and procedures for the analysis of underground structures that are more rigid than the emplacement medium, such as submerged trench-type tunnels that are placed in clay and soft soils. One approach (the seismic deformation analysis) assumes a sinusoidal shear wave propagating through the soil, inducing bending, shearing, and axial deformations in a tubular tunnel structure.[44-47] Strains are obtained by simple procedures from the mechanics of solids. Another approach (the seismic response analysis) develops a mathematical model of the soil-tunnel system (lumped masses, springs, and dashpots) or an experimental model for a shaking table, and then subjects the model to an earthquake time history.[46,48-51] Both of these approaches analyze the stresses in the tunnel liners.

Neither of the above analyses addresses the kind of tunnel envisaged for a waste repository. The repository tunnels will be excavated through rock and will require conventional stabilization methods, which generally will result in either a very flexible lining or no lining at all. Consequently, these approaches are not directly applicable to the repository tunnels with the exception of the thick concrete liners in the vertical shafts. No studies were found that analyzed strains due to seismic deformations along the longitudinal axis around openings in rock.

The literature discusses stresses around a cavity created by a plane wave propagating normal to the tunnel axis.[32,52-54] This motion causes deformations to the cross-sectional shape. Reference 32 presents expressions for stresses around a circular opening derived from two-dimension elastic wave theory using a sinusoidal shear wave with a wavelength that is large compared to the diameter of the cavity and concludes that liners will generally withstand an earthquake more effectively if they are resilient rather than rigid.

Reference 52 investigates an opening in rock using two-dimensional finite elements with earthquake time histories and concludes that seismic stresses are much smaller than the strength of granitic rock. Openings in homogeneous rock are found to have a fairly high degree of safety against earthquakes; however, the nature and extent of the rock jointing clearly influence the seismic safety.

Reference 54 studies the effect of plane dilatational and shear pulses on lined cylindrical cavities, using both classical and finite-element technology. If the liner is very stiff compared to the surrounding medium, the maximum dynamic hoop stress (due to a propagating stress pulse) will be approximately 10% to 20% larger than the equivalent maximum static hoop stress (due to a uniform stress field equivalent to the pulse). However, if the liner is very soft compared to the surrounding medium, the equivalent static hoop stresses are larger than the dynamic and provide conservative values. Reference 54 also studies so-called ringing and finds that it occurs around circular cavities only when the wavelengths are less than the radius.

Observations of earthquake and blast damage related to particle velocities or to accelerations form an important body of information in the literature.[55-58] Reference 56 reports that the limit for the fall of rock in unlined tunnels occurs for particle velocities of approximately 12 in./sec: "Unlined tunnels rarely experience visible damage at ranges where the free-field ground motions are on the order of 1-2 ft/sec, unless a loosened piece of rock is detached from the roof by the shaking." Reference 57 studies the response of 71 tunnels to earthquakes. No damage is found for peak surface accelerations below 0.19g; minor damage is observed for peak surface accelerations between 0.19g and 0.5g. The study concludes that "... tunnels are less susceptible to damage from shaking than aboveground structures at the same intensity level as determined from surface motions." Reference 58 reports the same findings in a more detailed fashion.

6.3 Characterization of Underground Seismic Motion

The following brief description of underground seismic motion is presented to assist in understanding the simple seismic stress analyses and the engineering evaluation of seismic effects employed in this study.[32,59-62]

6.3.1 Effects of Wave Types. Body waves, consisting of dilatational waves and shear waves, account for a significant portion of the seismic energy propagating at a particular point of depth. Body waves may arrive at that point along a number of paths: directly from the seismic source; as a reflection from the Mohorovicic discontinuity or other high-impedance contrast surface; as a reflection from the free surface; or as a reflection and refraction from interfaces below the surface. Thus, the body waves arriving

at a particular point will have been strongly influenced by the structure of the media intervening between the source and the point in question.

Plane dilatational waves (referred to as primary waves or simply as P-waves) propagate with velocity V_p and with particle motion parallel to the direction of propagation. The state of strain created by this wave is characterized by axial strains parallel to the propagation axis and by the absence of axial strains normal to that axis,[60] as illustrated in Figure 6.1b. Plane shear waves (referred to as secondary or S-waves) propagate with velocity V_s and with motion transverse to the direction of propagation. S-waves create shear strains, as illustrated in Figure 6.1c. It is convenient to characterize shear waves as horizontally (SH) and vertically (SV) polarized.

Surface waves may also account for a significant portion of the seismic energy at a particular point of depth. Rayleigh waves, one of the important types of surface waves, consist of displacements in a vertical plane, with vertical components (both up and down) and horizontal components (forward and backward) parallel to the direction of propagation.[61] Shape functions for the components are illustrated in Figure 6.2. The Rayleigh particle motion is basically elliptic and, in the classical solution for the elastic half-space, is retrograde at the surface. The velocity V_R of the Rayleigh wave is given approximately by $V_R \simeq .9\ V_s$. Surface waves also contain Love waves, which are horizontally polarized plane shear waves.[62] Love waves arise only when one or more layers of soil or rock of different composition exist over the base rock. These waves do not exist in the classical elastic half-space as do the Rayleigh waves. The proper characterization of surface waves is dependent upon the layering of soil and rock. This affects the generation of the Love wave and determines the modes for the Rayleigh waves.

The motion recorded at a single point below the ground surface can include all of these waves simultaneously. Dilatational and shear waves arrive from many directions as the result of multiple reflections from strata interfaces and from the ground surface. The record may reveal points in time at which the major dilatational and shear waves arrive; however, many such waves are arriving at different times and are being superimposed upon each other. The effects of surface waves are also being recorded along with the body waves although they begin to arrive somewhat later.

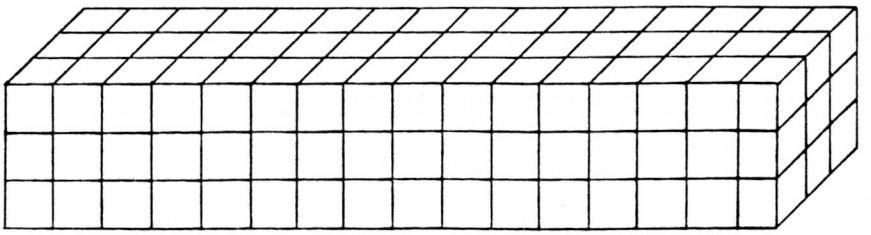

(a) Undeformed Ground

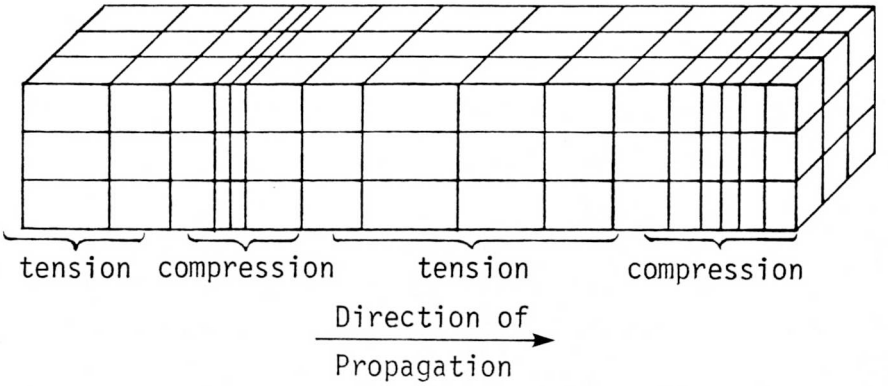

(b) Axial Deformation Due to P-Wave

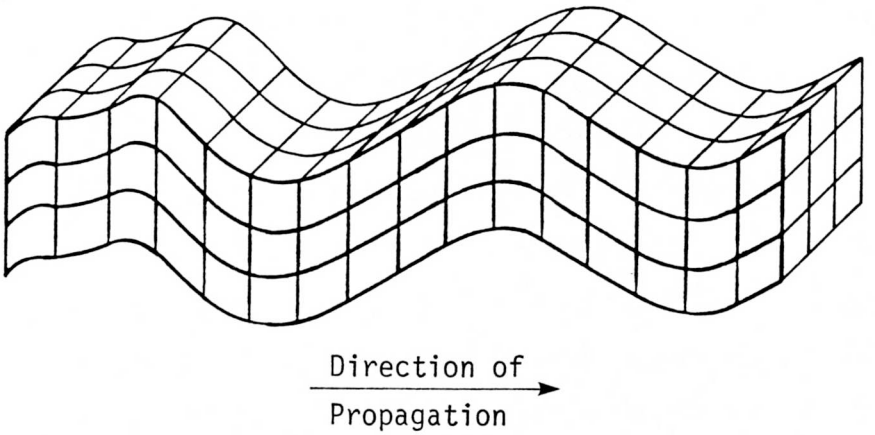

(c) Shear Deformation Due to S-Wave

FIGURE 6.1 DEFORMATION DUE TO BODY WAVES

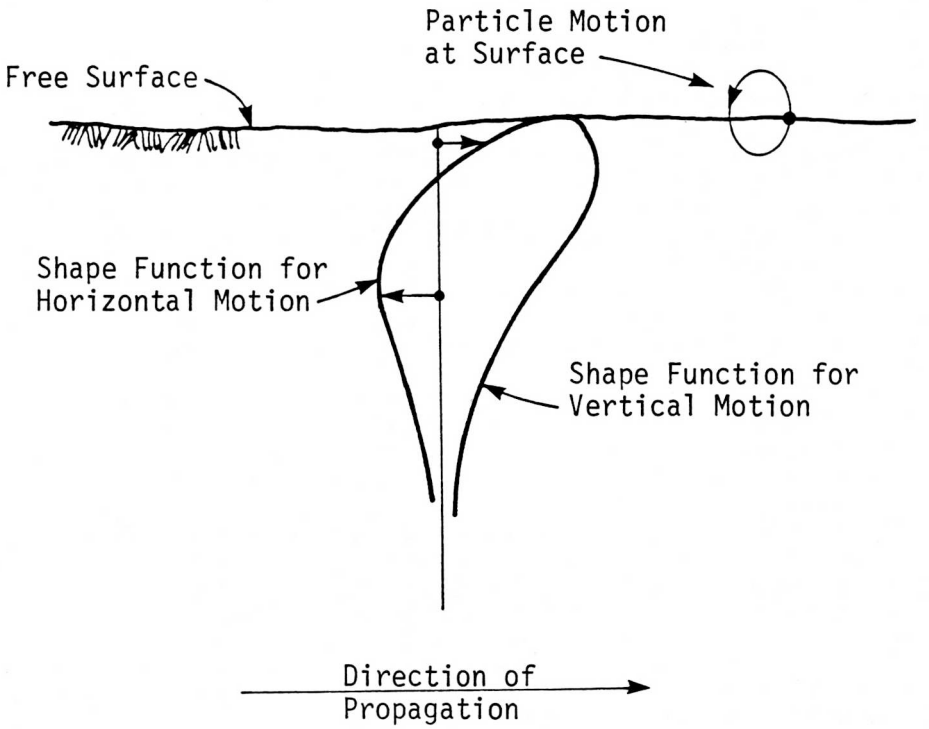

FIGURE 6.2 MOTION DUE TO RAYLEIGH WAVES

Time histories of the three components of motion at a given point contain all of these types of waves. For strong-motion records (i.e., at near field), it is difficult to discern the arrival time of each type. It is also currently impossible to resolve the motion into individual waves having specific amplitudes of motion.

6.3.2 Characterization for This Study. A rigorous approach to the prediction of seismic motion for deep tunnels requires consideration of the various wave types described above. Such seismic characterizations necessitate detailed and time-consuming analyses, which are not appropriate to the time constraints of this study. In addition, the current state-of-the-art technology for static tunnel design is largely empirical. Tunnel stabilization does not rely on detailed calculations of static stresses and strains. Consequently, simple seismic analyses are more useful to make a general engineering determination of appropriate tunnel-hardening procedures.

In the simplified but conservative approach employed in this study for the calculation of strains and stresses at depth, dilatational and shear waves were superimposed in various combinations in order to obtain the highest possible strains. The peak particle velocities of the various waves were added to produce the three components of peak particle velocities that a recording device might experience. (Peak particle velocities are outlined in Table 4.1.)

The vertical shafts may be strongly affected by surface waves. However, analysis of such effects requires extensive information both on the geology of the medium between source and receiver and on the magnitude of the surface waves. For the purposes of this study, simple analyses with large-magnitude body waves were employed to derive conservative estimates of strains in the shafts.

6.4 Effects of Seismic Motion on Tunnels

Seismic motion may affect the stability of a tunnel. The rigorous evaluation of tunnel behavior depends on the tunnel geometry, geology, and wave characterization. However, for this study a more general engineering approach was used to describe the mechanics of tunnel response. The importance of the various seismic effects was evaluated in an engineering context. This ap-

proach assumes plane waves propagating through an isotropic, homogeneous, elastic medium.

The effects of seismic motion on tunnels (lined or unlined) may be viewed as three principal types of deformation. Axial displacements that vary along the tunnel axis create axial strains parallel to the tunnel wall. Transverse displacements that vary along the tunnel axis deform an originally straight axis into a curved line. In addition, transverse displacements that vary over the cross section distort the cross-sectional shape. These three conditions are referred to as axial deformation, curvature deformation, and hoop deformation, respectively. Relative displacements are the only displacements of interest. Displacements that are constant along the tunnel axis or over the cross section simply impart rigid body motion whereas relative displacements cause strain.

Axial deformations develop when a P-wave propagates either parallel or obliquely to the tunnel or when an S-wave propagates obliquely. Alternating regions of compressive and tensile strain travel as a wave train along the axis, as shown in Figure 6.3. The dynamic strains are additive to the existing static strains in the rock and tunnel liner (if liner is present) and can cause several possible failure modes. Dynamic compressive strain added to static compressive strain could cause crushing of the rock or liner if the total strain exceeded the ultimate compressive strength of the materials. (A refined analysis would consider the triaxial state of strain and use the appropriate failure theory.[63,64]) Even at lower compressive strain levels, spalling may occur in an unlined tunnel because of local buckling of rock material. When the dynamic tensile strain exceeds the existing static compressive strain, intact rock may rupture or existing rock seams may open, allowing a momentary loosening of rock blocks and a potential fall of rock from the tunnel roof.

Curvature deformations develop when an S-wave travels parallel or obliquely to the tunnel axis or when a P-wave travels obliquely. This creates alternate regions of negative and positive curvature propagating along the tunnel. A tunnel liner that is very stiff compared to the surrounding soil responds as an elastic beam. With reference to Figure 6.4, for positive curvature, the liner will be in compression on the top and in tension on the bottom. This situation is assumed in much of the literature on seismic de-

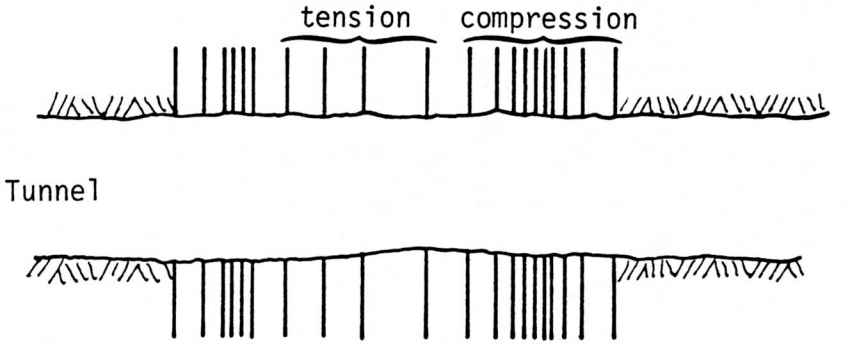

FIGURE 6.3 AXIAL DEFORMATION ALONG TUNNEL

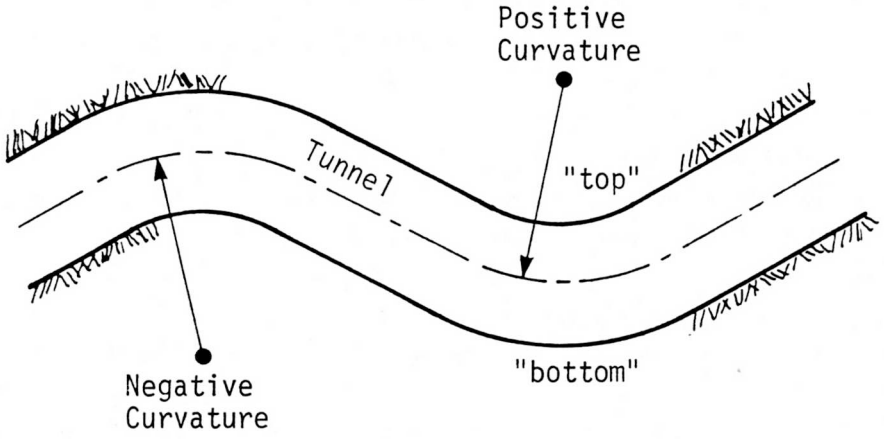

FIGURE 6.4 BENDING DEFORMATION ALONG TUNNEL

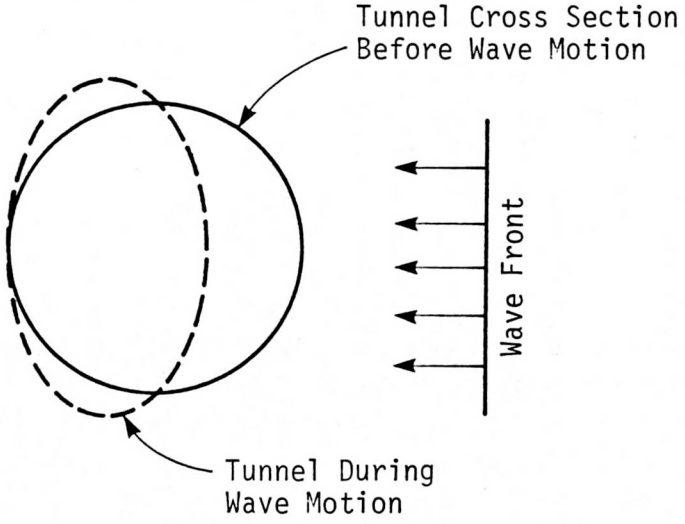

FIGURE 6.5 HOOP DEFORMATION OF CROSS SECTION

sign of tunnels.[44-51] However, it is not true for tunnels with flexible linings or no linings at all; in these cases, the tunnel in positive curvature experiences tensile strains on the top and compressive strains on the bottom. No simple theory (such as the Euler-Bernoulli theory for the deflection of elastic beams[65]) exists for the determination of these strains in an unlined tunnel. These axial strains are due to the presence of the free surface of the tunnel wall within the rock mass.

The possible tensile or compressive strains due to curvature in unlined tunnels are negligible in the context of this study. Without the presence of the tunnel, the rock would deform in pure shear because of the transverse displacements. Assuming that the dimensions of the rock mass in motion are extremely large in comparison to the diameter of the opening and that the wavelength values are large, the shear deformation of the rock will not be significantly affected by the presence of the tunnel.

In the present study, the assumption that the wavelength values are large compared to the tunnel diameters appears to be satisfied in general. Strong motion contains significant amplitudes for frequencies less than 15 Hz. At the slowest S-wave velocity (for shale it is 5,500 fps), the wavelength will exceed 360 ft. For the fastest P-wave velocity (granite, 15,300 fps) wavelengths will exceed 1,000 ft. Thus, the wavelength values are large compared to the assumed tunnel diameter of 18 ft.

Hoop deformations result when waves propagate normal or nearly normal to the tunnel axis. Only small wavelengths seem to be important in hoop effects. Two effects are observed. One is a distortion of the cross-sectional shape that creates stress concentrations in the hoop stresses, as shown in Figure 6.5. This would be most noticeable when the tunnel diameter is comparable to half the wavelength; that is, for wavelengths on the order of 2 x 18 ft = 36 ft. The other effect is that of ringing: the entrapment and circulation of seismic wave energy around the tunnel. Reference 54 states that this is possible only for circular cavities and only when wavelengths are approximately less than the tunnel radius. In this study, tunnel ringing is possible for wavelengths less than 9 ft. Thus, only very small values of wavelength produce hoop deformations. For the longer wavelengths associated with strong seismic motion, the tunnel cross section experiences essentially

uniform compression or tension. Consequently, cross-sectional distortions do not need to be considered in a preliminary determination of added costs for hardening.

For this study the effects of surface waves on tunnels were evaluated as discussed above. At great depth (2,000 ft or more) differential surface wave motion appears to be small and to have negligible effects on deep tunnels. Vertical shafts are nothing more than vertical tunnels and may be evaluated accordingly, given suitable analytical methodology.

A summary of tunnel deformations associated with various types of waves under different conditions of tunnel orientation is presented in Table 6.1.

6.5 Seismic Strains and Stresses

Seismic strains and stresses were determined by the simplified seismic wave analysis described above. Seismic motion was characterized as plane body waves propagating in an isotropic, homogeneous elastic medium. Strain states due to individual body waves were calculated, then appropriately superimposed to obtain the maximum stresses. This simple seismic analysis was used to make a general engineering evaluation of tunnel stability by comparing the magnitudes of seismic stresses to in-situ stresses and the ultimate compressive strength of the rock.

6.5.1 Peak Strains Due to Body Waves. Peak values of strain and curvature due to body waves can be easily estimated from wave behavior and rotation of coordinates. Figure 6.6 illustrates a plane body wave propagating in the x-direction with velocity, V (V_p for P-waves and V_s for S-waves). (No loss in generality occurs in considering a wave propagating parallel to the x-axis because the medium is assumed to be isotropic.) The particles behind the wave front move in the x-direction for P-waves and in the y-direction for S-waves. These motions satisfy the one-dimensional wave equation[66]:

$$\frac{\partial^2 u}{\partial x^2} = \frac{1}{V^2} \frac{\partial^2 u}{\partial t^2} \tag{6.1}$$

where:

u = the particle motion $u_x(x,t)$ for P-waves and $u_y(x,t)$ for S-waves at location x and time t.

TABLE 6.1

DEFORMATIONS ASSOCIATED WITH WAVE TYPE

AND WITH TUNNEL ORIENTATION

Wave Type	Direction of Wave Propagation Relative to Tunnel Axis		
	Longitudinal	Oblique	Transverse
P-Wave	Axial only	Axial Curvature Hoop (short wave-lengths only)	Hoop (short wave-lengths only)
S-Wave	Curvature only	Axial Curvature Hoop (short wave-lengths only)	Hoop (short wave-lengths only)
Surface	Deep horizontal tunnels: Effect is nil. Vertical shafts: Does not apply because wave direction can not be longitudinal or oblique to shaft axis.		Horizontal tunnels: Effect is nil Vertical shafts: Axial Curvature

The solution for a plane wave traveling in the positive x-direction is of the form:

$$u(x,t) = \phi(x - Vt) \tag{6.2}$$

where:

$\phi(x - Vt)$ is a function satisfying Equation (6.1).

Consequently,

$$\frac{\partial u}{\partial x} = -\frac{1}{V}\frac{\partial u}{\partial t} \tag{6.3}$$

The axial strain in the x-direction due to a P-wave is easily determined[67] from:

$$\varepsilon_x = \frac{\partial u_x}{\partial x} = -\frac{1}{V_p}\dot{u}_x \tag{6.4}$$

where the superimposed dot is the time derivative and $\dot{u}_x$ represents the particle velocity in the x-direction. The axial strains normal to the x-axis are zero because of the assumed planar nature of the wave; therefore, $\varepsilon_y = \varepsilon_z = 0$. The shear strains γ_{xy}, γ_{xy}, and γ_{xz} are also zero.

An S-wave due to the particle motion in the y-direction produces a pure shear strain:

$$\gamma_{xy} = \frac{\partial u_y}{\partial x} = -\frac{1}{V_s}\dot{u}_y \tag{6.5}$$

where $\dot{u}_y$ represents the particle velocity in the y-direction. The other shear strains (γ_{yz} and γ_{xz}) and the axial strains (ε_x, ε_y, ε_z) are all zero.

If a plane P- or S-wave propagates obliquely to a tunnel axis, the above states of strain may be transformed to the tunnel axes. For simplicity, consider a tunnel in the x-y plane with longitudinal and transverse coordi-

inates l and n (see Figure 6.6). Axial and shear strains are obtained for the new coordinate system, as shown in Table 6.2.

Curvature, K, along the l-axis is defined[65] by:

$$K = \frac{\partial^2 u_n}{\partial l^2} \tag{6.6}$$

This is also related to the particle motion due to the P- or S-wave propagating parallel to the x-axis, as shown in Table 6.2.

The maximum strains and curvatures may be estimated from the expressions in Table 6.2 using the peak ground particle velocity specified in Section 4.3.2 and PGA, respectively. The values may be maximized also by adjusting the angle θ. For example, the maximum strain parallel to a tunnel due to a P-wave will occur when the wave is propagating down the tunnel ($\theta = 0°$), so that:

$$\varepsilon_{max} = \pm \frac{\dot{u}_{peak\ (longitudinal)}}{V_p} \tag{6.7}$$

Axial strains could be either compressive or tensile, as indicated by + or -, respectively. Maximum curvature of a tunnel axis due to an S-wave will occur when the wave is propagating along the tunnel ($\theta = 0°$) so that[67]:

$$K_{max} = \frac{\ddot{u}_{peak\ (transverse)}}{V_s^2} \tag{6.8}$$

6.5.2 Stresses and Strains in Rock Around Tunnels. Considering various combinations of P- and S-waves propagating at various orientations, it is determined that maximum strains and stresses occur either for three orthogonally propagating P-waves or for three propagating S-waves.

Consider, first, three orthogonal P-waves. Two waves travel horizontally (one parallel to the tunnel in the x-direction, the other at right angles in the y-direction), and the third wave travels vertically (z-direction). The

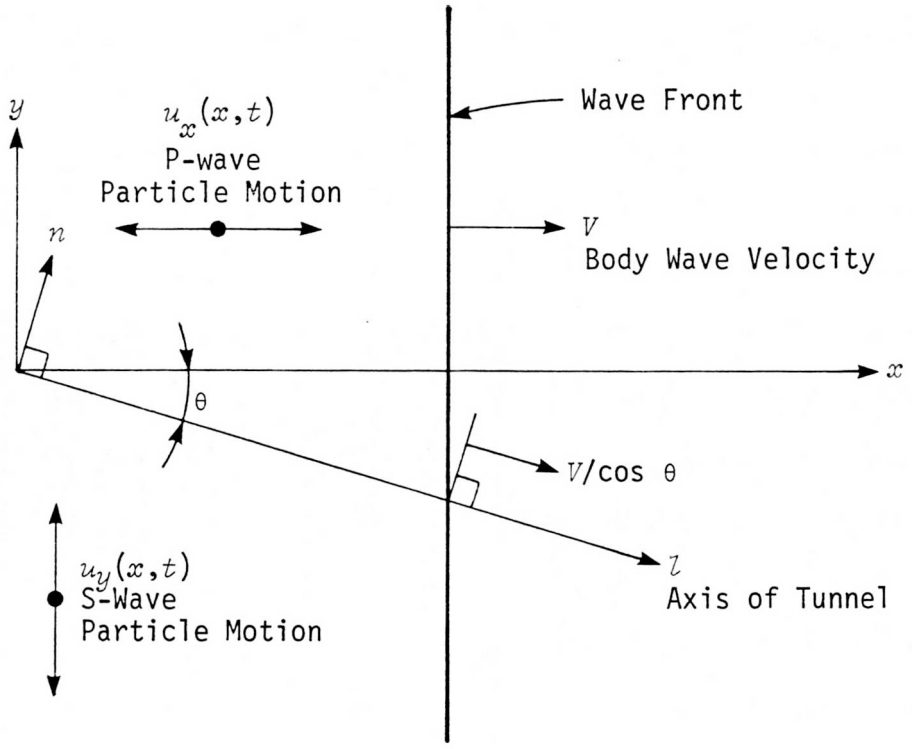

FIGURE 6.6 BODY WAVE MOTION RELATIVE TO TUNNEL ORIENTATION

TABLE 6.2

STRAINS AND CURVATURE DUE TO WAVES PROPAGATING OBLIQUELY TO TUNNEL AXIS

Wave Type	ε_l	ε_n	γ_{ln}	K
P-Wave	$-\frac{1}{V_p}\dot{u}_x \cos^2\theta$	$-\frac{1}{V_p}\dot{u}_x \sin^2\theta$	$-\frac{1}{V_p}\dot{u}_x 2\sin\theta\cos\theta$	$\frac{1}{V_p^2}\ddot{u}_x \cos^2\theta\sin\theta$
S-Wave	$+\frac{1}{V_s}\dot{u}_y \sin\theta\cos\theta$	$-\frac{1}{V_s}\dot{u}_y \sin\theta\cos\theta$	$-\frac{1}{V_s}\dot{u}_y(\cos^2\theta - \sin^2\theta)$	$\frac{1}{V_s^2}\ddot{u}_y \cos^3\theta$

Note:

1. Superimposed dot stands for time derivative.
2. The angle θ is measured clockwise between the direction of wave propagation and the tunnel axis.

non-zero strain in the direction of each propagating P-wave is given by Equation (6.7). Horizontal and vertical particle velocity components are set at the peak values given in Table 4.1 for the 1.0g case. (This case corresponds to PGAs of 1.0g in both of the horizontal directions and 0.67g in the vertical.) The resulting state of strain is given by:

$$\varepsilon_x = \varepsilon_y = \begin{cases} \pm \dfrac{48 \text{ in./sec}}{V_p} & \text{in shale} \\ \pm \dfrac{34 \text{ in./sec}}{V_p} & \text{in tuff and granite} \end{cases}$$

$$\varepsilon_z = \begin{cases} \pm \dfrac{32 \text{ in./sec}}{V_p} & \text{in shale} \\ \pm \dfrac{22 \text{ in./sec}}{V_p} & \text{in tuff and granite} \end{cases} \qquad (6.9)$$

Normal stresses are determined by the three-dimension constitutive relations for a linear elastic isotropic material, for example:

$$\sigma_x = \frac{E}{(1 + \nu)(1 - 2\nu)} [(1 - \nu)\varepsilon_x + \nu\varepsilon_y + \nu\varepsilon_z] \qquad (6.10)$$

where:

E = Young's modulus

ν = Poisson's ratio

Since the above strains are the principal strains ($\gamma_{xy} = \gamma_{yz} = \gamma_{xz} = 0$), Equation (6.10) yields the principal stresses. The maximum principal stress occurs when the three strains are all of the same sign. Maximum shear strain is determined by the difference between the largest and smallest principal strains; therefore, the maximum shear strain occurs when ε_x and ε_y are opposite in sign. Thus, for the P-waves:

$$\varepsilon_{max} = \varepsilon_x$$

$$\sigma_{max} = \frac{E}{(1 + \nu)(1 - 2\nu)} (\varepsilon_x + \nu\varepsilon_z)$$

$$\gamma_{max} = 2\varepsilon_x$$
$$\tau_{max} = G2\varepsilon_x \qquad (6.11)$$

Consider now the three S-waves which cause the largest strains or stresses. One SH-wave travels in the x-direction, another SH-wave travels in the y-direction, and an SV-wave travels in the x-direction. Non-zero shear strains are obtained by Equation (6.5) or the equivalent. The state of strain for the 1.0g case is given by:

$$\gamma_{xy} = \frac{\dot{u}_x + \dot{u}_y}{V_s} = \begin{cases} \dfrac{96 \text{ in./sec}}{V_s} & \text{in shale} \\ \dfrac{68 \text{ in./sec}}{V_s} & \text{in tuff and granite} \end{cases}$$

$$\gamma_{yz} = \frac{\dot{u}_z}{V_s} = \begin{cases} \dfrac{32 \text{ in./sec}}{V_s} & \text{in shale} \\ \dfrac{22 \text{ in./sec}}{V_s} & \text{in tuff and granite} \end{cases}$$

$$\gamma_{yz} = \varepsilon_x = \varepsilon_y = \varepsilon_z = 0 \qquad (6.12)$$

Principal strains, as determined from this state of strain[68], are:

$$\varepsilon_1 = \begin{cases} \dfrac{50.6 \text{ in./sec}}{V_s} & \text{in shale} \\ \dfrac{35.7 \text{ in./sec}}{V_s} & \text{in tuff and granite} \end{cases}$$

$$\varepsilon_2 = 0$$
$$\varepsilon_3 = -\varepsilon_1 \qquad (6.13)$$

Using subscripts 1, 2, and 3 in place of subscripts x, y, and z in Equation (6.10), the principal stress is determined. Thus, for three S-waves:

$$\varepsilon_{max} = \varepsilon_1$$

$$\sigma_{max} = \frac{E}{1 + \nu} \varepsilon_1$$

$$\gamma_{max} = 2\varepsilon_1$$

$$\tau_{max} = G2\varepsilon_1 = \sigma_{max} \qquad (6.14)$$

The engineering material properties to be used in Equations (6.11) and (6.14) are shown in Table 6.3. The values for the dilatational wave velocity (V_p), Poisson's ratio (ν), Young's Modulus (E), unit weight (ρ), and unconfined compressive strength (q_{ult}) are obtained from Table 3.3. The shear wave velocity (V_s) and the shear modulus (G) are determined from the other values.[61,65] The maximum strains and stresses calculated for the two cases are shown in Tables 6.4a and 6.4b.

It is observed that the largest normal stresses were calculated for the three P-waves whereas the largest shear stresses occurred for the three S-waves. For the purposes of a general engineering evaluation of tunnel stability, it is useful to consider normal stresses rather than shear stresses. Normal stresses may be compared to pretunnel in-situ stresses (overburden and horizontal) and to unconfined compressive strength, both of which quantities are reasonably well defined. However, shear stresses would be compared to ultimate shear strength, a quantity which is not easily determined. Thus maximum normal stresses resulting from three P-waves were used to evaluate tunnel stability.

6.5.3 Comparison of Calculated Seismic Stresses with In-Situ Stresses and Ultimate Strength. The maximum seismic stresses were added to the in-situ stresses and compared to the uniaxial strength properties of the rock in order to make a general engineering evaluation of tunnel stability. Although these stress analyses do not allow for the presence of the tunnel, they are acceptable for this study because the approach is strictly comparative. A rigorous analysis (such as may be required in a final design) would calculate stresses with the presence of the tunnel and would employ more refined failure criteria.

The maximum normal stresses predicted in section 6.5.2 for 1.0g were scaled linearly for other g-levels and are presented in Table 6.5. For comparative

TABLE 6.3

ASSUMED ENGINEERING MATERIAL PROPERTIES FOR THE THREE ROCK FORMATIONS

Rock Formation	V_p (fps)	V_s (fps)	ρ (pcf)	E (10^6 psi)	G (10^6 psi)	υ	$q^*_{ult.}$ (10^3 psi)
Eleana shale	11,000	5,500	162	2.85	1.07	0.33	3 to 8
Tuff	8,500	5,200	122	1.70	0.71	0.20	8 to 20
Granite	15,300	9,200	165	7.32	3.00	0.22	14 to 40

*Unconfined compressive strength.

TABLE 6.4a

CALCULATED MAXIMUM SEISMIC STRAINS AND STRESSES

FOR THE CASE OF THREE P-WAVES

(1.0g case)

Rock Formation	$\varepsilon_{max} = \varepsilon_x$ (10^{-6} in./in.)	ε_z (10^{-6} in./in.)	σ_{max} (psi)	τ_{max} (psi)
Eleana shale	360	240	2,800	800
Tuff	330	220	900	500
Granite	190	120	2,300	1,100

Note:

ε and σ may be either compressive (+) or tensile (-).

TABLE 6.4b

CALCULATED MAXIMUM SEISMIC STRAINS AND STRESSES

FOR THE CASE OF THREE S-WAVES

(1.0g case)

Rock Formation	ε_{max} (10^{-6} in./in.)	σ_{max} (psi)	τ_{max} (psi)
Eleana shale	770	1,600	1,600
Tuff	570	800	800
Granite	320	1,900	1,900

Note:

ε and σ may be either compressive (+) or tensile (-).

TABLE 6.5

COMPARISON OF CALCULATED MAXIMUM SEISMIC STRESSES TO IN-SITU STRESSES AND ULTIMATE COMPRESSIVE STRENGTH

Rock Formation	$\sigma_{overburden}$ at 2,000 ft (psi)	$\sigma_{horizontal}$ at 2,000 ft (psi)	$q^*_{ult.}$ (psi)	Calculated Seismic Stress σ_{max} (psi)			
				0.3g	0.5g	0.7g	1.0g
Eleana shale	2,300	1,100 to 3,500	3,000 to 8,000	800	1,400	2,000	2,800
Tuff	1,700	900 to 2,600	8,000 to 20,000	300	500	600	900
Granite	2,300	1,100 to 3,300	14,000 to 40,000	700	1,200	1,600	2,300

*Unconfined compressive strength.

purposes, the table also lists the estimated overburden and horizontal stresses at a depth of 2,000 ft. The horizontal stresses were taken as 50% to 150% of the overburden. The ultimate strength, q_{ult}, corresponds to the laboratory of field-observed unconfined compression test.

A compressive seismic stress pulse will add to the in-situ stresses, raising the question of potential compressive failure in the medium. If the total sum of the dynamic and static stress around the cavity were to exceed the ultimate strength of the rock, spalling and rock falls (due to crushed rock) might be expected. Comparisons of stress levels in the tuff and granite indicated that the ultimate strength will not be exceeded. The shale, however, presents a different situation. This simple stress predictor suggested a potential for crushing the shale at 0.7g and an even greater potential at 1.0g.

A tensile seismic stress pulse will subtract from the compressive in-situ stresses, and the resulting total stress may become tensile. The presence of tensile stresses in the rock implies that seams in the rock can open and permit surface rock blocks in the tunnel to loosen (and perhaps even to fall) as the tensile pulse passes. In the shale, this seems possible at 0.5g and at 0.7g and is quite likely at 1.0g. In granite, it seems possible at 0.7g and at 1.0g; it does not seem likely to occur in the tuff at all. The other potential danger from a tensile pulse is that the rupture strength of the intact rock might be exceeded, causing extensive fracturing of the rock mass. The rupture strength may be approximated as 10% of the ultimate compressive strength. Thus, rupturing might be expected within shale at 0.5g, 0.7g, and 1.0g; however, rupturing would not be expected in the tuff and granite.

The foregoing discussion indicates that the shale rock itself may experience damage at the 0.7g and 1.0g levels while the potential damage for tuff and granite may be very small or nonexistent. During a rigorous design of underground structures, the stresses in the shale should be carefully reviewed. More rigorous analytical models than were possible in this study, supplemented with better experimental data on horizontal in-situ stresses and shale strength properties, should be used.

6.5.4 Seismic Strains in Shaft Liners. Because the shafts were assumed to be heavily lined with reinforced concrete for watertightness, the liner needed to be investigated as an elastic beam subjected to S-wave motion. The liner prevents rock falls in the shaft during seismic motion; the previous analysis for tunnels was not useful for costing purposes. It was assumed that the liners do not constitute a part of the static rock stabilization system; therefore, seismically induced strains were considered independently from static strains. Because it is the tensile strains that may disturb the watertightness of the liner, ignoring the static compressive strains will produce conservative results.

Two wave situations were considered. First, a vertically propagating P-wave causing axial strains:

$$\varepsilon = \frac{\dot{u}_{vertical}}{V_p} \tag{6.15}$$

The second is an oblique SV-wave that yields axial strains:

$$\varepsilon = \frac{\dot{u}}{V_s} \sin\theta \cos\theta + \frac{\text{Diameter}}{2} \frac{\ddot{u}}{V_s^2} \cos^3\theta \tag{6.16}$$

The second expression in Equation (6.16), due to curvature, yields strains in the order of 5 microinches/inch (μin./in.) and was dropped from consideration. The strain due to the SV-wave was maximized using a $\theta = 45°$ and the vertical component of the particle velocity set equal to vertical peak ground velocity. The results for 1.0g are shown in Table 6.6.

The ultimate compressive strain (unconfined) for concrete is approximately 3,000 μin./in. Assuming the ultimate tensile strain is 10% to 12% of that value, concrete ruptures at tensile strains between 300 and 360 μin./in. Comparing these values to Table 6.6, the shaft liners are not expected to experience tensile cracks during seismic activity in any of the three materials at any g-level under consideration with one exception: the shaft liners in the Eleana shale may experience some hairline cracks at 1.0g.

TABLE 6.6

POSSIBLE TENSILE STRAINS IN THE SHAFT LINERS, 1.0g CASE

Rock Formation	Tensile Strain, ε, Due to P-Wave (10^{-6} in./in.)	Tensile Strain, ε, Due to SV-Wave (10^{-6} in./in.)
Eleana Shale	240	340
Tuff	220	250
Granite	120	140

6.6 Tunnel and Shaft Stabilization

The work reported in this section was performed by URS/Blume in consultation with Dr. Tor L. Brekke, Professor of Geological Engineering, University of California, Berkeley, California. Important information regarding current underground construction practices was provided by Mr. George E. Wickham of Jacobs Associates, San Francisco, California.

6.6.1 Background. To fulfill the purpose of the cost scoping studies, the additional stabilization measures required in connection with dynamic loads must be estimated. These additional stabilization needs were evaluated, in addition to those needs dictated by the static conditions, for the selected size and shape of the openings. Excavation methodology and prevailing geological factors were considered in the evaluation. In order to determine the additional and incremental improvements required in the support or rock-reinforcement system, it was necessary to assess the required stabilization system under static conditions. Because such information is currently being developed by others and was not available at the initiation of this study, it was necessary to develop a preliminary geological engineering assessment of the potential repository sites. The information given in Chapter 3 is meant to reflect the premises on which these assessments were based.

Appropriate background material was available to address only three of the four areas under consideration: the Eleana shale, the granite, and the tuff. The questions associated with openings in the alluvium could not be addressed because appropriate information on tunneling could not be obtained, as discussed in Chapter 3.

The following discussion assumes that the 18-ft-diameter tunnels are mined by a tunnel-boring machine. In general, this would be the modern economical excavation method for such an extensive network of tunnels. However several potential problems should be noted. Difficulties may arise in the shale when heavily squeezing ground is encountered, which may dictate alternative methods. Granite could also present a problem if extremely hard rock exists. However, in this preliminary study, it was assumed that the excavation methods should not significantly affect the incremental costs. Consequently, a common tunnel excavation system was assumed for all materials.

6.6.2 Static Support in the Eleana Shale. Laboratory data and core samples indicated that, although parts of the Eleana shale are quite competent and should not require substantial support, much of the shale slakes rather vigorously with environmental changes (such as drying and wetting). It appears likely that this shale will behave partly as squeezing ground at great depth. This condition may not prevail throughout the whole network of underground openings, and very careful exploratory work may allow the squeezing conditions to be avoided. However, for the tunnels in shale, squeezing must be assumed as the worst possible condition. The static loads were assigned in accordance with the guidelines given in Reference 69. At a depth of 2,000 ft, the tunnel supports are designed for squeezing ground at a great depth (a depth greater than 1,000 ft) using a rock load height of 2.2 x (2 x tunnel diameter). The ensuing tunnel support system consists of three-piece steel sets, W8 x 58, spaced 3 ft on centers (see Figure 6.7). Wood lagging (8 in. x 6 in.) with fire retardant spans the distance between the sets and fully covers the circumference of the tunnel. (Fire safety considerations may require a noncombustible material for lagging.) Sets are connected by longitudinal tie rods.

This support system is quite heavy for the size of the openings (18-ft diameter). It may be that the actual spacing of such sets in the network of openings could be doubled to about 6 ft and/or the weight of the sets could be somewhat reduced. However, it is prudent to evaluate the shale from the worst condition observed from the available data and to design accordingly. This assessment of tunnel support was based on conventional blocking and lagging of the sets, with occasional reblocking and relagging of sets where the squeeze would be heavy. Where the shale is somewhat better, spiling prereinforcement and shotcrete as a continuous lagging and blocking could be used. Where squeezing ground prevails, the traditional use of spiling and forepoling in combination with lagging would be the most appropriate measures.

The vertical shafts that connect the surface and underground facilities were assumed to be concrete lined to protect against possible aquifers. The lining would be constructed after excavation or sufficiently behind the excavation operations so that it would not be considered a part of the stabilization system. Shafts in shale must be supported to resist assumed squeezing ground; however, it is assumed that the vertical shafts can be sited to avoid

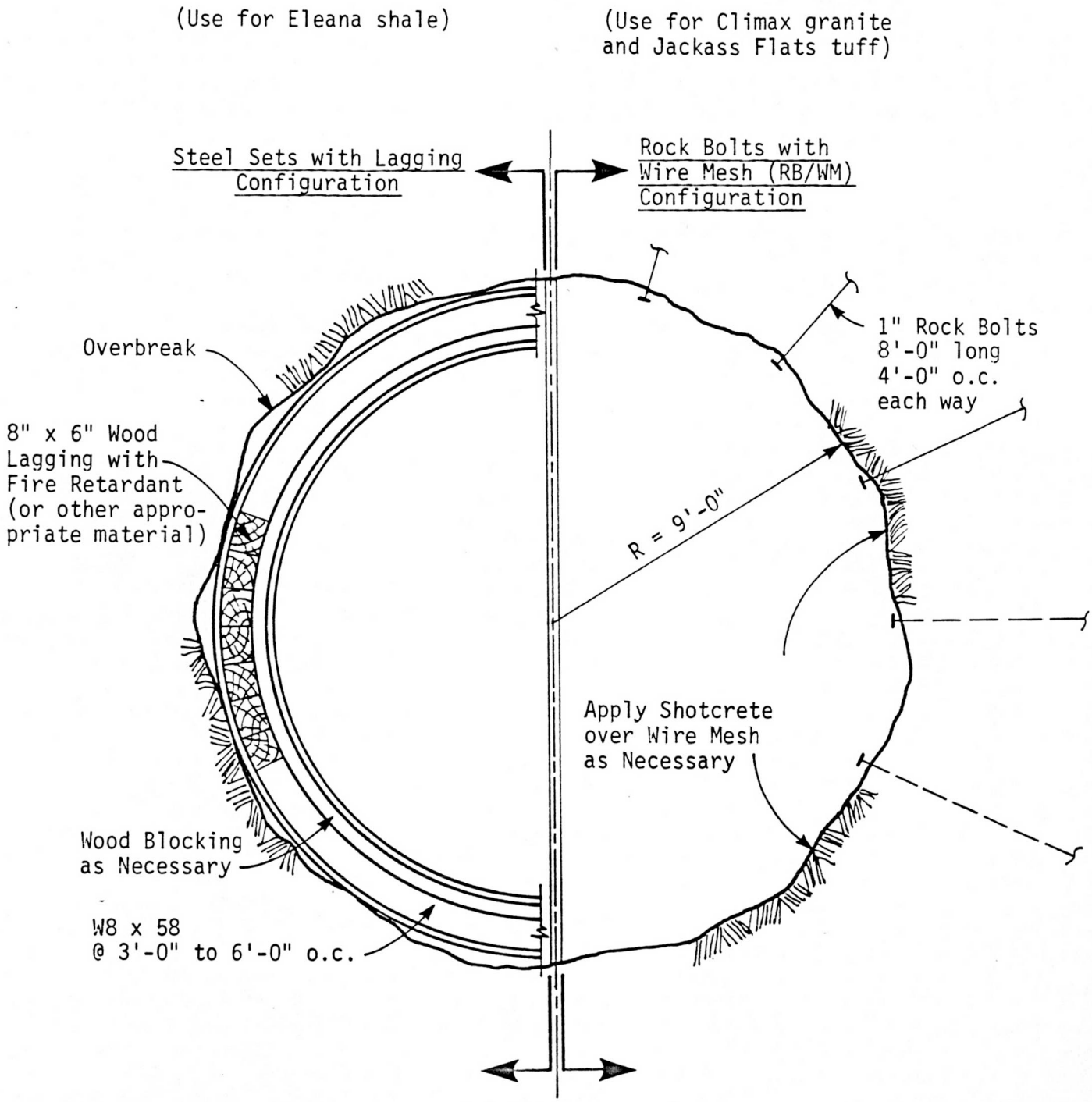

FIGURE 6.7 ASSUMED TUNNEL CROSS SECTION

the worst squeezing ground. Consequently, the recommended rock load is one-half of that used for tunnels.

The assumed static stabilization systems for tunnels and shafts in the Eleana shale are summarized in Table 6.7.

6.6.3 Static Support in the Tuff and the Granite. Both the tuff and the granite represent substantially better candidate rock than does the shale in terms of cost (except, perhaps, in terms of permeability). From a preliminary assessment, both of these rocks can be stabilized for static conditions using rock-bolt reinforcement. The length and spacing of the rock bolts for the static conditions were chosen from prevailing rules of thumb: the rock-bolt lengths are approximately one-half of the opening diameter, spaced at distances of approximately one-half the length of the bolts.[22] The static stabilization in tunnels therefore consists of anchor rock bolts, number 8 rebars, grade 60 steel, 8-ft lengths, spaced 4 ft on center in both the circumferential and longitudinal directions. Under static conditions, tunnels would require rock bolts with wire mesh, springline to springline (see Figure 6.7).

Vertical shafts in tuff and granite would also be concrete lined, and, as in the shale, the lining would not be part of the stabilization system. Anchor rock bolts should be used, with lengths and spacings determined by the procedure given above. Wire mesh would not be required assuming that the reinforced concrete lining (reinforced at least for temperature and shrinkage requirements) is placed following the advancement of the shaft. Tunneling experience in tuff at the NTS indicates the advisability of some kind of surface treatment because the tuff tends to deteriorate when exposed to drying and rewetting cycles.[70] Although such treatment could be provided with shotcrete or gunite, less expensive and effective sprays are available. Relative to this study, it is important that these sprays not have any structural effectiveness. Instead, they would be used to prevent deterioration of the rock arch through slaking. For the purpose of this study, a 1-in. layer of shotcrete was assumed for the tunnels excavated through tuff.

The assumed static stabilization systems for tunnels and shafts in tuff and granite are summarized in Table 6.7.

TABLE 6.7

SUMMARY OF THE ASSUMED STATIC SUPPORT SYSTEMS

Underground Structures	Diameter, Overall Dimension (ft)	Assumed Static Support	
		Shale	Tuff and Granite
All tunnels[a]	18.0	Steel sets: W8x58, 3 ft to 6 ft o.c. Wood lagging with fire retardant	RB/WM[b]: 8-ft lengths, 4 ft o.c. (1-in. shotcrete for tuff)
Man and materials shaft	26.0	Steel Sets: W10x72, 5 ft to 8 ft o.c. Wood lagging[c]	RB/WM: 12-ft lengths, 6 ft o.c.
HLW and construction ventilation shafts	16.5	Steel Sets: W8x31, 5 ft to 8 ft o.c. Wood lagging[c]	RB/WM: 8-ft lengths, 4 ft o.c.
HLW shaft	11.0	Steel Sets: W8x20 6 ft to 12 ft o.c. Wood lagging[c]	RB/WM: 6-ft lengths 3 ft o.c.

[a] See Figure 6.7.

[b] RB/WM = rock bolts with wire mesh, No. 8 rebars, grade 60 steel.

[c] Fire retardant not required because shafts are concrete lined.

6.6.4 Additional Support Required for Seismic Conditions. During UNE or earthquake ground motion, tunnels and shafts would be expected to maintain their structural integrity, to permit the continued normal access by machines and personnel, and to pose no threat to personnel from rock falls. Thus, the basic requirement of the support system is that it must prevent the dislodgement of large rock blocks or large quantities of debris although minor spalling could be tolerated. Furthermore, it is assumed that the shafts must remain watertight.

On the basis of the premises given, the additional measures needed because of the dynamic loads that the system of tunnels might be exposed to were evaluated. Two approaches were used. First, an analysis was conducted to obtain the stresses induced by earthquakes at different g-levels, assuming an elastic response of the media around the tunnels. It is valuable to view the incremental stresses that are induced above and beyond the in-situ stresses at the depth involved as incremental values that can bracket the magnitude of possible problems in terms of stresses. However, it is difficult to assess the importance of these incremental stress values with respect to some failure modes and criteria, both for the rock mass that surrounds the tunnels and for the composite structure of the rock mass support. This study did not attempt to develop firm conclusions about the relationship of numerical values for the dynamic stresses in the rock mass and the support and/or reinforcement system. The current technology for static design of tunnels is not yet compatible with detailed and refined dynamic analysis.

The second approach evaluated effects of dynamic motion along with the qualitative assessment of calculated seismic stresses. The response of the two systems (steel supports and rock reinforcement) was reviewed in terms of experience from tunnels exposed to dynamic loads; qualitative consideration of the interaction between supports and surrounding rock; and the behavior of a reinforced rock arch or cylinder. On this basis, the following conclusions were reached:

1. Consider first the stabilization system selected for the tunnels in shale. Inherently, this system carries a substantial reserve, or resilience, in that both the assessment of static load and the assessment of the capacity of the system, derived from the squeezing-ground load condition, are rather conserva-

tive. It is well known that when steel sets fail it is seldom because the ultimate strength of a given, continuous member of the steel set is exhausted. Rather, it is a question of the failure of connections between the different parts of the set, or a situation of unbalanced loading. Consequently, the incremental support that would be needed to stabilize the system for dynamic loads requires greater attention to construction detail and workmanship than normally would be required if only the static loads were considered. For example, it would be appropriate to weld rather than simply to bolt together the different pieces of a steel set. Blocking that is made as continuous as possible is preferable to spot blocking. Finally, it is necessary to continuously support the system by lagging or by shotcrete (with wire mesh) to prevent severe downfall between steel sets.

2. Similar considerations are applicable for the rock reinforcement systems selected for the tuff and the granite. However, it is necessary to increase the amount of rock reinforcement by bringing it around the full circumferential area of the opening, rather than springline to springline as dictated by static conditions. It will be necessary in this case to prevent the spalling of rock blocks between the fully grouted bolts. This can be accomplished by the use of reinforced shotcrete. The incremental cost for this system may appear to be more significant than that for the steel-set-supported system. Note, however, that the starting point in terms of cost per linear foot of tunnel is substantially lower with the premises and assumptions adopted at the present time.

3. An important common denominator for the two systems is that it is not advantageous to harden them in terms of stiffening them. An approach of maintaining flexibility is the better one, and the incremental effort and cost associated with dynamic loads should be focused on the quality of the details of the support and reinforcement systems selected for static loads and on the prevention of possible spalling or popping of minor blocks or sheets of rock. In principle, a carefully executed, flexible stabilization system is preferable to a very stiff system of stabilization. This is true from a technical as well as from an economic viewpoint.

In order to protect the tunnels from seismic damage, attention is given to improving construction details to achieve a more coherent medium-tunnel system. This means improving rock bolt details by grouting the full length of the bolt and shotcreting between the wire mesh and the overbreak (to obtain

intimate contact between rock and wire mesh during ground motion.) Furthermore, it means packing or grouting between lagging and overbreak to ensure contact and to tie steel sets together securely in the longitudinal direction. Such measures can be scaled to various peak acceleration levels, the full improvement program being applied to the 1.0g level, with various reductions for decreasing g-levels.

The attention given to the details of the support systems in tunnels under strong ground motion must also be applied to the vertical shafts. In addition, the concrete lining and the reinforced concrete collars for the shafts require special consideration. Calculations of possible dynamic strains indicate that the lining of a shaft in shale is likely to experience hairline cracking at 1.0g. This is not indicated for acceleration levels less than 1.0g in the shale or for any levels (including 1.0g) in the tuff and granite. The hairline cracks created during the dynamic state will close after the motion has ceased if sufficient steel is present to maintain an elastic condition. Assuming that the liners contain only the minimum steel reinforcement area required for shrinkage and temperature control (0.25% of the gross concrete area), an increase to 2.0% of the gross concrete area is recommended.

To protect against damage in the collar region, attention must again be given to details. Assuming that the collar itself would normally be heavily reinforced, no additional steel is needed. However, where the collar connects to the lining, stress concentrations and hammering action between the two are to be avoided.

For this study, the additional reinforcing bars required in the collar region of the four shafts will contribute negligible incremental cost and are ignored. However, future studies should seriously address the dynamic problems associated with the shaft collars.

The proposed programs for the improvement of construction details for tunnels and shafts to withstand various peak acceleration levels are outlined in Tables 6.8 and 6.9. Only those items expected to affect the cost are included.

TABLE 6.8

TUNNEL SUPPORT SYSTEMS FOR VARIOUS PEAK GROUND ACCELERATIONS

Support System	Static Load	PGA			
		0.3g	0.5g	0.7g	1.0g
Rock bolts (RB) with wire mesh:					
Extent of RB around perimeter	Upper 1/2	Upper 1/2	Upper 1/2	Upper 2/3	Full circle
RB attachment	Epoxy anchor	Epoxy anchor	Epoxy anchor	Epoxy full length	Epoxy full length
Shotcrete (thickness)	none[a]	none[a]	3 in.[b]	3 in.	3 in.
Steel sets with wood lagging:					
Packing between lagging and overbreak	none	none	none	Completely grouted	Completely grouted
Tie rods (number and diameter)	12, 3/4 in. ø	12, 3/4 in. ø	12, 1 in. ø	18, 1 in. ø	18, 1 in. ø

[a]For tuff, 1 in. shotcrete required only to prevent drying; not required as part of support system.

[b]Tuff only.

TABLE 6.9

SHAFT SUPPORT SYSTEMS FOR VARIOUS PEAK GROUND ACCELERATIONS

Support System	Static Load	PGA			
		0.3g	0.5g	0.7g	1.0g
Rock bolts (RB):					
Extent of RB	Full circle	Full circle	Full circle	Full circle	Full circle
RB attachment	Epoxy anchor	Epoxy anchor	Epoxy full length	Epoxy full length	Epoxy full length
Shotcrete[a] (thickness)	none	none	none	none	none
Steel sets with wood lagging:					
Packing between lagging and overbreak	none	none	none	Completely grouted	Completely grouted
Tie rods (diameter)	3/4 in.	3/4 in.	1 in.	1 in.	1 in.

[a]For tuff, 1 in. shotcrete required only to prevent drying; not required as part of support system.

7. SECONDARY STUDIES OF EARTHQUAKE HARDENING COSTS

Additional brief studies of earthquake hardening costs were conducted in order to compare the cost of structural hardening data available from various other projects with the added costs for hardening obtained for the repository. As stated earlier, hardening, as used here, is defined as strengthening of a structure to resist specified ground motion (from earthquakes and UNEs) beyond conventional static design. Cost for hardening is defined as the total direct, additional cost for such hardening (in January 1978 dollars), which includes the cost of materials, architectural and engineering design, and construction. It does not include interest during construction; escalation; indirect engineering support services such as scheduling, licensing, planning, estimating, quality assurance, purchasing, etc. The types of structures selected to compare to the Category I waste repository structures were those that best simulated the surface and underground repository structures. Information on the strengthening requirements, details of the structural modifications, associated costs, and associated changes in the ground motion design criteria was obtained from the project reports and from the project engineers and other individuals recommended by them. The results of the secondary studies are summarized below.

7.1 Study of Underground Structures

Cost data for hardening conventionally engineered (and designed) underground structures to accommodate increased design ground motion magnitude could not be found. Several underground projects that were engineered and required the consideration of seismic design were investigated. These included the San Francisco Bay Area Rapid Transit (BART) subway, subways in the eastern part of the United States, and tunnels located at the NTS.

Typical NTS tunnels are about 16 ft wide by 16 ft high and are lined with about a 3-in. thickness of concrete reinforced with welded wire mesh. These tunnels were constructed without a formal engineering design procedure and were hardened on the basis of experience of damage from UNEs; they have been subjected to UNE ground accelerations as high as 70g without serious damage although limited concrete spalling has occurred.

Seismic load combinations did not control the design of the subways and tunnels of the San Francisco BART system. A reference[45] often cited for the seismic design of subways concludes that seismic design requirements will control in underground structural design only when (1) there are weak soil conditions such that the soil may compact due to shaking or (2) a structure is built across a known active fault line.

The limited amount of information on the seismic design of underground structures suggests that, on the basis of practical empirical experience and normal design procedures, the seismic capacity of these structures (even when they are not specifically designed under seismic criteria) is high in areas of properly compacted soils. Performing a direct statistical comparison between the cost of hardening the repository underground structures and the cost of hardening other, similar underground structures is not currently feasible because of the absence of relevant data.

7.2 Study of Surface Structures

The Category I waste repository surface structures include:

- HLW building
- Control building
- Emergency power building
- HLW hoist building
- Suspect waste and laundry building
- Mine storage filter building
- Two water pumphouses

These are reinforced concrete shear-wall structures that are similar to nuclear power plant auxiliary structures in that both types of structures may require thick roof slabs and walls (overall thicknesses of approximately 18 in.) in order to provide adequate resistance against tornado-generated missiles, as discussed in Chapter 2.

Similar structures that were investigated in this secondary study included the structures of two nuclear power plants (a pressurized water reactor [PWR] plant and a boiling water reactor [BWR] plant), two hospital buildings, a warehouse building, and nine commercial buildings. Five surface structures

were investigated at the two nuclear power plant sites. The other buildings investigated included old brick buildings and buildings of several construction types: reinforced concrete shear wall and flat slab; reinforced concrete frame; precast wall and slab; steel frame; and timber frame. Their heights varied from two stories (20 ft high) to 15 stories (160 ft high), and their floor plans were of rectangular, box, L, and cross shapes. The total gross area of the buildings ranged from about 4,000 ft^2 to about 500,000 ft^2.

Information obtained from various project reports and discussions with the project engineers included:

- Project name and location
- Type of construction
- Dimensions of structure
- Year of completion and year of strengthening
- Original seismic design criteria and final seismic design criteria
- Method of strengthening original structure
- Additional construction cost (materials and labor) from the original to the final structural design

Of the 17 different structures that were investigated, 16 involved the strengthening of a structure already built, and one involved the conceptual strengthening of an architectural layout. Strengthening of a structure already constructed is usually much more costly than conceptual strengthening of an architectural design.

The following criteria were established for selecting the project information that could best be applied to the repository surface structures:

1. The structural construction materials should be reinforced concrete because all Category I waste repository surface structures are reinforced concrete structures.
2. The method of strengthening a structure that has already been built should be simple enough to be acceptable for conceptually strengthening the original structure.
3. The original and final seismic design PGAs and the total gross area of the structure must be known.

4. The final incremental cost (and the year in which this cost was established) must include only the additional construction cost (labor and materials) and not other costs such as those related to the relocation of equipment, the temporary relocation of people, architectural and engineering services, etc.

The selection criteria reduced the sample size to five structures. The most frequent reason for disqualifying a building was failure of the project to meet the second criterion. For example, one project involved a two-story brick building built in 1900; as a result of the new seismic design criteria, the entire interior was demolished and redesigned, and only the exterior brick wall facing was retained. This example clearly does not apply to the conceptual hardening of a repository surface structure. Another example involved strengthening the roof slab of an existing nuclear power plant structure to comply with increased seismic design criteria. The solution in this example involved the installation of steel trusses anchored to the top of the slab, not an increase in the thickness of the reinforced concrete (which is an acceptable method for conceptually strengthening the original structure).

Because the added costs for hardening an existing structure are generally much higher than the same costs for a structure under design, it was necessary to estimate a cost-scaling factor that would equate the two figures. As used in this section, the cost-scaling factor is defined as the ratio of the modification cost of an existing structure to the conceptual cost that would have been incurred if the structure had been hardened in the design phase.

A summary of the important information on the five selected structures that were strengthened is given in Table 7.1. Structure A is part of the turbine building of a PWR nuclear power plant. The associated cost-scaling factor is 8. Structure B is a commercial building for which the costs are a direct result of a conceptual study, and a cost-scaling factor is not required. Structure C is a hospital building with a cost-scaling factor of 7. Structure D is a warehouse building with a cost-scaling factor of 3. Structure E is a hospital building with a cost-scaling factor of 5. Cost-scaling factors for each project were obtained from project personnel. The cost-scaling factors were estimated on the basis of reviews of the construction procedures for structurally modifying the structures already built.

TABLE 7.1

STRUCTURAL, DESIGN, AND COST DATA ON THE STRUCTURES SELECTED FOR STUDY

Structure[a]	Type of Construction	Structural Dimensions	PGA[b] Original/Final	Incremental Construction Cost	
				Total[c]	Total per ft^2 per 0.1g[d]
A	Peripheral shear walls (t = 18 in.) Intermediate floor slabs (t = 12 in.) Interior steel columns	3 stories; 137 ft by 371 ft by 55 ft high; 173,000 ft^2	0.043g/0.54g	$540,000	$0.63
B[e]	Precast concrete slabs (t = 9 in.) Poured-in-place square columns (14 in. by 14 in.)	2 stories; 127 ft by 318 ft by 20 ft high; 81,100 ft^2	0.05g/0.25g	$155,000	$0.96
C	Reinforced concrete columns Concrete flat slabs	15 stories; 158 ft by 153 ft by 150 ft high; 362,610 ft^2	0.02g/0.25g	$694,000	$0.83
D	Reinforced concrete columns Concrete flat slabs Peripheral shear walls	7 stories; 150 ft by 400 ft by 85 ft high 420,000 ft^2	0.016g/0.07g	$220,000	$0.97
E[f]	Peripheral shear walls (t = 10 in.) Waffle slabs (t = 6 in.) Interior concrete columns	9 stories; 300 ft by 300 ft by 90 ft high; 485,500 ft^2	0.02g/0.22g	$1,800,000	$1.85

[a] In accordance with the request of the interviewed project engineers, the structures are not identified.

[b] PGA refers to the peak ground acceleration on a typical response spectrum curve; 1.0g is the acceleration of gravity (32.2 ft/sec^2).

[c] Total incremental construction costs listed are conceptual costs that have been scaled from the costs required to modify the already-built original structure. These costs are adjusted to January 1978 dollars.

[d] The total incremental cost per gross square foot of floor space for an incremental increase in PGA of 0.1g.

[e] Structure B was the only building for which cost scaling was not required.

[f] Structure E was geometrically shaped as a cross (+) in floor plan.

The methods of seismic hardening used for the five structures selected are as follows:

1. Exterior peripheral shear walls were added on all four elevations from top to bottom for structures A and C.
2. The structural connections were strengthened and the member sizes were increased to strengthen structure B.
3. Several interior architectural brick walls were replaced with structural concrete shear walls to strengthen structure D.
4. Exterior shear wing walls were added to the existing structure to strengthen structure E.

The original and final PGA design values were derived in two different ways. Final PGA values for structures A and E were obtained directly from earthquake response spectra because these two structures were hardened using earthquake response spectra. The other structures were designed to meet *Uniform Building Code*[43] design criteria. All of the original structures were designed for a particular base shear coefficient (C_b) before and/or after the strengthening modification. The design base shear coefficient was then related to a design spectral acceleration (S_a) by the relationship $C_b/S_a = .75$.[71] This relationship was derived by using an average value of C_b/S_a (given on page 73 of Reference 71). The computed S_a was then converted to an equivalent design PGA using the NRC *Regulatory Guide 1.60* response spectra.[28]

The total incremental construction costs shown in Table 7.1 consist of the direct material and labor costs (in January 1978 dollars) required to harden the main structural frames. Most of the cost figures were from the period 1970 to 1978 and had to be adjusted to account for an annual inflation rate of 8% in order to conform to January 1978 dollars. Costs involved with seismic strengthening of piping and mechanical and electrical equipment were not included.

From Table 7.1, the average total incremental construction cost per ft^2 for all five structures for an incremental increase in PGA of 0.1g is $1.05. Note that five data points are not sufficient for firm conclusions, especially when the original-to-final-design-range PGAs are mostly limited to

the range of 0.02g to 0.25g (four structures of the five). However, it seems that the added costs for hardening per ft^2 per 0.1g increment would be larger near the lower part of the original-to-final-design-range PGA (0.02g to 0.25g) than near the upper part of the range (0.7g to 1.0g) for the following reasons:

1. A conceptual hardening from 0.02g to 0.25g is equivalent to adding a few new shear walls to increase the lateral seismic strength (primarily to provide for wind resistance) of a buildings that originally had little lateral seismic strength. The additional conceptual construction costs for a new wall include the forming, all materials, and labor. Forming and the associated labor usually constitute a major portion of the additional cost.
2. A conceptual hardening from 0.5g to 0.8g is equivalent to thickening an already thick shear wall. The added conceptual construction costs in this case would include extra concrete, reinforcing steel, and little or no additional forming or labor. Therefore, these added construction costs are lower. This assumption is verified to some degree by the incremental construction costs that are summarized in Table 7.1. The lowest incremental cost in the table, for structure A, is for the largest increment in PGA (0.497g).

Therefore, an average value of \$1.05 per ft^2 per 0.1g incremental increase is conservative for an incremental seismic design modification from 0.3g to 1.0g. For the modification from 0.3g to 1.0g, the cost can probably be reduced by 80%, to \$0.21. This reduction factor was assumed on the basis of the engineering judgement of the project engineers involved and can not be substantiated without extensive cost data. Therefore, for the PGA values being considered for the design cost scoping studies (all above 0.3g), it was assumed that \$0.21 per ft^2 per 0.1g is a reasonable value. This incremental value was applied to the Category I surface structures of the repository. The resulting added costs for hardening are shown in Table 7.2.

As stated earlier, it is difficult to arrive at firm conclusions from only five hardening cases that are within a narrow PGA range. However, even though the values in Table 7.2 are not firm values, it is felt that they can be used to estimate added costs for hardening associated with incremental PGA seismic design values for the repository surface structures.

TABLE 7.2

ADDED COSTS FOR HARDENING FOR THE CATEGORY I REPOSITORY SURFACE STRUCTURES BASED ON THE RESULTS OF THE SECONDARY STUDIES (without tornado hardening)

Structure	Above-Grade Gross Surface Area[a] (ft^2)	Added Costs[b] for Hardening for Incremental PGA Ranges				
		0g to 0.3g	0.3g to 0.5g	0.5g to 0.7g	0.7g to 1.0g	0g to 1.0g
HLW building	25,400	$ 80,000	$10,700	$10,700	$16,000	$117,000
Control building	5,400	17,000	2,300	2,300	3,400	25,000
Emergency power building	30,700	97,000	13,000	12,900	19,400	142,000
HLW hoist building	2,500[c]	8,000	1,000	1,000	1,600	12,000
Suspect waste and laundry building	5,500	17,000	2,300	2,300	3,500	25,000
Mine storage filter building	18,600	59,000	7,800	7,800	11,800	86,000
Total	88,100	$278,000	$37,100	$37,000	$55,700	$407,000

[a] From Reference 5.

[b] Cost values are based on $1.05 per ft^2 per 0.1g and are expressed in January 1978 dollars.

[c] Hoist building is an underground structure.

Further comparisons and correlations between the results of the secondary studies and the results of the cost scoping studies of the hardened repository structures are discussed in Chapter 8.

8. HARDENING COSTS

This chapter summarizes the preliminary estimates of added costs for hardening the conceptual repository at the candidate NTS sites against the specified ground motions. The results are presented separately for the surface structures and for the underground structures (shafts and tunnels). At the initiation of the work, it was planned to compute the added costs for hardening only as a percentage of the total construction costs. However, as the work progressed it became necessary to compute realistic construction costs for all structures. These URS/Blume cost estimates are for conventional structures, such as rapid transit tunnels, that do not involve costs such as those incurred for licensing, nuclear quality assurance, security at the NTS, etc. Thus, all dollar costs cited in this chapter should be viewed as costs to be used for relative comparisons between the candidate sites. At the conclusion of the chapter, the added costs for hardening are summarized as percentages of the total construction costs in the absence of ground motion. These figures are the only ones that should be used as the added costs for hardening at the candidate sites.

Construction costs for the Eleana shale were estimated[72] concurrently by Fenix & Scisson, Inc., Las Vegas. Those costs should not be compared with the costs computed by URS/Blume because they are based on different assumptions. Further, the estimates are sensitive to the conceptual design. At present, no conceptual design for a waste repository at the NTS exists.

The added costs for hardening, when taken as a percentage of the construction cost, can be used in conjunction with the final estimated construction costs for the candidate sites. These percentages are believed not to be very sensitive to changes in the total costs (even changes as significant, for example, as a doubling of the URS/Blume estimated total dollar costs).

At the initiation of the cost scoping studies, it was planned to report the added hardening costs separately for UNE and earthquake ground motions. However, due to the high stiffnesses (frequencies) of the subject structures and the similarities between the assumed spectral shapes of the two types of motion at high frequencies (see Chapter 4), the added costs for hardening are identical for a given PGA for both types of motion. Thus, the following

results are presented for the different PGAs, which range from 0.3g to 1.0g, and no distinction is made between UNE and earthquake ground motion.

The added costs for hardening for the surface structures were not given extensive treatment in the cost scoping because these costs are governed to a large extent by the assumed non-seismic loads, such as tornado-induced loads. Furthermore, the overall repository costs are most heavily influenced by the underground structures.

8.1 Added Costs for Hardening for the Surface Structures

Table 5.1 summarizes the assumed structural properties and the incremental quantities of reinforced concrete that are required to harden the surface structures against ground motion. An average cost of in-place concrete for nuclear-type structures is about $300 per cubic yard. The cost of the concrete was based on the following:

1. The current in-place cost of concrete at a job site is approximately $150 per cubic yard.
2. It is assumed that the cost of the concrete would double for a Category I structure that houses waste material. That increase would be caused by additional engineering, additional quality assurance requirements, and additional expenses usually incurred for nuclear structures.
3. No cost multiplier for NTS construction is included.

The added costs for hardening are shown in Table 8.1. These costs are small when compared to the total constructed costs of the structures, which are estimated to be in excess of $40 million. Also, it is apparent that if state-of-the-art tornado-resistant design is used, as assumed, the added ground motion hardening costs are small. Table 7.2, which presents results from separate estimating procedures, lists some extrapolated seismic hardening costs for all of the assumed Category I surface structures. Note that, for example, for the HLW building the incremental cost for the range of 0.7g to 1.0g is $16,000, as compared to the $60,000 incremental cost for the same range in Table 8.1. The total estimated increase in seismic hardening cost for the range 0.0g to 1.0g from Table 7.2 is $117,000. Tornado hardening costs for the structures would be expected to be much more because the thick

TABLE 8.1

SUMMARY OF THE ADDED COSTS FOR HARDENING FOR THE SURFACE STRUCTURES

Structure	Incremental Cost[a] (January 1978 dollars) PGA			
	0.3g	0.5g	0.7g	1.0g
HLW building	none[b]	none	30,000	90,000
Control room building	none	none	none	none
Emergency power building	none	none	none	15,000
HLW hoist building	none	none	none	none
Suspect waste and laundry building	none	none	none	none
Mine storage filter building	none	none	none	none
Water pumphouses	none	none	none	none

[a]Based on an assumed cost of $300 per yd^3 of concrete.

[b]Tornado hardening design governs wherever "none" appears.

Note:

These dollar amounts should be used only in the context of this report. They are relative figures and may vary significantly.

concrete walls are primarily necessitated by the assumed tornado-induced loads, and any additional seismic hardening costs would be small.

In summary, if tornado hardening of the surface structures of the repository is required, as was assumed in this study, the added ground motion hardening costs are small. If, however, tornado hardening is not required, the costs would be much greater. A preliminary indication of these costs may be obtained from Table 7.2; at 1.0g, the added costs are more than $400,000.

In reinforced concrete construction for conventional facilities, engineering costs account for roughly 6% of the total project cost. Of that figure, 1/6, or 1%, is used for seismic analysis and other analyses. In typical high-technology projects, such as a repository, the analytical effort is often 1/3 to 1/2 of the engineering effort. At the NTS, the engineering costs vary between 12% and 35% of the total cost.[73] Thus, the incremental design engineering cost for all of the design PGAs could vary between 2% and 18% of the total construction cost for the surface structures.

8.2 Added Costs for Hardening for the Underground Structures

The added costs for hardening the underground structures of the repository are based on the various hardening procedures discussed in Chapter 6. The costs were computed by Jacobs Associates, tunnel construction management engineers, using results from the hardening studies discussed in Chapter 6.

For the underground structures, it was assumed, as discussed previously, that no hardening is required at or below 0.3g.

The costs and the added costs for hardening were computed on the basis of the following general assumptions:

1. Direct costs were determined for labor, equipment, and materials on the basis of crew sizes and advance rates established for each tunnel or shaft excavation.
2. Materials include both expendable items, such as cutters and dynamite, and permanent support items, such as rock bolts, steel ribs, etc., as applicable to the particular operation.

3. All labor was computed at a rate of $16.00 per hour and includes base, fringe benefits, insurance, and taxes.

4. The equipment and material charges are based on current costs and prices.

5. An allowance of 35% to 45% of direct costs was used for the indirect costs of overhead, general administration, plant, and profit.

6. The costs are represented in January 1978 prices.

7. Tunnel boring machines were considered feasible for all tunnels. This will not be the case if sections of extremely hard granite or squeezing shale are encountered.

8. All shafts are sunk with conventional methods, keeping the concrete lining close to the bottom. It is possible that the HLW shaft (11-ft diameter) and the HLW and construction ventilation shafts (16.5-ft diameter) in tuff and shale can be bored full face from the surface.

9. The costs for the shafts are based on a depth of 2,000 ft and continuous operation. The costs for the tunnels assume continuous 24-hour operation over many years and represent many thousands of linear feet for the tunnels.

10. The costs for the underground structures do not reflect higher costs that may be incurred at the NTS. However, the relative costs will remain unchanged.

11. The hardening features are designed to be conservative. Thus, the stated costs could probably be considered to be the upper limit of hardening costs up to a 1.0g PGA level.

Table 8.2 summarizes the total estimated costs for the tunnels and the shafts per linear foot. All of the estimated added costs for hardening can be computed from the table.

8.2.1 Tunnels. Figure 8.1 shows the total costs per linear foot of tunnel for the three different rock materials. The base cost in the range of 0.0g to 0.3g PGA for the Eleana shale is $1,400, almost double the cost for tuff ($770) and for granite ($730). The added costs for hardening do not significantly alter the differences in cost between the materials.

Table 8.3 simplifies the information on added costs for hardening by illustrating these costs as percent of base cost. Up to 0.5g, all but the tuff increments are negligible (easily within the accuracy of the information).

TABLE 8.2

ESTIMATED COSTS FOR THE TUNNELS AND SHAFTS FOR VARIOUS PEAK GROUND ACCELERATIONS

(per linear foot; in January 1978 dollars)

PGA	Tunnels (18 ft ø)			Man and Materials Shaft (26 ft ø)			Ventilation Shafts (16-1/2 ft ø)			HLW Shaft (11 ft ø)		
	Granite	Tuff	Shale	Granite	Tuff	Shale	Granite	Tuff	Shale	Granite	Tuff	Shale
Static and 0.3g	$730	$ 770	$1,400	$3,400	$3,500	$4,900	$2,700	$2,700	$3,500	$1,800	$1,900	$2,100
0.5g	750	910	1,430	3,500	3,500	4,900	2,700	2,800	3,500	1,900	2,000	2,100
0.7g	930	970	1,580	3,500	3,500	4,900	2,700	2,800	3,500	1,900	2,000	2,100
1.0g	980	1,040	1,580	3,500	3,500	5,400	2,700	2,800	3,800	1,900	2,000	2,300

Note:

These dollar amounts should be used only in the context of this report. They are relative figures and may vary significantly.

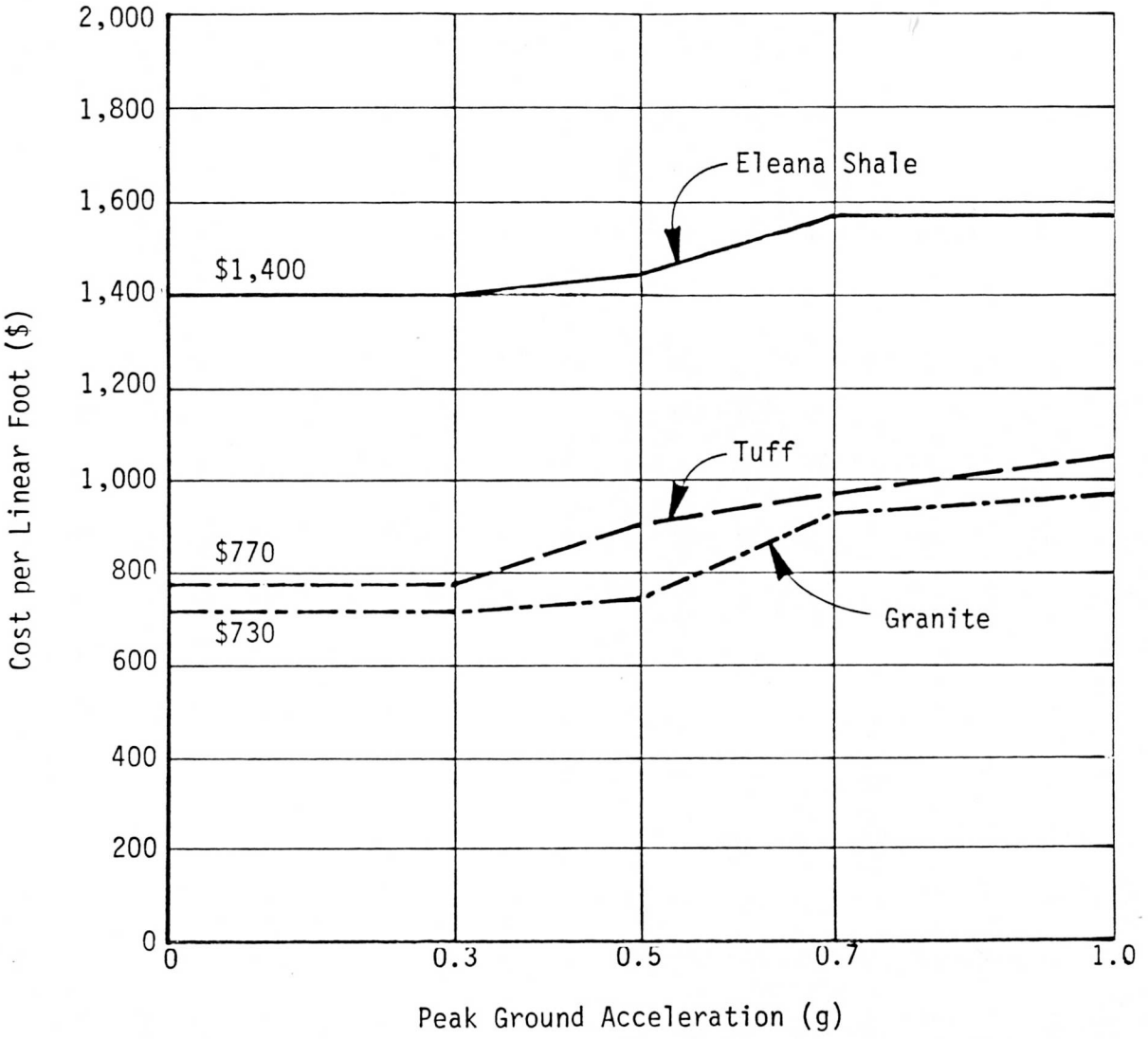

Note:

These dollar amounts should be used only in the context of this report. They are relative figures and may vary significantly.

FIGURE 8.1 SUMMARY OF ESTIMATED TUNNEL COST PER LINEAR FOOT

TABLE 8.3

SUMMARY OF ESTIMATED HARDENING COSTS AS PERCENTAGE INCREASE

PGA Range (g)	Cost Increase per Linear Foot (%)					
	Tunnels			Four Shafts Combined		
	Granite	Tuff	Shale	Granite	Tuff	Shale
0.0 to 0.3	0	0	0	0	0	0
0.0 to 0.5	3	18	2	1	1	1
0.0 to 0.7	27	26	13	1	1	1
0.0 to 1.0	34	35	13	1	1	10

At 0.7g and higher, the incremental percentage costs for the shale are less than half of those for the tuff and granite.

For the granite, the increase in cost at 0.7g is primarily due to the addition of 3 in. of shotcrete. The same increase occurs for the tuff at the 0.5g level, where an additional 2 in. of shotcrete is added. If further, more detailed analyses show that these additional thicknesses of shotcrete are unncessary, the incremental increases in cost for hardening of the tuff and granite tunnels will probably be less than half of those indicated in Table 8.3. The increase in the cost at 0.7g for the shale is due to the additional cost of packing (with grout) between the lagging and the overbreak of the tunnel. This cost is based on the assumption that this packing will further enhance the support system. It should be understood that hardening by the addition of shotcrete or grout will be necessary only if the final tunnel design criteria do not allow spalling or minor rock breakage.

In summary, the preliminary added costs for hardening against ground motion can be quite significant at or above 0.5g. Although there is generally little difference in the costs between tuff and granite, the granite seems to be somewhat less costly. The shale is the least economically desirable material. It is approximately twice as costly to design the tunnels in shale for the static condition. The added costs for hardening are, however, somewhat smaller than those for tuff and granite.

8.2.2 Shafts. The various costs for the three types of shafts are given in Table 8.2. In general, the costs for the shafts significantly exceed those for the tunnels per linear foot.

Table 8.3 summarizes the added cost for hardening as a percentage of the cost of the shafts in the absence of ground motion design criteria. It is apparent that only the shale incurs a significant increase (10%), and that is only at the 1.0g level. This is due to an increase in the amount of reinforcing steel to prevent possible tensile cracking. All other increases are easily within the margin of error of the assumptions.

9. CONCLUSIONS

From the reported analyses, the following general conclusions were reached regarding the added costs required for hardening repository structures at three candidate NTS locations against ground motion caused by earthquakes and weapons testing. These conclusions are preliminary in nature and should be considered and weighed in the context of the assumptions and idealizations that have been made.

9.1 Surface Structures

The major conclusions for surface structures are as follows:

1. Assuming that tornado hardening will be required for the surface structures, as it is for nuclear power plant facilities, such hardening will also provide adequate seismic resistance at PGAs of 0.3g and 0.5g. Added costs due to ground motion considerations will be incurred for the HLW building at a PGA of 0.7g (earthquake and UNE) and also for the emergency power building at 1.0g (UNE only). No other surface structures are expected to incur significant added costs due to ground motion (see Table 8.1).
2. The total added cost for seismic hardening of the surface structures is approximately $105,000 at 1.0g assuming tornado hardening is required. These costs are negligible compared to the estimated overall repository cost of over $400 million.
3. If tornado hardening is not required, the added costs for seismic hardening will be in excess of $400,000 for 1.0g (see Table 7.2).
4. A significant analysis-and-design engineering effort is generally expected for Category I structures (particularly if licensing is required) for protection against earthquakes and UNEs. A minimum increase of 2% in the total construction cost for the surface structures can be expected whether or not additional hardening is found to be necessary. For a repository at the NTS, this increase could be as high as 18%.

9.2 Underground Structures

The major conclusions for the underground structures are as follows:

1. No significant added costs for hardening are expected at 0.3g in the shafts or the tunnels.

2. The added costs for hardening the tunnels against ground motion become significant at levels above 0.5g and may increase the total cost of the underground portion of the repository as much as 35% (see Figure 8.1 and Table 8.3).

3. Assuming that the Eleana shale is characterized by squeezing ground behavior, the tunnel support for static stability is estimated to be almost twice as costly in the shale as in the tuff and granite. However, the added costs for seismic hardening of the tunnels in the shale at 0.7g and 1.0g are somewhat lower than those for the other two materials (see Figure 8.1).

4. The cost estimates for the tunnels are sensitive to the assumptions and procedures used to design the additional supports for seismic conditions.

5. The final performance criteria will strongly influence the required tunnel-hardening procedures.

6. On the basis of items 4 and 5, above, the hardening costs would be significantly reduced for the tunnels if the assumed performance criteria for this study are relaxed and some minor spalling and rock breakage are acceptable.

7. Except for the shale at 1.0g (UNE only), the added costs for the shafts are negligible at all ground motion levels (see Table 8.3).

8. At present, the static design of tunnels and similar underground structures is generally accomplished on the basis of engineering experience and modification during construction. It is possible to determine accurately the upper bound of seismic stresses in the rock; however, the lithostatic stresses and the ultimate strengths are not well known. Therefore, it is difficult to obtain an assessment or a quantification of the actual effects of motion on the tunnels. The seismic design of tunnel support systems might also need to be modified during construction.

9.3 Further Studies

No further cost scoping studies are deemed necessary until more detailed information is available concerning:

1. A complete conceptual design for a repository located at a specific site.

2. Preliminary performance criteria for tunnel stability.

3. A rigorous ground motion characterization procedure for the prediction of underground motion.

4. Engineering geological data for the repository site.

5. A comprehensive failure model (or stabilization evaluation procedure) for tunnels that includes static, dynamic, and thermal loadings.

URS/Blume will continue to be involved in related or parallel activities: the NTS Seismic Deisgn Criteria Study[1] and a study on the earthquake engineering of large underground structures funded by the National Science Foundation and the Federal Highway Administration.

10. REFERENCES

1. U.S. Department of Energy, Nevada Operations Office, *NTS Terminal Waste Storage, Program Plan for FY 1978*, Las Vegas, Nevada, March 1978.

2. Letter dated October 5, 1977, from R. E. Skjei of URS/John A. Blume & Associates, Engineers, San Francisco, to P. N. Halstead, U.S. Department of Energy, Nevada Operations Office, Las Vegas, Nevada.

3. Office of Waste Isolation, *Waste Isolation Facility Description -- Bedded Salt*, Report No. Y/OWI/SUB-76/16506 to the U.S. Energy Research and Development Administration, Oak Ridge, Tennessee, September 1976.

4. U.S. Nuclear Regulatory Commission, Office of Nuclear Material Safeguards and Safety, *Workshop Material for State Review of USNRC Site Suitability Criteria for High-Level Radioactive Waste Repositories*, NUREG-0326, Washington, D.C., September 1977.

5. Sandia Laboratories, *WIPP Conceptual Design Report*, Report No. SAND77-0274 to U.S. Energy Research and Development Administration, Albuquerque, New Mexico, June 1977.

6. Weart, W. D., "New Mexico Waste Isolation Pilot Plant, A Status Report," *Proceedings of the Symposium on Waste Management*, Tucson, Arizona, October 1976.

7. Rippon, S., "Prospects Look Good for Gorleven Center," *Nuclear News*, Vol. 21, No. 2, 1978.

8. Atlantic Richfield Hanford Company and Kaiser Engineers, *Retrievable Surface Storage Facility Alternative Concepts Engineering Studies*, Report No. ARH-2888 REV to the U.S. Atomic Energy Commission, Richland, Washington, July 1974.

9. Rockwell International, Atomics International Division, *Spent Unreprocessed Fuel Facility Engineering Studies*, Draft Report No. RHO-LD-2 to the U.S. Energy Research and Development Administration, Rockwell Hanford Operations, Richland, Washington, October 1977.

10. U.S. Atomic Energy Commission, *Regulatory Guide 1.76 -- Design Basis Tornado for Nuclear Power Plants*, Washington, D.C., April 1974.

11. URS/John A. Blume & Associates, Engineers, *Seismic Evaluation and Structural Consultation for Conceptual Design of the Safety Research and Experiment Facility at the Idaho National Engineering Laboratory, Idaho*, report to CH_2M-Hill, San Francisco, California, September 1975.

12. Bechtel Power Corporation, *Tornado and Extreme Wind Design Criteria for Nuclear Power Plants*, BC-TOP-3-A, Revision 3, San Francisco, California, August 1974.

13. Bechtel Power Corporation, *Design of Structures for Missile Impact*, BC-TOP-9, Revision 1, San Francisco, California, July 1973.

14. Sandia Laboratories, *Full-Scale Tornado-Missile Impact Tests*, Report No. EPRI NP-440, to Electric Power Research Institute, Palo Alto, California, July 1977.

15. Rotz, J. V., "Evaluation of Tornado-Missile Impact Effects on Structures," Symposium on Tornados: Assessment of Knowledge and Implications for Man, Texas Tech University, Lubbock, Texas, June 1976.

16. Hoover, D. L., "Geology of the UE17e Drill Hole in the Eleana Formation, Nevada Test Site," unpublished.

17. Cornwall, H. R., *Geology and Mineral Deposits of Southern Nye County, Nevada*, Bulletin 77, Nevada Bureau of Mines and Geology, 1972.

18. Gibbons, A. B., E. N. Hinrichs, W. R. Hansen, and R. W. Lemke, *Geology of the Rainier Mesa Quadrangle, Nye County, Nevada*, Map GQ-215, U.S. Geological Survey, Menlo Park, California, 1963.

19. Hoover, D. L., "Core Description of U12e.14 UG10," U.S. Geological Survey, unpublished.

20. Ege, J. R., and R. E. Davis, "Preliminary Appraisal of Proposed Tiny Tot Site #2 and Exploratory Drill Hole UE15f, Area 15, Nevada Test Site," technical letter, Area 15-6, 1965.

21. King, M. J., "Engineering Resource Unit Approach to Engineering Land-Use Planning," *Bulletin of the Association of Engineering Geologists*, Vol. XV, No. 3, 1978, in press.

22. Brekke, T. L., Professor of Geological Engineering, University of California, Berkeley, private communication, January 1978.

23. Hoover, D. L., and J. N. Hodson, "Engineering Geology Related to Mineability of the Argillite in the Syncline Ridge Area, Nevada Test Site," U.S. Geological Survey, Mercury, Nevada, unpublished report, January 18, 1978 (revised February 18, 1978).

24. Newmark, N. M., and E. Rosenblueth, *Fundamentals of Earthquake Engineering*, Prentice-Hall, Englewood Cliffs, New Jersey, 1971.

25. Hoover, D. L., Special Projects Branch, U.S. Geological Survey, Denver, Colorado, private communications, January-March 1978.

26. "Physical Property Data for (HW-6) J-11, Nevada Test Site, Nye County, Nevada," provided by J. Ohl, Special Projects Branch, U.S. Geological Survey, Denver, Colorado, private communication, January 1978.

27. Maldonado, F., *Summary of the Geology and Physical Properties of the Climax Stock, Nevada Test Site*, Open-File Report 77-356, U.S. Geological Survey, Denver, Colorado, 1977.

28. U.S. Nuclear Regulatory Commission, *Regulatory Guide 1.60 -- Design Response Spectra for Seismic Design of Nuclear Power Plants*, Revision 1, December 1973.

29. John A. Blume & Associates, Engineers, *Recommendations for Shape of Earthquake Response Spectra*, report to the Directorate of Licensing, U.S. Atomic Energy Commission, Washington, D.C., February 1973.

30. McEvilly, T. V., and W. A. Peppin, "Source Characteristics of Earthquakes, Explosions, and Afterevents," *Geophysical Journal of the Royal Astronomical Society*, Vol. 31, 1972.

31. Stevens, P. R., *A Review of the Effects of Earthquakes on Underground Mines*, Open-File Report 77-313, U.S. Department of the Interior, Geological Survey, Reston, Virginia, April 1977.

32. Okamoto, S., *Introduction to Earthquake Engineering*, John Wiley, New York, New York, 1973.

33. Kanai, K., T. Tanaka, S. Yoshizawa, T. Morishito, K. Osada, and T. Suzuki, "Comparative Studies of Earthquake Motions on the Ground and Underground, II," *Bulletin of the Earthquake Research Institute*, Vol. 44, 1966.

34. Iwasaki, T., S. Wakabayashi, and F. Tatsuoka, "Characteristics of Underground Seismic Motions at Four Sites around Tokyo Bay," *Wind and Seismic Effects*, H. S. Lew, ed., U.S. Department of Commerce, May 1977.

35. Tanaka, T., S. Yoshizawa, T. Morishita, K. Osada, and Y. Osawa, "Observation and Analysis of Underground Earthquake Motions," *Proceedings of the Fifth World Conference on Earthquake Engineering*, Rome, Italy, 1973.

36. Kuribayashi, E., and T. Iwasaki, "Effects of Soil Deposits on Seismic Behavior of Prefabricated Highway Tunnels," *Proceedings of the Fifth World Conference on Earthquake Engineering*, Rome, Italy, 1973.

37. Banister, J. R., D. M. Ellett, C. R. Mehl, and F. F. Dean, "Stress and Strains Developed by the Reflection of Seismic Waves at a Free Surface," draft of Report No. SAND77-0673, Sandia Laboratories, Albuquerque, New Mexico, February 1978.

38. Newmark, N. M., and W. J. Hall, "Seismic Design Criteria for Nuclear Reactor Facilities," *Proceedings of the Fourth World Conference on Earthquake Engineering*, Vol. II, Santiago, Chile, 1969.

39. Newmark, N. M., "Earthquake Response Analysis of Reactor Structures," *Nuclear Engineering and Design*, Vol. 20, No. 2, 1972.

40. Newmark, N. M., J. A. Blume, and K. K. Kapur, "Seismic Design Spectra for Nuclear Power Plants," *Journal of the Power Division*, American Society of Civil Engineers, Vol. 99, No. PO2, November 1973.

41. Mohraz, B., "A Study of Earthquake Response Spectra for Different Geological Conditions," *Bulletin of the Seismological Society of America*, Vol. 66, No. 3, June 1976.

42. *Building Code Requirements for Reinforced Concrete*, ACI 318-21, American Concrete Institute, Detroit, Michigan, 1971.

43. *Uniform Building Code*, International Conference of Building Officials, Whittier, California, 1976.

44. San Francisco Bay Area Rapid Transit District, *Trans-Bay Tube, Technical Supplement to the Engineering Report*, Parsons, Brinckerhoff-Tudor-Bechtel, San Francisco, California, July 1960.

45. Kuesel, T. R., "Earthquake Design Criteria for Subways," *Journal of the Structural Division*, American Soeicty of Civil Engineers, Vol. 95, No. ST6, June 1969.

46. Kuribayashi, E., T. Iwasaki, and K. Kawashima, "Dynamic Behavior of a Subsurface Tubular Structure," *Bulletin of the New Zealand National Society for Earthquake Engineering*, Vol. 7, No. 4, December 1974.

47. Aoki, Y., and S. Hayashi, "Spectra for Earthquake-Resistive Design of Underground Long Structures," *Proceedings of the Fifth World Conference on Earthquake Engineering*, Rome, Italy, June 1973.

48. Okamoto, S., and C. Tamura, "Behavior of Subaqueous Tunnels during Earthquakes," *Earthquake Engineering and Structural Dynamics*, Vol. 1, 1973.

49. Okamoto, S., C. Tamura, K. Kato, and M. Hamada, "Behavior of Submerged Tunnels During Earthquakes," *Proceedings of the Fifth World Conference on Earthquake Engineering*, Rome, Italy, June 1973.

50. Goto, Y., J. Ota, and T. Sato, "On the Earthquake Response of Submerged Tunnels," *Proceedings of the Fifth World Conference on Earthquake Engineering*, Rome, Italy, June 1973.

51. Hamada, M., T. Akimoto, and H. Izumi, "Dynamic Stress of a Submerged Tunnel During Earthquakes," *Proceedings of the Fifth World Conference on Earthquake Engineering*, Rome, Italy, 1973.

52. Yamahara, H., Y. Hisatomi, and T. Morie, "A Study on the Earthquake Safety of Rock Cavern," *Proceedings of the Rockstore Conference*, Stockholm, Sweden, September 1977.

53. Fukushima, D., M. Hamada, and T. Hanamura, "Earthquake-Resistant Design of Underground Tanks," *Proceedings of the Rockstore Conference*, Stockholm, Sweden, September 1977.

54. Glass, C. E., *Seismic Considerations in Siting Large Underground Openings in Rock*, Ph.D. dissertation, University of California, Berkeley, 1976.

55. Engineering Research Associates, "Underground Explosion Test Program, Final Report," *ROCK*, Vol. 2, U.S. Army, Corps of Engineers, Sacramento District, April 1953.

56. Hendron, A. J., "Engineering of Rock Blasting on Civil Projects," *Structural and Geotechnical Mechanics*, E. J. Hall, ed., Prentice-Hall, Englewood Cliffs, New Jersey, 1977.

57. Dowding, C. H., "Seismic Stability of Underground Openings," *Proceedings of the Rockstore Conference*, Stockholm, Sweden, September 1977.

58. Dowding, C. H., and A. Rozen, "Damage to Rock Tunnels from Earthquake Shaking," *Journal of the Geotechnical Engineering Division*, American Society of Civil Engineers, Vol. 104, No. GT2, 1978.

59. Richter, C. F., *Elementary Seismology*, W. H. Freeman, San Francisco, California, 1958.

60. Richart, F. E., J. R. Hall, and R. D. Woods, *Vibrations of Soils and Foundations*, Prentice-Hall, Englewood Cliffs, New Jersey, 1970.

61. Fung, Y. C., *Foundations of Solid Mechanics*, Prentice-Hall, Englewood Cliffs, New Jersey, 1965.

62. Ewing, W. M., W. S. Jardetzky, and F. Press, *Elastic Waves in Layered Media*, McGraw-Hill, New York, New York, 1957.

63. Cook, N. G. W., and J. C. Jaeger, *Fundamentals of Rock Mechanics*, 2nd ed., John Wiley, New York, New York, 1976.

64. Stagg, K. G., and D. C. Zienkiewicz, *Rock Mechanics in Engineering Practice*, John Wiley, New York, New York 1969.

65. Popov, E. P., *Introduction to Mechanics of Solids*, Prentice-Hall, Englewood Cliffs, New Jersey, 1968.

66. Kolsky, H., *Stress Waves in Solids*, Dover Publications, New York, New York, 1963.

67. Newmark, N. M., "Problems in Wave Propagation in Soil and Rock," *Proceedings, International Symposium on Wave Propagation and Dynamic Properties of Earth Materials*, University of New Mexico Press, Albuquerque, New Mexico, August 23-25, 1968.

68. Timoshenko, S., and J. N. Goodier, *Theory of Elasticity*, McGraw-Hill, New York, New York, 1951.

69. Proctor, R. V., and T. L. White, *Rock Tunneling with Steel Supports*, Commercial Shearing and Stamping Company, Youngstown, Ohio, 1946, revised 1968.

70. LaComb, J., Department of Defense, Nevada Test Site, private communication, December 1977.

71. *Effects Prediction Guidelines for Structures Subjected to Ground Motion*, JAB-99-115, URS/John A. Blume & Associates, Engineers, San Francisco, California, 1975.

72. Fenix & Scisson, Inc., *Mineability Study of the Terminal Waste Storage Program: Eleana Investigation*, draft, Mercury, Nevada, March 10, 1978.

73. Kunich, M. P., U.S. Department of Energy, Las Vegas, Nevada, private communication, March 1978.

DISTRIBUTION: JAB-99-123

David B. Clemens, DOE/HQ, Washington, D.C.
Carl R. Cooley, DOE/HQ, Washington, D.C.
George W. Cunningham, DOE/HQ, Washington, D.C.
Kevin P. Donovan, DOE/HQ, Washington, D.C.
Mark W. Frei, DOE/HQ, Washington, D.C.
Critz H. George, DOE/HQ, Washington, D.C.
John L. Gilbert, DOE/HQ, Washington, D.C.
Colin A. Heath, DOE/HQ, Washington, D.C.
Carl W. Kuhlman, DOE/HQ, Washington, D.C.
Robert L. Morgan, DOE/HQ, Washington, D.C.
Donald L. Vieth, DOE/HQ, Washington, D.C. (2 copies)
James B. Cotter, DOE/NV, Las Vegas, Nevada
Mahlon E. Gates, DOE/NV, Las Vegas, Nevada
P. N. Halstead, DOE/NV, Las Vegas, Nevada
David G. Jackson, DOE/NV, Las Vegas, Nevada
Mitchell P. Kunich, DOE/NV, Las Vegas, Nevada
Robert R. Loux, DOE/NV, Las Vegas, Nevada
Henry L. Melancon, DOE/NV, Las Vegas, Nevada
Billy C. Moore, DOE/NV, Mercury, Nevada
Allen J. Roberts, DOE/NV, Las Vegas, Nevada
Robert W. Taft, DOE/NV, Las Vegas, Nevada
Technical Library, DOE/NV, Las Vegas, Nevada (10 copies)
Delacroix Davis, DOE/AL, Albuquerque, New Mexico
John J. Schreiber, DOE/OR, Oak Ridge, Tennessee
Technical Information Center, Oak Ridge, Tennessee (27 copies)
David J. Squires, DOE/RL, Richland, Washington
Dale Cook, DOE/SAN, Oakland, California
Roger Richter, DOE/San, Oakland, California
D. M. Ellett, SL, Albuquerque, New Mexico
Orval E. Jones, SL, Albuquerque, New Mexico
Richard Lincoln, SL, Albuquerque, New Mexico
Richard W. Lynch, SL, Albuquerque, New Mexico
W. A. Von Riesemann, SL, Albuquerque, New Mexico
Howard Stephens, SL, Albuquerque, New Mexico

Lynn D. Tyler, SL, Albuquerque, New Mexico
Wendell D. Weart, SL, Albuquerque, New Mexico
Alan Stephenson, SL, Las Vegas, Nevada
William P. Bishop, NRC, Washington, D.C.
Regis Boyle, NRC, Washington, D.C.
James Malaro, NRC, Washington, D.C.
J. C. Frye, GSA, Washington, D.C.
George A. Dinwiddie, USGS, Denver, Colorado
William W. Dudley, USGS, Denver, Colorado
William S. Twenhofel, USGS, Denver, Colorado
George D. DeBuchananne, USGS, Reston, Virginia
Peter R. Stevens, USGS, Reston, Virginia
Bruce B. Arkell, State of Nevada, Carson City, Nevada
Noel Clark, State of Nevada, Carson City, Nevada
Bruce Crowe, LASL, Los Alamos, New Mexico
Larry Germain, LASL, Los Alamos, New Mexico
Darleane C. Hoffman, LASL, Los Alamos, New Mexico (2 copies)
Alfred Holtzer, LLL, Livermore, California
Lawrence Ramspott, LLL, Livermore, California
William W. Hambleton, Kansas State Geological Survey, Topeka, Kansas
Sam Basham, BMI, Columbus, Ohio
Wayne Carbiner, BMI, Columbus, Ohio
John W. Barlett, BNW, Richland, Washington
Alan M. Platt, BNW, Richland, Washington
W. J. McClain, UC/OWI, Oak Ridge, Tennessee
Conway Chan, EPRI, Palo Alto, California
Raul A. Deju, Rockwell International Co., Richland, Washington
H. B. Dietz, Rockwell International Co., Richland, Washington
Tor L. Brekke, University of California, Berkeley, California
Fred D. Waltman, Fenix & Scisson, Inc., Las Vegas, Nevada
George E. Wickham, Jacobs Associates, San Francisco, California